People's Democratic Republic of Algeria

Ministry of Higher Education and Research Scientist

UNIVERSITY DR. YAHIA FARÈS OF MEDÉA

Faculty of Technology

Department of Civil Engineering



Graduation Project

Presented for graduation from Master

Specialty: Civil Engineering

Option: Construction and materials

Theme:

Numerical study of a masonry wall

Realized by Mrs: KERMEZLI Youcef et ELGHERIBI Mahdi

Directed by : Mr.BOUKESSANI Omar

June 2018

République **A**lgérienne **D**émocratique et **P**opulaire
Ministère de l'**E**nseignement **S**upérieur et de **R**echerche la **S**cientifique
UNIVERSITÉ YAHIA FARÈS DE MÉDÉA

Faculté de **T**echnologie

Département de **G**énie **C**ivil



Projet de Fin d'études

Présenté pour l'obtention du diplôme de Master

Option : Matériaux en genie civil

Théme :

Etude numérique d'un mur en maçonnerie

Etudié par : KERMEZLI Youcef et ELGHERIBI Mahdi

Encadré par : Mr.BOUKESSANI Omar

Promotion Juin 2018

Dedications

I want to dedicate this memoir:

To my dear Mother and my dear Father, in testimony and gratitude for their dedication, their constant support during all my years of study, their unlimited sacrifices, their moral comfort, they who have made so much effort for my education, and to see myself reach that goal, for all that and for what cannot be said, my boundless affections.

I thank my friend and binomial ***Mahdi*** *who contributed to the realization of this modest work.*

I thank ***AbdeRahman, islam, omran, Ayad Abed Razak, Abelkader*** *and all my friends*

To all the promo of June 2018 especially civil engineering and to all the people I know



Youcef

Dedications

I want to dedicate this memoir:

To my dear Mother and my dear Father, in testimony and gratitude for their dedication, their constant support during all my years of study, their unlimited sacrifices, their moral comfort, they who have made so much effort for my education, and to see myself reach that goal, for all that and for what cannot be said, my boundless affections.

I thank my friend and binomial ***Yousef*** *who contributed to the realization of this modest work.*

I thank ***Islam, omran, zinou, Abdelmadjid, Hamza, amine, dahmen, Ahmed*** *and all my friends*

To all the promo of June 2018 especially civil engineering and to all the people I know



Mahdi

Thanks

*First, we thank **ALLAH**, the merciful for giving us the strength and courage to carry out this modest work.*

It is not difficult to thank all those who have participated in this work, but it must be admitted that the formulas are numerous and that the choice of good words has always been difficult. We would like to thank:

*Our supervisor **Dr. Bouksani Omar** for having accepted to supervise us, and for his precious advices during the realization of this work. For the honor he gives us to supervise this work, for their availability, for their listening, for the very precious help and the constant interest that they have kindly shown for this work they have guided. by judicious advice, who were able to communicate us to best lead this study.*



We express our deep appreciation for his enlightening reading of this research work.

A big thank you is sent to all the engineers and workers of the University of Medea

Our sincere thanks also go to all the teachers of the Department of Civil Engineering of the University of Medea, who offered us all this knowledge especially ***Mr. Kermezli Tayeb*** *&* ***Mr. Rebhi Karim***

And we certainly do not forget our parents our friends and all those who have helped us in our task, we will thank them.

Finally, we thank all those who contributed directly or indirectly to the realization of this memoir.

.



Abstract

The main objective of this project is to obtain an adequate set of numerical data based on ANSYS APDL concerning masonry structures, with a complete stress-strain behaviour description including a characterization of the failure modes (crack, deformation) with different mortar resistance and paths, using applied horizontal and vertical loads.

The obtained results show that the mechanical effects of properties of mortar are not that important in the masonry wall reinforcement composed with different resistance with too close results and behavior). Also results show that the most vulnerable areas in the masonry wall is the intersection area of horizontal and vertical mortar.

ملخص

الهدف الرئيسي من هذا المشروع هو الحصول على مجموعة كافية من البيانات التجريبية (باستخدام ANSYS APDL) فيما يتعلق بهياكل البناء. بما في ذلك وصف كامل لسلوك الإجهاد والتشوه مع وصف أنماط الانهيار (التشقق، والتشوه الكلي) باستخدام مقاومة ومسارات مختلفة للملاط، و هذا بتطبيق قوى أفقية وعمودية.

تظهر النتائج التي تم الحصول عليها ان الخصائص الميكانيكية للملاط ليست بتلك الأهمية في تعزيز جدار البناء (مقاومة مختلفة مع سلوك ونتائج متقاربة جدا) مقارنة مع نتائج المناطق الأكثر ضعفا في البناء و هي منطقة تقاطع الملاط الافقي والعمودي.

Résumé

L'objectif principal de ce projet est d'obtenir un ensemble adéquat de data base numérique (en utilisant ANSYS APDL) concernant les structures de maçonnerie, avec une description complète du comportement contrainte-déformation y compris une caractérisation des modes de rupture (fissure, déformation) en utilisant différentes résistances et types de mortier, sous des charges horizontales et verticales appliquées.

Les résultats obtenus montrent que l’effet mécaniques du mortier ne sont pas si importantes dans le renforcement des murs en maçonnerie comparé avec (résistance différente avec des résultats et un comportement trop proche). Les résultats montrent également que les zones les plus vulnérables dans le mur de maçonnerie est l'intersection du mortier horizontal et vertical.

Dedication
Thanks
Abstract
Summary
List of tables
List of figures
Symbols and Abbreviations

GENERAL INTRODUCTION ..... Error! Bookmark not defined.

CHAPTER 1 : BIBLIOGRAPHIC SYNTHESIS

INTRODUCTION 2

I.1 **HISTORICAL MASONRY STRUCTURES** ..... Error! Bookmark not defined.

MASONRY STRUCTURES THROUGH TIME ..... **Error! Bookmark not defined.**

I.2 **Experimental research on masonry structures** ..... Error! Bookmark not defined.

Uniaxial Behavior ..... **Error! Bookmark not defined.**

Compressive Testing 9

Shear Testing 9

Biaxial behavior ..... Error! Bookmark not defined.

Numerical modelling of masonry structures ..... **Error! Bookmark not defined.**

I.3 **Structural Behaviour** 11

A. Linear elastic behaviour 13

B. Plastic Behaviour 13

C. Non linear behaviour 14

Modelling techniques for masonry structures 15

I.4 **MECHANICAL TESTS ON STONE AND BRICK MASONRY** **16**

I.5 **Numerical Simulations done by others** ..... Error! Bookmark not defined.

Numerical Model ..... **Error! Bookmark not defined.**

Setting of ATENA ..... **Error! Bookmark not defined.**

Materials ..... **Error! Bookmark not defined.**

Solution Parameters.....**Error! Bookmark not defined.**
Meshing.....**Error! Bookmark not defined.**
2D analysis vs. 3D analysis .....**Error! Bookmark not defined.**
Influence of Geometry.....**Error! Bookmark not defined.**
Thickness of Joints .....**Error! Bookmark not defined.**
Head Joints.....**Error! Bookmark not defined.**
I.6 Influence of Material Properties..... Error! Bookmark not defined.
Young's Modulus.....**Error! Bookmark not defined.**
Fracture Energy.....**Error! Bookmark not defined.**
Tensile Strength .....**Error! Bookmark not defined.**
Compressive Strength.....**Error! Bookmark not defined.**

CHAPTER 2 : MATERIAL AND TESTS

II.1 Introduction..... Error! Bookmark not defined.
II.2 Materials ..... Error! Bookmark not defined.
II.3 Loads ..... Error! Bookmark not defined.
II.4 Modeling ..... Error! Bookmark not defined.
II.5 Execution ..... Error! Bookmark not defined.
Vertical loads.....**Error! Bookmark not defined.**
Horizontal loads .....**Error! Bookmark not defined.**

CHAPTER 3 : RESULTS AND INTERPRETATION

III.1 Influence of mortar parameters on wall resistance .. Error! Bookmark not defined.
Stress .....**Error! Bookmark not defined.**
Strain.....**Error! Bookmark not defined.**
III.2 Influence of applied loads sense on wall deformation Error! Bookmark not defined.
Vertical loads.....**Error! Bookmark not defined.**
Horizontal loads.....**Error! Bookmark not defined.**
III.3 Influence of mortar parameters on the crack path .... Error! Bookmark not defined.

III.4 Conclusion and pespective..... Error! Bookmark not defined.

List of Tables

CHAPTER 01 : BIBLIOGRAPHIC SYNTHESIS

Tableau 1. 1: Material parameters of cocciopesto mortar 19
Tableau 1. 2: Material parameters of clay brick 20
Tableau 1. 3: Material parameters of steel plate 20
Tableau 1. 4: Summary of solution parameters 21
Tableau 1. 5: Summary of peak values for different thicknesses of joints 27
Tableau 1. 6: Peak values for walls with 10 mm thick bed joints and with/without head joints 31
Tableau 1. 7: Peak values for walls with 45 mm thick bed joints and with/without head joints 33
Tableau 1. 8: Summary of peak values for different Young's modulus 36
Tableau 1. 9: Summary of peak values for different fracture energies 39
Tableau 1. 10: Summary of peak values for different tensile strengths 41
Tableau 1. 11: Summary of peak values for different tensile strengths 43

CHAPTER 02 : MATERIALS AND TESTS

Tableau 2. 1: Type of materials 45
Tableau 2. 2 : Type of materials 63
Tableau 2. 3 : Type of materials 63
Tableau 2. 4: Type of materials 68
Tableau 2. 5: Type of materials 73

List of Figures

CHAPTER 01 : BIBLIOGRAPHIC SYNTHESIS

Fig 1. 1: Egyptian pyramids 04
Fig 1. 2: Lion Gate at Mycenae 05
Fig 1. 3: The Parthenon at Athens 06
Fig 1. 4: Roman masonry walls 07
Fig 1. 5: Dry stone constructions 07
Fig 1. 6: Different kinds of stone masonry 08
Fig 1. 7: Different arrangements for brick masonry 08
Fig 1. 8: Compressive testing model (ANSYS APDL). 09
Fig 1. 9: Different modes of failure of solid clay brickwork panels under biaxial loading 11
Fig 1. 10: Different modes of material behavior 12
Fig 1. 11: General load-displacement diagrams of a structural analysis 12
Fig 1. 12: Distinct regions of the stress strain curve 14
Fig 1. 13: Plain concrete tensile response 15
Fig 1. 14: Modelling strategies for masonry structures 16
Fig 1. 15: Shear wall scheme 18
Fig 1. 16: Samples of cocciopesto mortar in laboratory 18
Fig 1. 17: Newton-Raphson method vs. Arc-length method 21
Fig 1. 18: Influence of fineness of meshing 22
Fig 1. 19: 2Danalysis vs. 3D analysis 23
Fig 1. 20: Crack pattern of 2D shear wall 24
Fig 1. 21: Crack pattern of 3D shear wall 24
Fig 1. 22: Crack pattern of experimental shear wall 25
Fig 1. 23: Shear wall with 10 mm thick joints 26
Fig 1. 24: Shear wall with 45 mm thick joints 26
Fig 1. 25: Shear walls with 10 mm thick joints and with 45 mm thick joints 28
Fig 1. 26: Behavior of wall with 10 mm thick joints in vicinity of peak 29
Fig 1. 27: Behavior of wall with 45 mm thick joints in vicinity of peak 30
Fig 1. 28: Shear wall with 10 mm thick joints without head joints 30
Fig 1. 29: Shear walls with 45 mm thick joints without head joints 31
Fig 1. 30:Shear walls with 10 mm thick bed joints and with/without head joints 32
Fig 1. 31: Crack pattern of wall with 10 mm thick bed joints without head joints 33
Fig 1. 32: Shear walls with 45 mm thick bed joints and with/without head joints 34
Fig 1. 33: Crack pattern of wall with 45 mm thick bed joints without head joints 35
Fig 1. 34: Shear wall with 45 mm thick joints. 35
Fig 1. 35: Crack pattern of wall with 45 mm thick joints and Young's modulus 2200 MPa 37
Fig 1. 36: Shear walls with different values of fracture energy. 38
Fig 1. 37: Crack pattern of wall with 45 mm thick joints and different fracture energies 39
Fig 1. 38: Shear walls with different values of tensile strength 40

Fig 1. 39: Crack pattern of wall with 45 mm thick joints and different tensile strengths 41
Fig 1. 40: Shear walls with different values of compressive strength 42
Fig 1. 41: Crack pattern of wall with 45 mm thick joints and compressive strength 5 MPa ...43

CHAPTER 02 : MATERIALS AND TESTS

Fig 2. 1 : Main model (Ansys APDL) 45
Fig 2. 2 : Element types 46
Fig 2. 3 : Linear isotropic properties for material (1) 46
Fig 2. 4 : Parameters for material (1) 47
Fig 2. 5 : Linear isotropic properties material (2) 47
Fig 2. 6:. Loads distribution 47
Fig 2. 7: First crack 48
Fig 2. 8: Stress 2D 48
Fig 2. 9: Stress 3D 48
Fig 2. 10: Stress in function of time 49
Fig 2. 11: Elastic strain 2D 49
Fig 2. 12: Elastic strain 3D 49
Fig 2. 13: Elastic strain in function of time 50
Fig 2. 14: Stress (a) and elastic strain (b) in function of time by EXCEL 50
Fig 2. 15 : Parameters for material (1) 51
Fig 2. 16: Stress 2D 51
Fig 2. 17: Stress 3D 51
Fig 2. 18: Stress in function of time 52
Fig 2. 19: Elastic strain 2D 52
Fig 2. 20: Elastic strain 3D 52
Fig 2. 21: Elastic strain in function of time 53
Fig 2. 22: Stress (a) and elastic strain (b) in function of time by EXCEL 53
Fig 2. 23: Parameters for material (1) 54
Fig 2. 24: Stress 2D 54
Fig 2. 25: Stress 3D 54
Fig 2. 26: Stress in function of time 55
Fig 2. 27: Elastic strain3D 55
Fig 2. 28: Elastic strain 2D 55
Fig 2. 29: Elastic strain in function of time 56
Fig 2. 30: Stress (a) and elastic strain (b) in function of time by EXCEL 56
Fig 2. 31: Parameters for material (1) 57
Fig 2. 32: Stress 2D 57
Fig 2. 33: Stress 3D 57
Fig 2. 34: Stress in function of time 58
Fig 2. 35: Elastic strain 2D 58
Fig 2. 36: Elastic strain 3D 58
Fig 2. 37:. Elastic strain in function of time 59
Fig 2. 38: Stress (a) and elastic strain (b) in function of time by EXCEL 59
Fig 2. 39: Parameters for material (1) 60
Fig 2. 40: Stress 2D 60
Fig 2. 41: Stress 3D 60

Fig 2. 42: Stress in function of time 61
Fig 2. 43: Elastic strain 2D 61
Fig 2. 44: Elastic strain 3D 61
Fig 2. 45: Elastic strain in function of time 62
Fig 2. 46: Stress and elastic strain in function of time by EXCEL 62
Fig 2. 47: Distribution of material 63
Fig 2. 48: Properties of material (1) 64
Fig 2. 49: Properties of material (2) 64
Fig 2. 50: Properties for material (3) 64
Fig 2. 51: Distribution of loads 65
Fig 2. 52:. The first crash path 65
Fig 2. 53:. Stress 2D 66
Fig 2. 54: Stress 3D 66
Fig 2. 55: Stress in function of time 66
Fig 2. 56: Elastic strain 2D 67
Fig 2. 57: Elastic strain 3D 67
Fig 2. 58: Elastic strain in function of time 67
Fig 2. 59: Displacement of wall 67
Fig 2. 60:. Distribution of materials 68
Fig 2. 61: Distribution of loads 69
Fig 2. 62: The first crash path 69
Fig 2. 63: Stress 2D and 3D 70
Fig 2. 64: Stress in function of time 70
Fig 2. 65: Elastic strain 2D 71
Fig 2. 66: Elastic strain 3D 71
Fig 2. 67: Elastic strain in function of time 71
Fig 2. 68: Displacement 72
Fig 2. 69: Distribution of materials 72
Fig 2. 70: Distribution of loads 73
Fig 2. 71: The first crash 74
Fig 2. 72: Stress 2D 74
Fig 2. 73: Stress 3D 74
Fig 2. 74: Stress in function of time 75
Fig 2. 75: Elastic strain 2D 75
Fig 2. 76: Elastic strain 3D 75
Fig 2. 77: Elastic strain in function of time 76
Fig 2.78 : Displacement 76
Fig 2.79 : Stress in function of time 77
Fig 2.80 : Elastic strain in function of time 77
Fig 2.81 : Stress in function of time 77
Fig 2.82 : Elastic strain in function of time 77
Fig 2.83 : Stress in function of time 78
Fig 2.84 : Elastic strain in function of time 78

CHAPTER 3 : RESULTS AND INTERPRETATION

Fig 3. 1:. Stress in function of time 79
Fig 3. 2:. Elastic strain in function of time 80
Fig 3. 3:. Elastic Strain 81
Fig 3. 4:. Elastic Strain 81
Fig 3. 5:. Elastic Strain 81
Fig 3. 6:. Elastic Strain 81
Fig 3. 7:. Elastic Strain 81
Fig 3. 8:. Elastic Strain 82
Fig 3. 9:. Elastic Strain 82
Fig 3. 10:. Elastic Strain 82
Fig 3. 11:. Crack path Left side 83
Fig 3. 12:. Crack path Right side 83
Fig 3. 13:. Crack path Both sides 83

Symbol and abbreviation

ANSYS APDL: ANSYS Parametric Design Language

F: The applied force (load)

σ: Stress

ε: Strain

E: Young’s modulus of elasticity

P: Plain concrete tensile response

T: Shear stress

2D: 2 dimension

3D: 3 dimension

μ: Poisson's ratio

ft: Tensile strength

fc: Compressive strength

Gf: Specific fracture energy

Wd: Critical compressive displacement

e: Fail. surface eccentricity

ρ: Specific material weight

ε_{cp} : Plastic strain at compressive strength

α : Coefficient of thermal expansion

NRM: Newton-Raphson method

ALM: Arc-length method

Ex : Young’s modulus

Prxy : Major Poisson's ratio, x-y

Masonry is the oldest building material that still finds wide use in today's building industries. The most important characteristic of masonry construction is its simplicity. Laying pieces of stone, bricks or blocks on top of each other, either with or without cohesion via mortar, is a simple, though adequate, technique that has been successfully used ever since remote ages. Naturally, innumerable variations of masonry materials, techniques and applications occurred during the course of time. The influence factors were mainly the local culture and wealth, the knowledge of materials and tools, the availability of material and architectural reasons. The decay of masonry as a structural material and the lack of standardization of the material resulted in a lack of resources used for masonry research. This applies both for new and old masonry structures. Time shows that many historical constructions have collapsed. Europe possesses notorious examples, like the ones related to the earthquake of Lisbon in 1755 **[1]**, Nevertheless, not only exceptional events affect historical constructions. Fatigue and strength degradation, accumulated damage due to traffic, wind and temperature loads, soil settlements and the lack of structural understanding of the original constructors are high risk factors for the architectural heritage.

Recent examples of irreversible losses of the cultural and architectural damage can be found, for example, in Italy: Campanile of St. Marcus in Venice (total collapse in 1902 after being repeatedly struck by lightning) **[2]**, Civic Tower of Pavia (total collapse in 1989 with hardly any warning) **[3]**and Cathedral of Noto (collapse of the dome in 1996) **[4]**. Famous examples of historical constructions in risk due to soil settlements are the Cathedral of Mexico City and the tower of Pisa, and constructions in risk due to a deficient structural conception are the Cathedral of Pavia and the Cathedral of Florence. Nevertheless, only very recently the scientific community began to show interest in advanced testing (under displacement control) and advanced tools of analysis for historical constructions. The lack of experience in this field is famous in comparison with more advanced research fields like concrete, soil, rock or composite mechanics

Chapter 1 :

BIBLIOGRAPHIC SYNTHESIS

INTRODUCTION

This study is concerned with the experimental and numerical analysis of masonry structures submitted to loading. numerical studies have been carried out, focusing on the structural behaviour of masonry.

Numerical studies should, whenever possible, be complemented with appropriate experimental programs like ANSYS in our case, which provide appropriate material data necessary to calibrate advanced nonlinear numerical models. The objectives of this study are:

- ✓ To obtain an adequate set of experimental data concerning historical masonry components and structures, capable of being used for numerical purposes. This material characterization should include a complete stress-strain behaviour description with emphasis on the cyclic behaviour, a characterization of the failure modes (crack, deformation)

- ✓ To verify the developed model by comparing the predicted numerical response with the behaviour measured in reliable experiments. In spite of the wide scatter that characterizes masonry tests, the developed model should be able to provide a good agreement in terms of ultimate load, global behaviour and failure mode with experimental results.

These two objectives are directly related, since the performance of the numerical model depends on the existence of reliable and appropriate experimental data concerning inelastic behaviour. On the other hand, the use of a numerical tool (ANSYS) beforehand may allow enhancing the definition of experimental testing programs.

I.1 HISTORICAL MASONRY STRUCTURES

Historical masonry constructions inevitably suffer damage with time. Earthquakes, soil settlements, material degradation and lack of maintenance are the main reasons for structural damage to these constructions **[5]**. Therefore, careful periodic inspections are necessary in order to evaluate their actual structural safety levels. However, performing the structural analysis of a historical masonry construction is, in general, a very complex and difficult task, since structural engineering is only one of the disciplines of a multidisciplinary group that should be constituted when a consistent plan of intervention for a given historical construction is intended to be drawn. Indeed, all the components of a historical construction must be taken into account when dealing with the design of

an intervention. A given historical construction can be seen as a complex entity, where the structural skeleton together with the visual image and the architectural style are significant parts of it. Another important part that also carries important cultural significance is its age, which means that historically, these constructions have been a part of human lives. Therefore, besides the expected structural strengthening, it is required that both image and substance of historical constructions be preserved after any structural intervention **[6]**.

MASONRY STRUCTURES THROUGH TIME

There are two fundamental structural problems when building with masonry: how to achieve height and how to span an opening, i.e. how to span vertical and horizontal spaces **[7]**. Spanning vertically is done by using columns, walls and towers, and spanning horizontally is done by using lintels, beams and arches. In addition, some structural elements such as vaults and domes can simultaneously span vertically and horizontally.

Masonry is the oldest building material that is still commonly used nowadays. The placing of stone or brick units on top of each other, laid dry or bonded with mortar has revealed itself to be a very successful technique, which is mainly justified by its simplicity and the durability of the constructions.

The first masonry was a simple stack of selected natural stones and mortar, if any, was earth packed between the stones. As tools became available and skills developed, stone units were shaped in regular forms. The first bricks were made of mud or clay, shaped to form bricks and dried by the sun. The bricks were then laid with mud mortar into walls. This simple process has been widely used for millennia to construct dwellings, particularly in the valleys of the Nile and Mesopotamia **[8]**. The practice of burning brick represented a natural evolution and the first prefabricated component.

Due to environmental degradation, religious structures, built with better materials and skill than dwellings, supplied the oldest preserved constructions. In this way, the structural form of the pyramids, which represents one of the most stable structural shapes, was the logical development of the initial stone piles. Apart from possible settlements, their structural behaviour does not present any particular problem, as the inner space is limited and the stresses are low and perfectly compatible with the material strength. The most famous pyramids are undoubtedly the Egyptian pyramids at Giza, see Figure 1.1, which are the only survivors of the Seven Wonders of the World and remained the tallest structure (=140 m) in the world until the 20th century.



Fig I.1. Egyptian pyramids **[9]**

With time, the structural behaviour started to play a more important role in the construction of temples. The use of stone lintels to support the masonry above openings in walls, as the one used to build the Lion Gate at Mycenae, Greece (13^{th} century), which spanned about 3 m and weighed between 25 and 30 tons **[10]**, shows the beginning of the arched behaviour that would dominate the following millennium, see Figure I.2.

During the classical period, columns and the corresponding capitals rose as their most distinctive elements. The reduced distance between the columns was mostly a structural need. Spanning large distances could not be achieved because it was difficult to transport large stone blocks and at the same time stone has a rather low tensile strength



Fig I.2. Lion Gate at Mycenae **[11]**

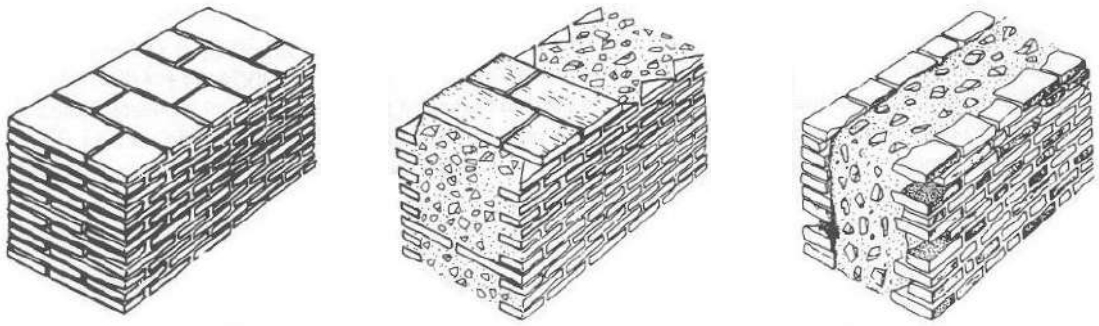
Greek architecture in general, and temples in particular, were aesthetically perfect and based on strict rules of proportion and symmetry between the different elements, which represented an important milestone in the history of buildings. Limestone was usually the stone used to build structural elements as walls, columns and beams. The Parthenon (5^{th} century B.C.) represents the most famous construction of the Greek architecture, see Figure I.3.



Fig 1.3. The Parthenon at Athens. **[12]**

The Romans, with a strong and centralized empire, provided one of the most important steps in the construction of buildings. Contrasting with the Greeks, their architecture was not only concerned with temples and amphitheaters, but also with roads, bridges, aqueducts and harbors. They introduced many innovations directly related to materials, structural concepts and construction processes.

Together with an improvement of the quality of bricks, the brick size became more standardized and different shapes were produced for special purposes. Apart from that, the production of concrete, made of rubble, lime and special volcanic sand (pozzolana) revolutionized building construction. During the Roman period, innovative techniques were introduced in the construction of walls, using bricks or stones as facing, finely finished, and filling the inner space with concrete, as shown in Figure I.4.



(a) (b) (c)

Fig I.4. Roman masonry walls: (a) bonded brick wall; (b) brick faced wall with header courses; (c) brick faced wall **[13].**

The technique of dry stone block was also greatly improved and remarkable structures were built, such as the Colosseum (1st century A.D.) and Segovia's aqueduct (1st century A.D.), represented in Figure I.5.



(a) (b)

Fig I.5. Dry stone constructions: (a) the Colosseum **[14]**; (b) the Segovia's aqueduct **[15]**.

I.2 Experimental research on masonry structures

Masonry is a heterogeneous material composed of units of natural or artificial origin jointed by dry or mortar joints. Irregular stones, ashlars, adobes, bricks and blocks have been used as units. The units can be joined together using mortar (commonly clay, lime or cement based mortar) or just by

simple superposition. With these two components, a large number of arrangements can be accomplished, generated from the different combinations of units and joints. A possible classification of stone masonry is shown in Figure I.6 For brick masonry, the most used combinations are illustrated in Figure I.7

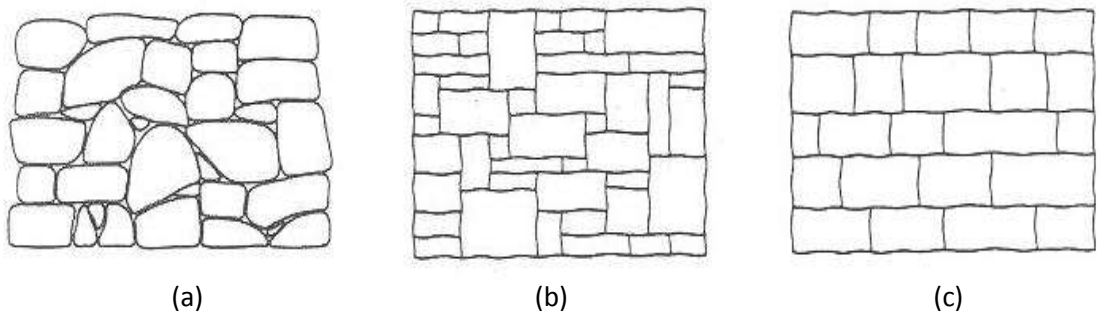


Fig I.6. Different kinds of stone masonry: (a) rubble masonry; (b) ashlar masonry; (c) coursed ashlar masonry **[16]**.

However, the mechanical behaviour of the different types of masonry generally exhibits a common feature: a very low tensile strength. This property is so important that it has determined the structural form of historical constructions.

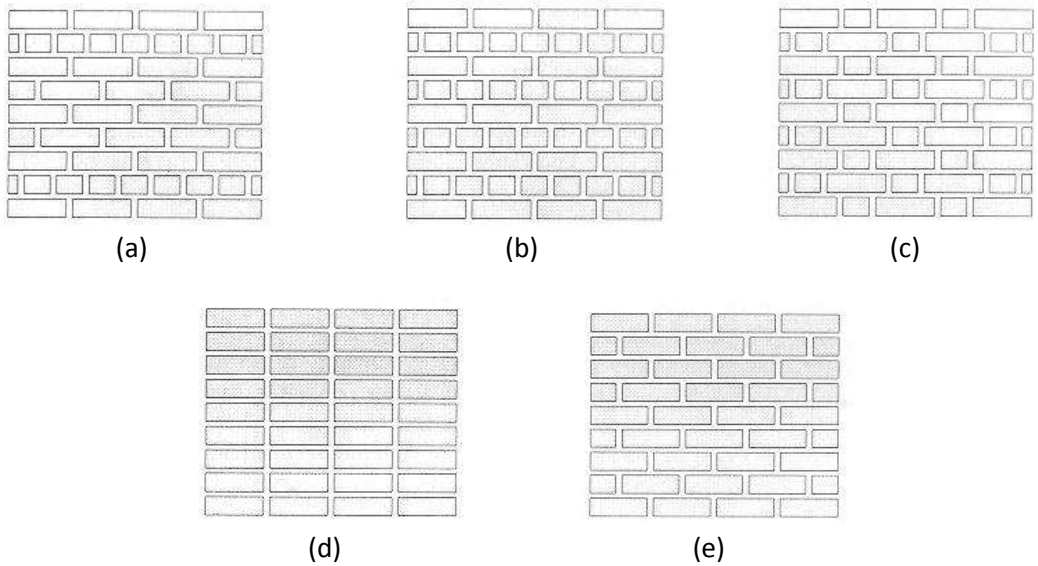


Fig 1.7 – Different arrangements for brick masonry: (a) American (or common) bond; (b) English (or cross) bond; (c) Flemish bond; (d) stack bond; (e) stretcher bond **[16].**

Uniaxial Behavior

The uniaxial behaviour, obtained under displacement-controlled tests, is usually characterized by the establishment of a stress-displacement diagram, in which the most important features that characterize the behaviour of the material should be included, namely the complete pre-peak branch, the peak load and significant part of the post peak branch. In the case of cyclic experiments, features such as strength and stiffness degradation as well as energy dissipation should be also adequately characterized. An important feature, common to all frictional materials, is the occurrence of softening after peak, which is defined as a progressive decrease of the mechanical strength under continuous imposed displacement. Softening behaviour is experimentally observed in uniaxial compressive, tensile and shear failure.

Compressive Testing

Compressive strength experiments on masonry prisms are rather easy to carry out. Until a few years ago, importance was only given to the evaluation of the ultimate load and, due to that, post-peak behaviour of the masonry is practically non-existent. This gap in knowledge was an encouragement to the execution of uniaxial compressive tests in both masonry prisms and unit specimens, including the characterization of the post-peak behaviour, which are described in detail in Chapter II.

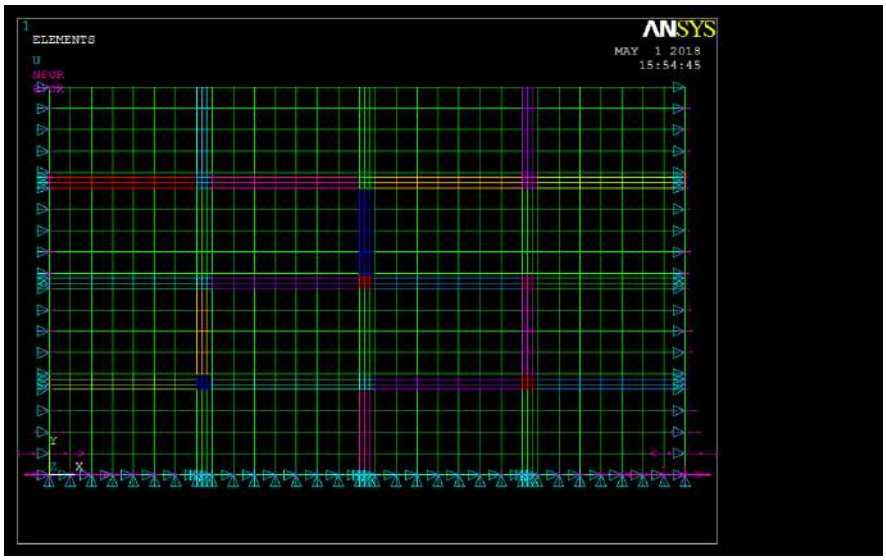


Fig I.8. Compressive testing model (ANSYS APDL).

Shear Testing

Shear has been identified as the governing mode of failure in masonry constructions subjected to lateral loads like wind and earthquakes. A certain degree of confinement present in the masonry walls is associated to these shear actions. Thus, pure shear mode is altered to shear-compression mode. This issue must be considered in testing, where direct shear loading applied to the joint has to be accompanied by normal loading. Direct shear tests are very demanding experiments because the test set- up, to be used idealistically, should generate a uniform state of stress on the joint. Moreover, this stress state should be kept constant during testing. These requisites are very difficult to attain since most of the time the shear load cannot be applied in line with the joint, originating, in consequence, an undesirable overturning moment for the joint stress.

Biaxial behavior

Masonry can be regarded as a discontinuous material. Bed and head joints are responsible for its discontinuous nature. This feature becomes evident when considering dry joint masonry. By acting as planes of weakness, the joints induce an anisotropic behaviour in both elastic and plastic domains. Therefore, the strength of masonry is highly dependent on the orientation of the principal stresses with respect to the material axes. Moreover, this anisotropic behaviour is further marked if the units exhibit anisotropic strength properties. Therefore, constitutive behaviour of masonry under biaxial stress states cannot be completely described from the constitutive behaviour under uniaxial loading conditions **[17]**. Due to its anisotropic nature, the biaxial strength envelope of masonry is described by a three- dimensional surface, either in terms of the full stress vector in a fixed set of material axes or in terms of the two principal stresses and the rotation angle between the principal stresses and the material axes.

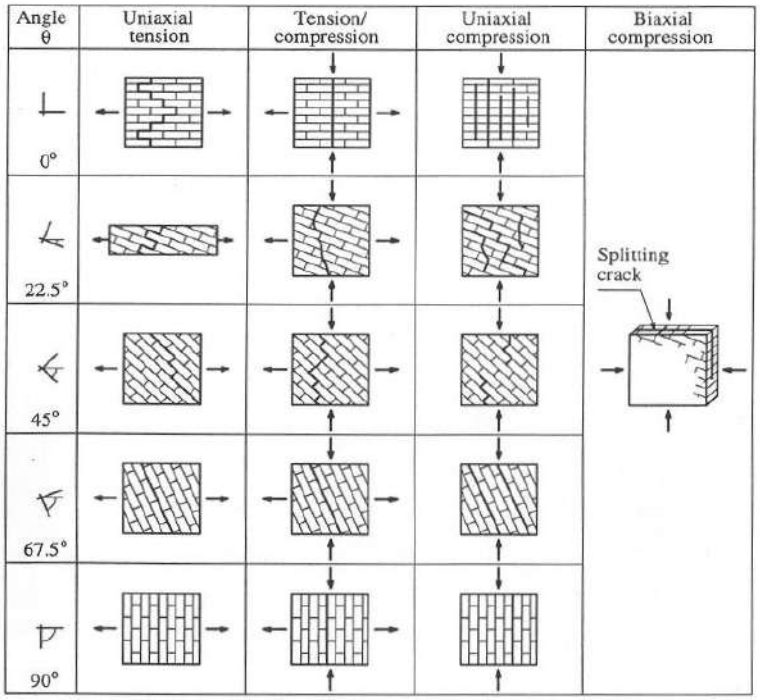


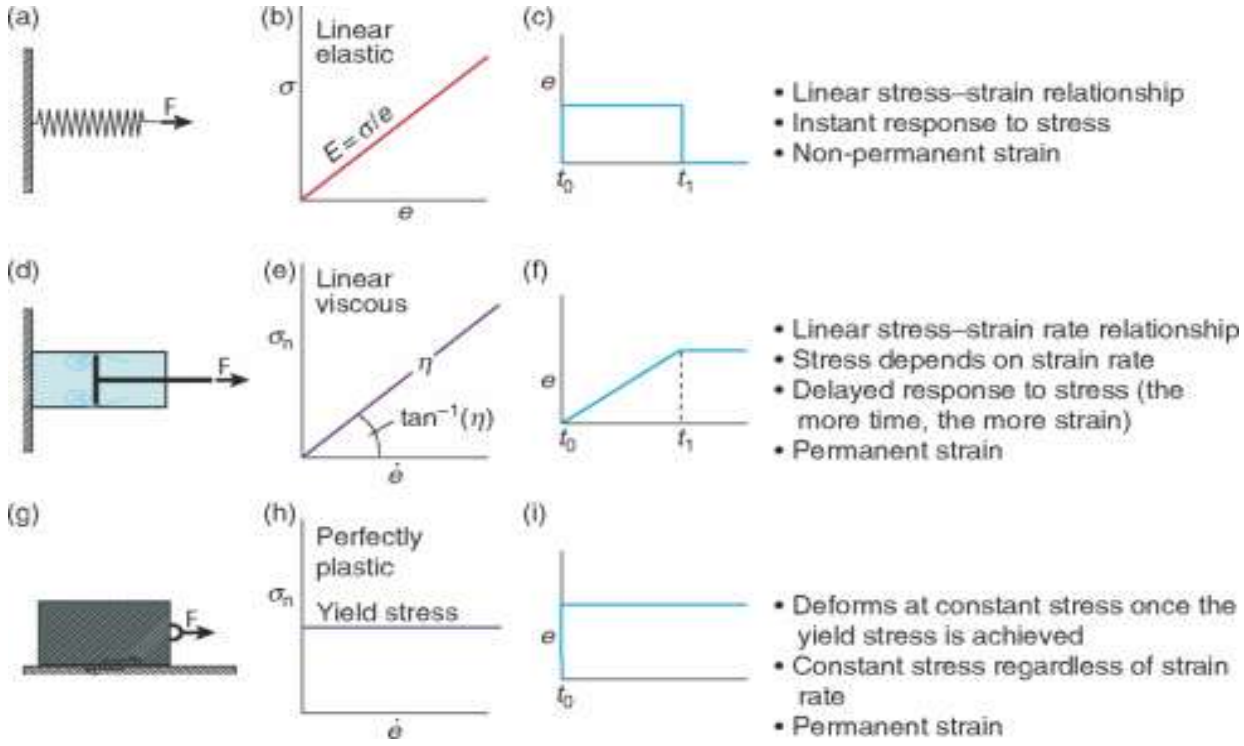
Fig I.9. Different modes of failure of solid clay brickwork panels under biaxial loading **[18]**.

Numerical modelling of masonry structures

Due to the high complexity of masonry behaviour, the approach towards the numerical simulation of its structural behaviour has led researchers to develop several constitutive models characterized by different levels of complexity. From the solutions based on the classical plastic methods **[19]** to the most advanced computational formulations, a wide series of numerical methods is available nowadays. The definition of the most suitable method depends on, among other factors, the structure under analysis, the available input data and the analyst's experience and qualifications **[20].**

I.3 Structural Behaviour

In order to solve a given structural problem, several idealizations of material behaviour can be established, each of them being necessarily associated with different degrees of complexity. Naturally, different types of constitutive models (i.e. different descriptions of the material behaviour, associated with different idealizations of the geometry, such as two- or three- dimensional description), originate a sequence, or hierarchy, of models, which allow the analysis to include more complex response effects as well as costlier solutions



. **Fig I.10**. Different modes of material behavior **[21].**

When dealing with masonry structures, the most common idealizations of material behaviour are elastic behaviour, plastic behaviour and non- linear behaviour. These different idealizations are schematically represented in Figure 4.2, where each idealization is represented by a typical general load-displacement diagram.

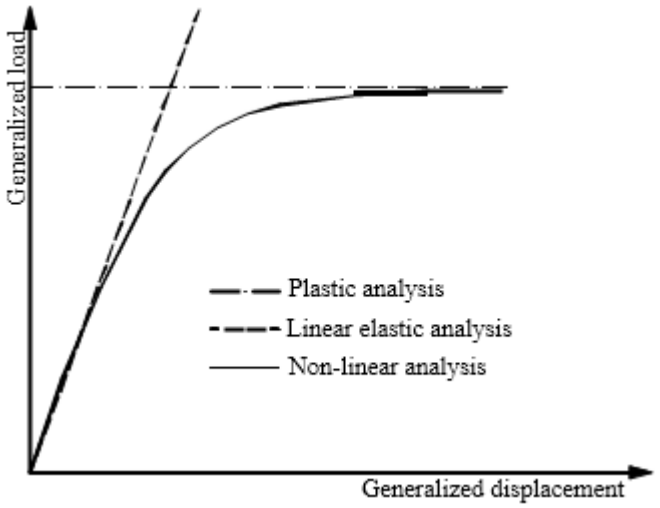


Fig I.11 – General load-displacement diagrams of a structural analysis.

By adopting a non- linear analysis instead of a linear analysis, a more comprehensive insight into the structural response can be obtained, with a higher cost, both in terms of necessary input data and required knowledge of the analyst. In the following, a brief description concerning the three idealizations referred to above is given and the most relevant issues are discussed. Emphasis is given to non- linear behaviour, since the development of a non-linear constitutive material model able to perform cyclic analyses is one of the objectives of this study.

A. Linear elastic behaviour

The linear elastic analysis is the procedure usually followed in structural analysis, where the material is considered to exhibit an infinite linear elastic behaviour, both in compression and tension. In the case of masonry structures, where joints possess relatively low tensile strength, or even no-tensile strength in the case of dry joints, cracks arise at low stress levels and, therefore, the assumption of elastic behaviour is quite debatable.
In general, linear elastic analyses are not appropriate for ancient constructions **[22]**.

However, in a first stage of analysis, the hypothesis of linear elastic behaviour can be of great help to the analyst. Linear analysis requires little input data, being less demanding, in terms of computer resources and engineering time used, when compared with non-linear methods. Moreover, for materials with tensile strength, linear analysis can provide a reasonable description of the process leading to the crack pattern.

B. Plastic behaviour

Plastic analysis, or limit analysis, is concerned with the evaluation of the maximum load that a structure can sustain (limit load). The assumption of plastic behaviour implies that, on one hand, the maximum load is obtained at failure and, on the other hand, the material should possess a ductile behaviour. Apparently, this last requirement seems to be unrealizable since the plastic deformations may exceed the ductility of the masonry. However, the limited ductility in compression does not play a relevant role as collapses, except in the case of columns, are generally related to the low tensile strength **[23]**.

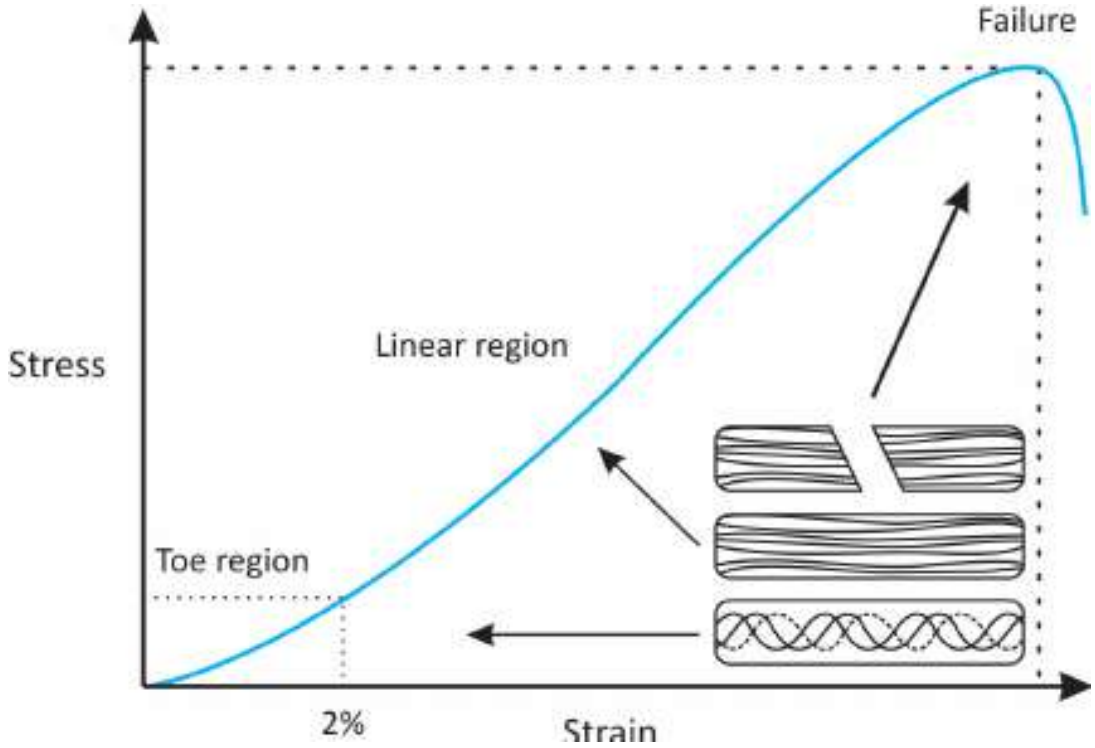


Fig I.12. distinct regions of the stress strain curve **[24]**

C. Non-linear behavior

Non-linear analysis is the most powerful method of analysis, the only one able to trace the complete structural response of a structure from the elastic range, through cracking and crushing, up to failure. On the other hand, the existence of mortar or dry joints, generally the weakest link in a masonry assemblage and characterized by a marked non- linear behaviour, induces a non- linear response on masonry structures, even for moderate loads, e.g. serviceability loads. Therefore, non-linear behaviour, being the most complete method of numerical analysis, appears as the most adequate approach to be used in numerical simulations of masonry structures. But, as stated before, its use depends on which objectives are required from the analysis. If the sought information can be attained using a simpler method, which turns out to be less expensive or more in agreement with the expertise of the analyst, then its use is advised.

Nonlinear finite element modelling can be an extremely useful and powerful approach in determining the behavioral response of complex concrete structures but extreme care is needed in the setting up of the models, in the verification of the model, in assessing the models capability to correctly identify critical behaviour and in the interpretation of results. Non-linear finite element analysis based on advanced constitutive models can be well used for the simulation of a real behaviour of reinforced concrete structures. Using the nonlinear finite element method can greatly contribute to improve

construction quality and safety performance of actual structures. **[25]**

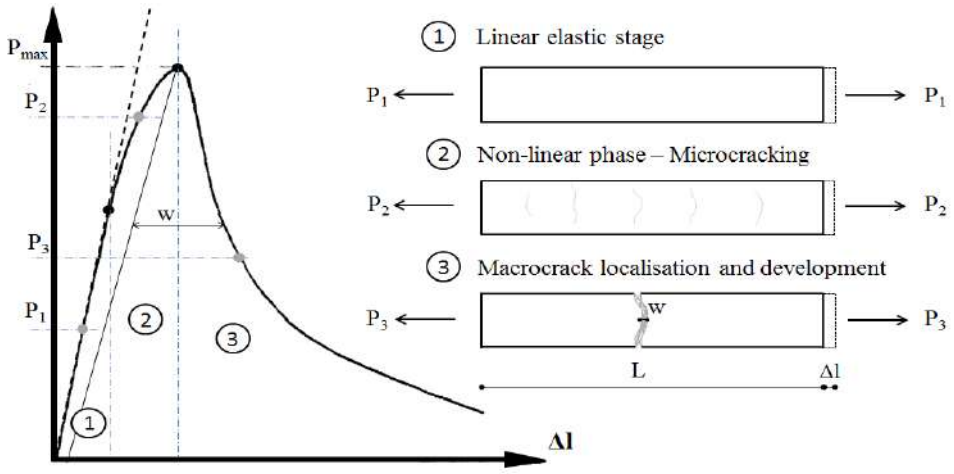


Fig I.13. plain concrete tensile response **[26]**

Modelling techniques for masonry structures

In the analysis of masonry structures, the existence of (mortar) joints is the major source of weakness and material non- linearity. Different levels of refinement have been used for the structural analysis. Depending on the degree of accuracy and the simplicity desired, the following modelling strategies can be used **[27]**, see also Figure I.14:

- Detailed micro-modelling: both units and mortar are discretized and modeled with continuum elements whereas the unit- mortar interface is represented by discontinuum elements.
- Simplified micro- modelling: expanded units are modeled with continuum elements, while the behaviour of the mortar joints and unit- mortar interface is lumped in discontinuum line interface elements.
- Macro- modelling: units, mortar joints and unit- mortar interface are smeared out in a homogeneous anisotropic continuum.

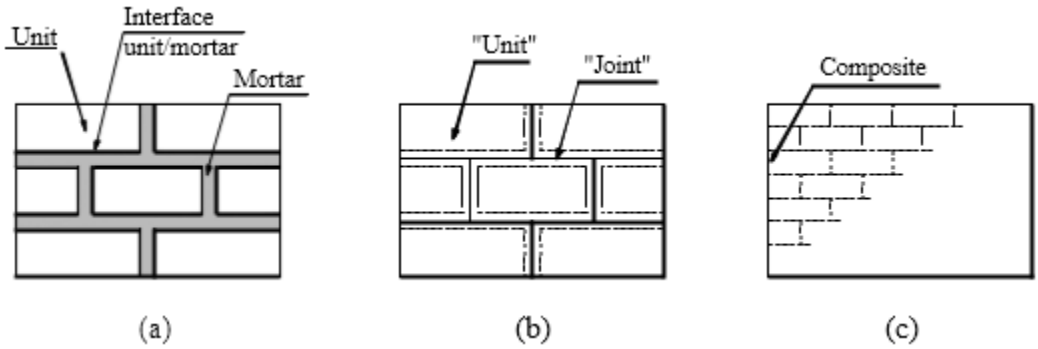


Fig I.14. Modelling strategies for masonry structures:(a) detailed micro-modelling;(b) simplified micro-modelling; (c) macro- modelling **[27]**

Following the description given above, it is clear that micro- and macro- modelling have different fields of application and one modelling strategy cannot be preferred over the other. The choice of the modelling strategy to be used, as well as the degree of refinement and accuracy, depends basically on the objectives of the study and the sought information. Moreover, this choice is constrained by the existing experimental data, required by numerical modelling.

In the following, the most important numerical modelling techniques concerning the analysis of masonry structures are presented. Particular emphasis is devoted to discontinued finite element modeling since this approach will be amply used in the analysis of masonry structures in Chapter 2.

I.4 MECHANICAL TESTS ON STONE AND BRICK MASONRY

The use of natural stones and bricks as structural building materials has been known since ancient times. Over the centuries, their use has been improved and they have been applied in different forms all over the world, varying with culture and time. In fact, it can be observed that most of our historical constructions utilize stone and brick, laid dry or bonded with mortar, as a key building material. Historical constructions are defined here as buildings constructed before the advent of Portland cement, at the end of the 19th century. Nowadays, the role of these materials has become less important due to the progressive adoption of other structural materials, particularly concrete and steel, and therefore, their use has been limited mainly to non-structural elements.

In order to understand the mechanical behaviour of a given material or structure, it is fundamental to perform experimental tests. In this way, it is possible to characterize the material behaviour from

the undamaged state through peak and also including the post-peak behaviour. But, if on one hand, it is almost impossible to carry out any kind of destructive test on elements belonging to masonry constructions, on the other hand, the possibility of performing non- destructive tests, such as flat jacks, dynamic identification tests, impact echo or ultrasonic tests, e.g. **[28]**, Numerical tools (ANSYS APDL in our case) can only give reliable results if adequate experimental data are available.

I.5 Numerical Simulations done by others

These numerical simulations were originally done by others **[29]** so the plan was to use a paper by Baronio, Binda, Lombardini (1997) **[30]**, which has already served as a source for mixing ratios of mortar samples prepared in a laboratory and there is also presented an experiment of a masonry structure with thick joints. The experiment should have been repeated by a numerical simulation and the parameters used in ATENA then fitted to results of the real experiment. However, after thorough study it was found useless, because they use fresh mortar. It is obvious that the monitored displacements were huge even without an external loading and stresses the structure was able to withstand were very small.

Because the cocciopesto is not a usual type of mortar, it was not possible to find another experiment dealing with cocciopesto, which would be suitable for comparison and fitting of results. Therefore, a new research of a literature began, in order to find a suitable type of experiment settings, no matter what mortar was used.

Numerical Model

It is a masonry wall with fixed foot and the top of the wall has enabled rotations and horizontal displacements only. Self-weight is not taken into account. There is a steel plate placed on the top, to distribute the stresses caused by a prescribed displacement u in x-direction. This simulates a laboratory setting with restricted push-over mode, when the tested walls are placed into a steel frame with hydraulic jacks. There were monitored two quantities. Number one is load monitored just next to the applied displacement and number two is displacement monitored in the right top corner of the wall. It is schematically illustrated in Figure I.15.

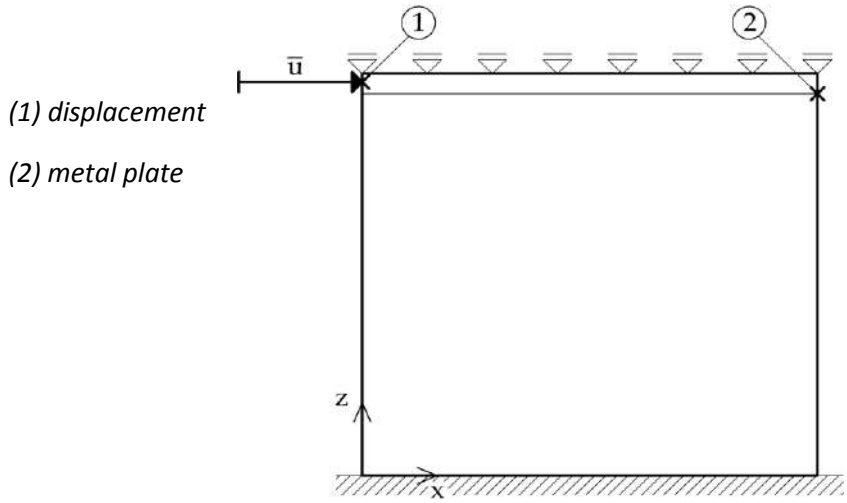


***Fig. I.15**: Shear wall scheme* **[29]**

It was planned to compare a response of structures with cocciopesto mortar and "standard" mortar. Nevertheless, to find all necessary mechanical properties of the standard mortar in one paper turned out to be impossible and find them in several papers is very disputable, because the individual mortars evaluated in different papers and laboratories are always different as well, depending very strongly on mix ratios, setting and hardening conditions, curing time etc. Therefore, such a procedure of obtaining mechanical properties would result in hybrid mortar with unreasonable characteristics. The sound method of comparing two mortars is to get own results from own testing. Unfortunately, our own samples of the cocciopesto mortar are still in molds and not ready for testing, as you can see in Figure I.16. **[31]**



Fig I.16. Samples of cocciopesto mortar in laboratory **[29]**

From the reasons stated above, the strategy was changed from comparing two mortars, to comparing one mortar with various mechanical properties and used on different types of walls, while observing trends rather than absolute peak or collapse values.

I.6.3 Setting of ATENA

There were carried out both analyses, 2D and 3D. 2D pre-processing was done in ATENA 2D version 3.2.0.0, while analysis and post-processing were done in ATENA 2D version 4.2.2.0. In a case of 3D, the pre-processing was done in ATENA 3D version 3.2.0 and analysis with post-processing in ATENA 3D version 4.2.5.3252.

Materials

There were used two different material models and three materials. Material model 3D nonlinear cementitious 2 was used for both, the cocciopesto mortar and the clay bricks in 2D and 3D analyses. All the material parameters, which are possible to set for the cocciopesto mortar, are shown in Table I.1. Only the parameters E, μ, fc and ft were set different from default values. It was done according to preliminary results of micromechanical homogenization by Nežerka (2011) **[32].**

Table I.1*. Material parameters of cocciopesto mortar*

Elastic modulus E [MPa]:	2200	Fail. surface eccentricity e [-]:	0,52
Poisson's ratio μ [-]:	0,202	Specific material weight ρ [kgm^{-3}]:	2300
Tensile strength f_t [MPa]:	0,7	Plastic strain at compressive strength ε_{cp} [-]:	-3,489E-4
Compressive strength f_c [MPa]:	-5,0	Coefficient of thermal expansion α [K^{-1}]:	1,2E-5
Specific fracture energy G_f [Nm^{-1}]:	19,55	Fixed crack model coefficient [-]:	1,0
Critical compressive displacement w_d [mm]:	-0,5	Multiplier for plastic flow direction β [-]:	0,0

The parameters for the clay brick appear in Table I.2. Again, only the parameters E, μ, fc and ft were changed. These were taken from paper by Brencich et al. [**33**].

***Table 1.2**. Material parameters of clay brick*

Elastic modulus E [MPa]:	2400	Fail. surface eccentricity e [-]:	0,52
Poisson's ratio μ [-]:	0,2	Specific material weight ρ [kgm^{-3}]:	2300
Tensile strength f_t [MPa]:	3,4	Plastic strain at compressive strength ε_{cp} [-]:	-7,045E-4
Compressive strength f_c [MPa]:	-18,7	Coefficient of thermal expansion α [K^{-1}]:	1,2E-5
Specific fracture energy G_f [Nm^{-1}]:	47,11	Fixed crack model coefficient [-]:	1,0
Critical compressive displacement w_d [mm]:	-0,5	Multiplier for plastic flow direction β [-]:	0,0

For the steel plate on the top of the wall, plane stress elastic isotropic material model was used for 2D analysis and 3D elastic isotropic for 3D analysis respectively. All material parameters, which are possible to change, are shown in Table I.3 and all of them were left as they were set by default.

***Table I.3.** Material parameters of steel plate* **[29]**

Elastic modulus E [GPa]:	210	Specific material weight ρ [kgm^{-3}]:	2300
Poisson's ratio μ [-]:	0,3	Coefficient of thermal expansion α [K^{-1}]:	1,2E-5

Solution Parameters

The objective is to trace the load-displacement curve up to the post-failure softening regime. It would be possible to prescribe loading in terms of forces and use the arc-length method, which automatically changes the sign of load increment once a peak is attained. Alternatively, displacement can be prescribed. Since displacement will keep on increasing even after the wall fails, either the Newton-Raphson method or arc-length method can be employed. Due to its better stability, the Newton-Raphson solution method was chosen. **[29]**

To speed up convergence of the solution, the full Newton-Raphson method with tangent stiffness updated in each iteration was employed. To automatically adjust the speed of analysis according to the non-linearity of the response, the line search method was utilized. All the parameters are summarized in Table I.4.

***Table I.4**. Summary of solution parameters*[29]

Solution method:	Newton-Raphson
Update stiffness:	Each iteration
Stiffness type:	Tangent
Iteration limit for step:	40
Error tolerances:	0,01
Line search:	on, with iterations

However, before the solution method was finally decided, comparison of the Newton-Raphson method and arc-length method was done, in order to be sure that the methods do not differ significantly in any phase of the loading. Because then it would be necessary to find the reason of the difference and maybe even to change the solution method. A graph showing the results of both methods is in Figure 1.17. As you can see, both methods are perfectly corresponding up to the peak and even in post-peak phase the correspondence is almost perfect. Since the NRM was less time demanding, the above made choice was just approved by this comparison.

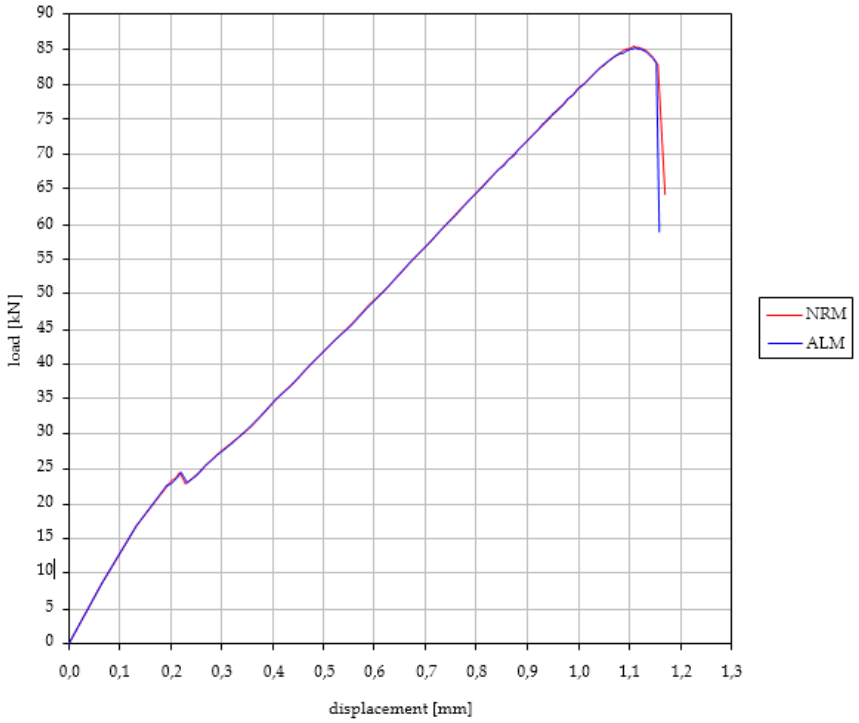


Fig. I.17. Newton-Raphson method vs. Arc-length method[29]

As mentioned in Section 4.2.3, for large or brittle beams, a snap-back behavior may occur, in which case both displacement and force increments change their sign upon failure. In such situation, the arc-length solution would be the only applicable method.

Meshing

The quadrilateral elements in 2D and the brick elements in 3D analyses were used, wherever it was possible. Since the wall was modeled as bricks and mortar joints separately, without any homogenization, the size of the elements varied from case to case. **[29]**

To know the importance of a fineness of meshing on the solution, comparative analyses were carried out. The result is depicted in Figure I.18. It is apparent that the curves are different in values but not so much different in shapes.

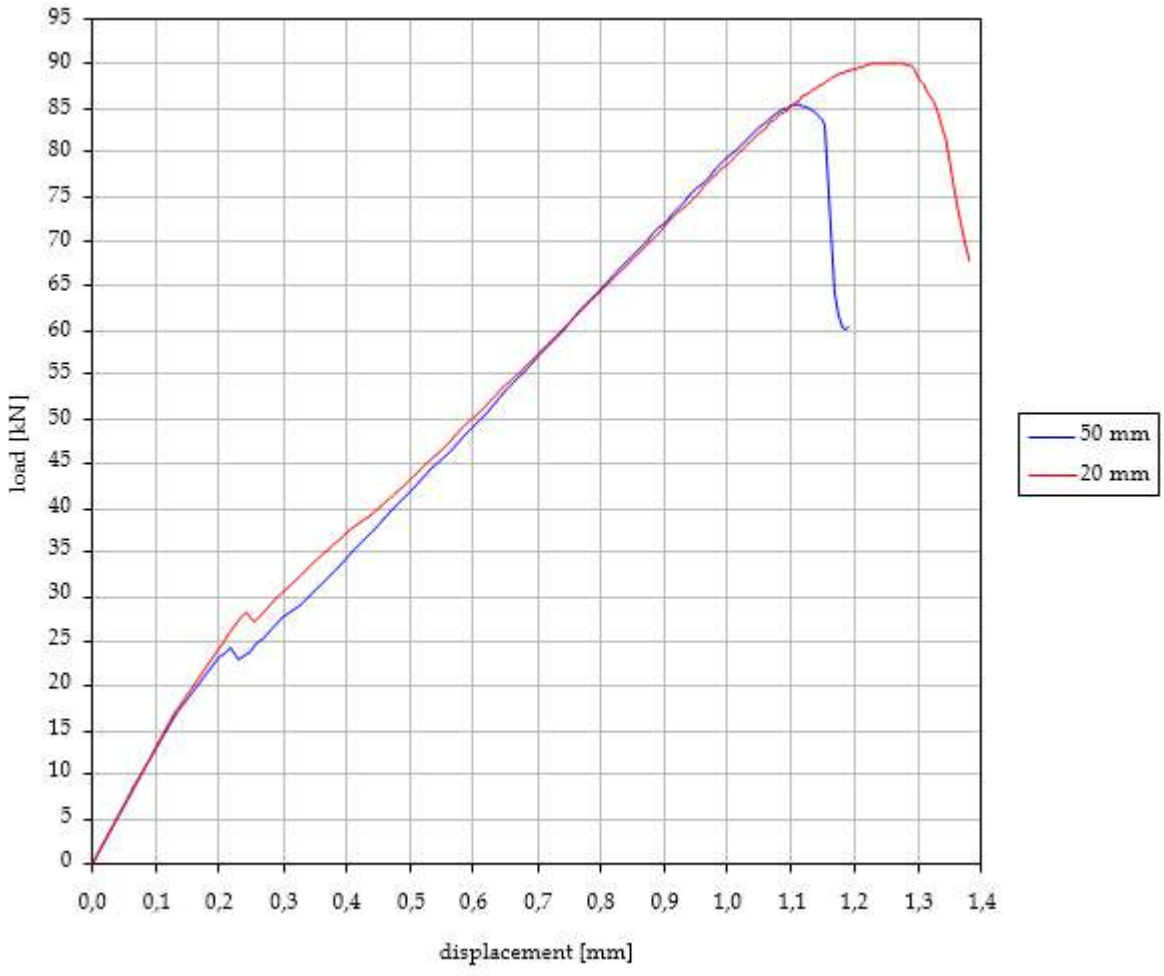


Fig. 1.18. Influence of fineness of meshing**[29]**

However, the finer meshing was extremely demanding on a computer and time. Executing more such analyses would have been unfeasible. In addition, as mentioned in Section 5.1, the aim is to observe trends rather than precise peak or collapse values. From these reasons, the absolute accuracy of the results is not essential and the less fine meshing was chosen for further analyses.

2D analysis vs. 3D analysis

Another important decision was, whether use 2D or 3D analysis. It is obvious that 2D analysis needs fewer elements and therefore it is much more time efficient than 3D analysis. Nevertheless, before the 2D analysis was adopted for its advantages, it was necessary to check a correspondence of these two analyses. For this comparison, a standard wall with 10 mm thick joints was chosen. The concrete dimensions of the wall and bricks will be discussed in the following sections. A graphical result of the comparison is shown in Figure 1.19. Apparently, in this case not only values differ, but also the shapes are quite different, especially in the peak zone. Generally, the 3D analysis is usually more realistic, but it was necessary to prove that this is also the case.

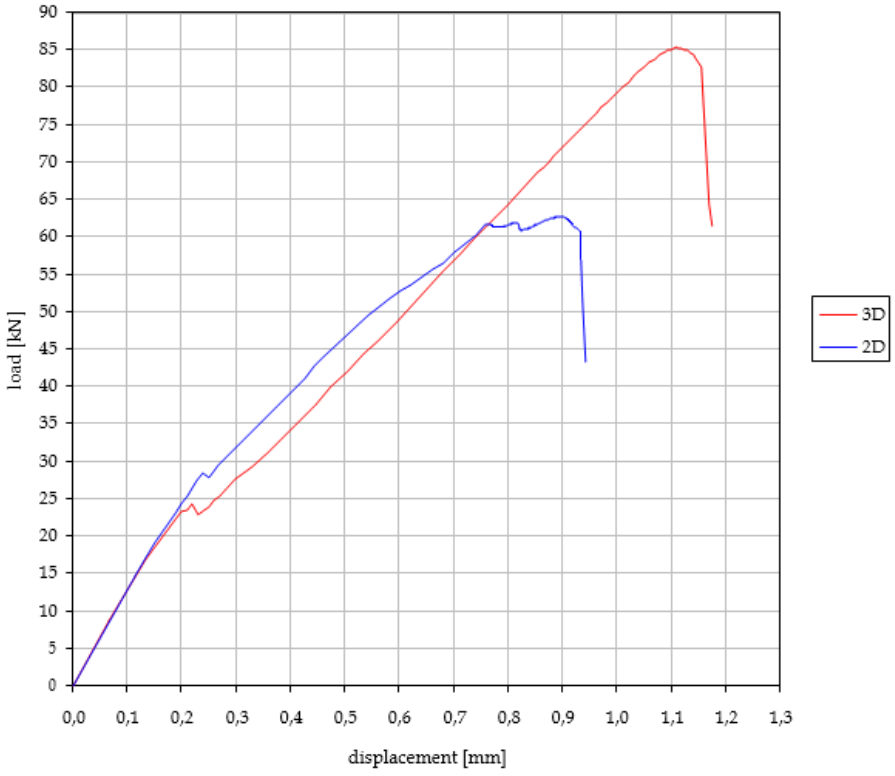


Fig. I.19. 2Danalysis vs. 3D analysis**[29]**

Pictures of the cracked walls were very helpful in this issue. As you can see in Figures I.20 and I.21, the distribution of cracks is in both cases very different. One would have naturally expected a crack pattern similar to Figure I.21, especially when taking into account the direction of maximum principal stress, respectively the direction of the tensile diagonal. Moreover, when this assumption was supported by Figure I.22 from an experiment made by Maheri et al. (2008) **[34]**, there were no doubts that the 3D analysis really gives more reasonable and realistic results. Therefore, all the following analyses are performed in 3D.

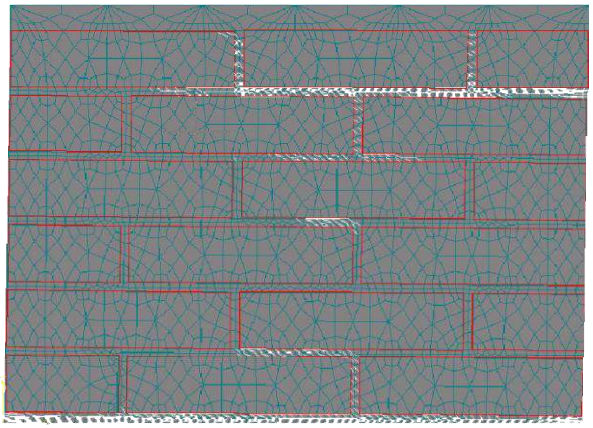


Fig. I.20. Crack pattern of 2D shear wall**[29]**

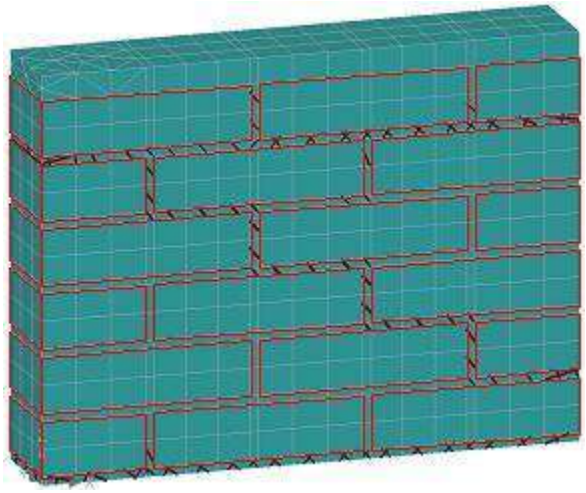


Fig. I.21. Crack pattern of 3D shear wall**[29]**



Fig. I.22. Crack pattern of experimental shear wall **[29]**

Influence of Geometry

In this section, an influence of different wall geometries on a structural behavior is examined. There are used the clay bricks with properties describe and they are so-called small format full bricks with dimensions 250 x 120 x 65 mm. The same or similar type of bricks was used in several papers, e.g. Brasile et al. (2007) or Brencich et al. [**33**]. This type of bricks was used in all analyses in this thesis and there are always six rows of the bricks, with two and half brick in each row.

The properties of the used cocciopesto mortar are described in and they do not change throughout the current section.

Thickness of Joints

To find out the influence of the thickness of the joints is very interesting task. It was investigated on two different walls.

The first wall has standard 10 mm thick cocciopesto mortar joints. The geometry of this wall, with all important dimensions, is depicted in Figure I.23.

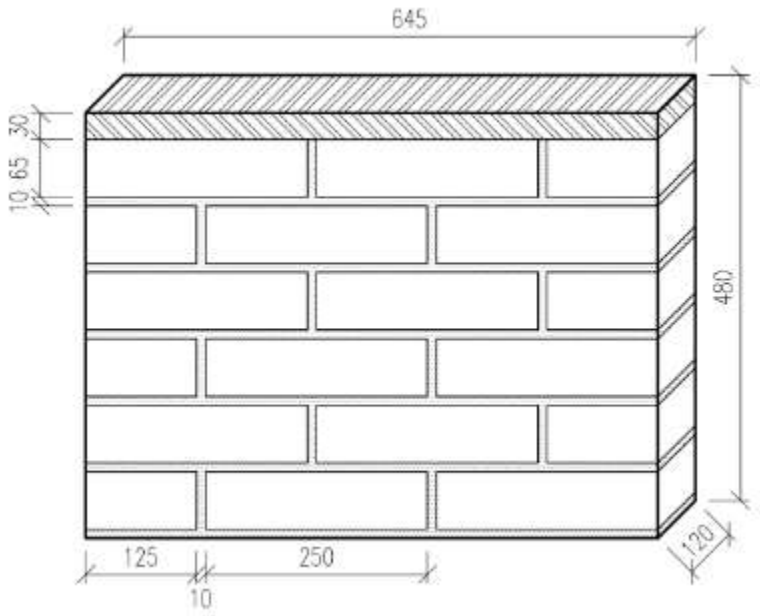


Fig. I.23. Shear wall with 10 mm thick joints **[29]**

The second wall has 45 thick joints, made of cocciopesto mortar. This thickness was chosen according to Baronio, Binda, Lombardini (1997) **[30]**, who studied the coociopesto mortar coming from the remaining of the original walls of St. Michele in Africisco. The geometry and dimension are shown in Figure 1.24. The wall may seem little bit ridiculous, in comparison with the first wall. However, you can see that the thickness of the bricks is still bigger than thickness of the joints, and as you know it was no exception in ancient times, if the joints were even thicker than the bricks.

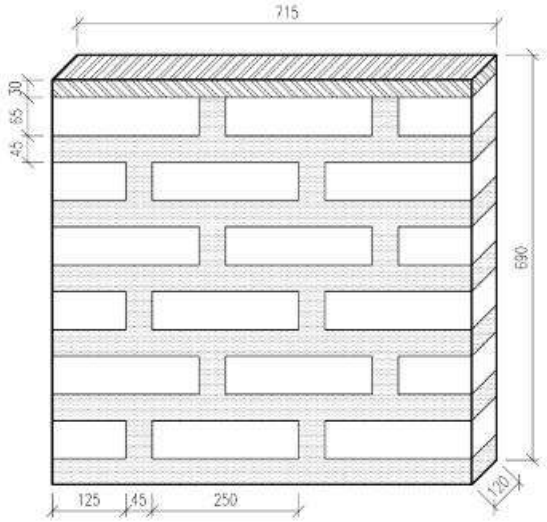


Fig. I.24. Shear wall with 45 mm thick joints **[29]**

Both walls were subjected to the same prescribed displacements and deformed a little beyond the peak values. Again, this loading procedure was done in all performed analyses. The load-displacement graphs of both analyses are depicted in and coordinates of peak values are in Table I.5.

***Table I.5**. Summary of peak values for different thicknesses of joints* **[29]**

Thickness of joints [mm]	Displacement [mm]	Load [kN]
10	1,11	85,38
45	1,74	83,85

We can observe several interesting facts in the graphs. For example, note the small discontinuities of the curves, around the loading of 20 kN. These are caused by a sudden propagation of cracks in the right top horizontal joint, because the joint tries to "open", as the right top corner of the wall is being pushed aside.

Another interesting fact is that the wall with 45 mm thick joints is apparently more compliant than the wall with 10 mm thick joints, but practically without any loss of resistance. This is rather remarkable. This is due to a bigger content of the "weak" member, i.e. mortar, in the wall, which makes the wall with 45 mm thick joints less stiff. The higher compliance is advantageous in situations, when e.g. differential settlement or other non-force loading can occur. Most importantly, the compliant structures are also able to resist dynamic effects in a bigger extent than the stiff ones. This can be one of the reasons, why the ancient structures with thick joints were able to withstand a high seismicity for many hundreds of years, as for example Hagia Sofia in Istanbul. **[29]**

You have also probably noticed the shape difference of the peak zones of both walls. It is smooth in the case of the 10 mm thick joints and very sharp in the case of the 45 mm thick joints. Neither different solution method nor finer meshing changed the sharp character of 45 mm joints curve. The explanation is in different reasons of the collapse. The internal strain energy is calculated as a product of stress and strain. Since the wall with 10 mm thick joints reaches almost the same loading as the wall with 45 mm thick joints, but smaller displacement, it also attains lower internal strain energy. Therefore, the wall with 10 mm joints fails due to exhausting its load-bearing capacity, which is quite gradual, whereas the wall with 45 mm thick joints collapses due to reaching its fracture energy and this is manifested by a sudden failure. What happens if the fracture energy is increased will be shown.

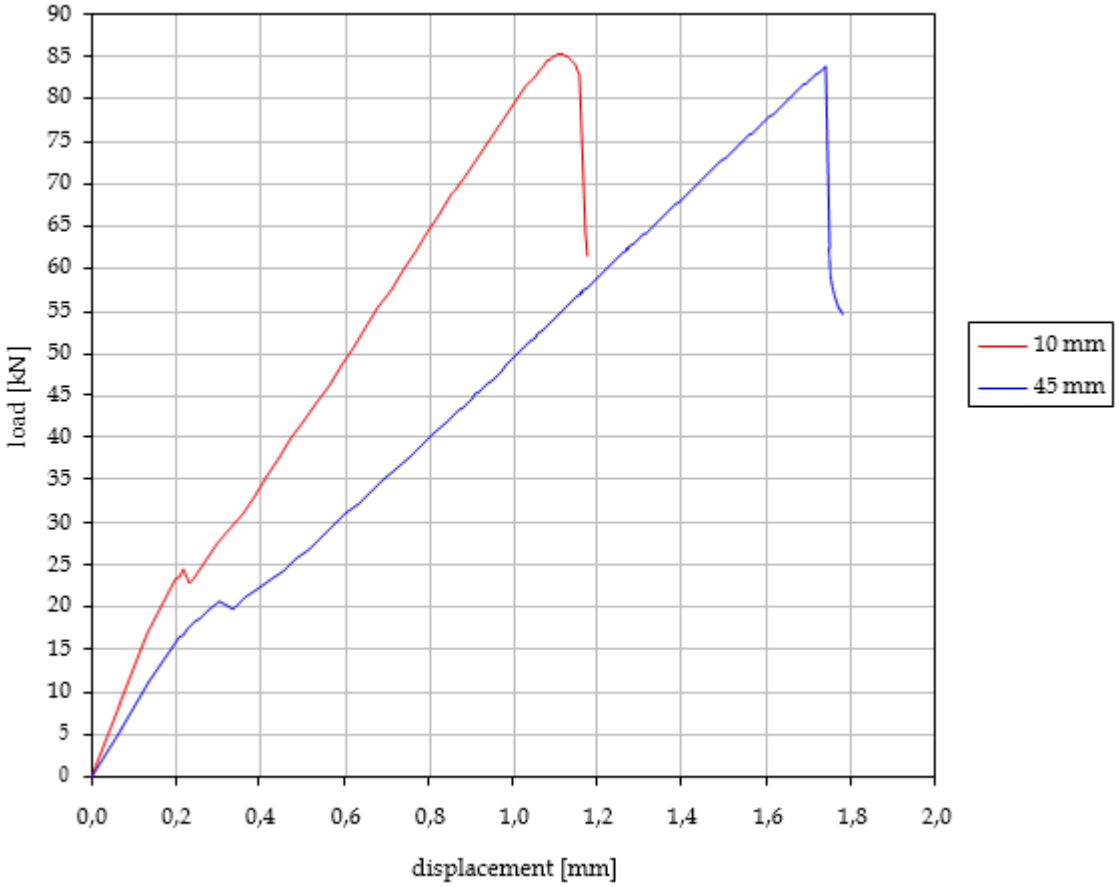
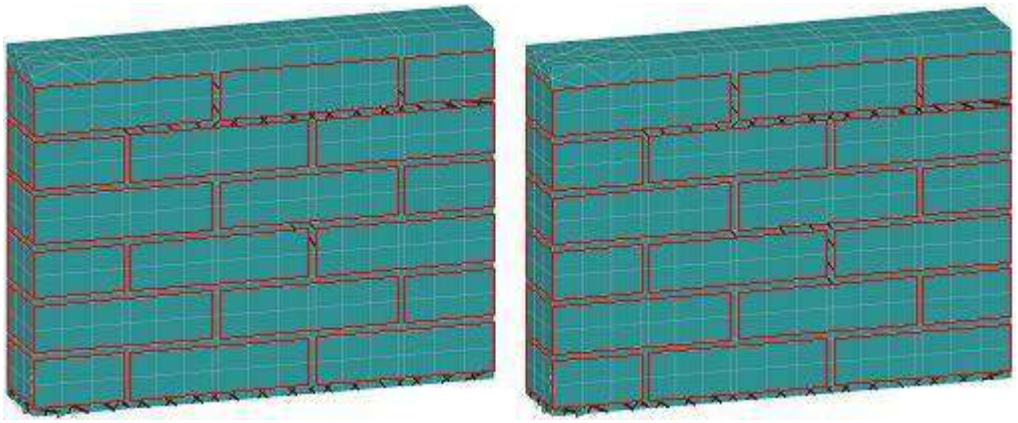


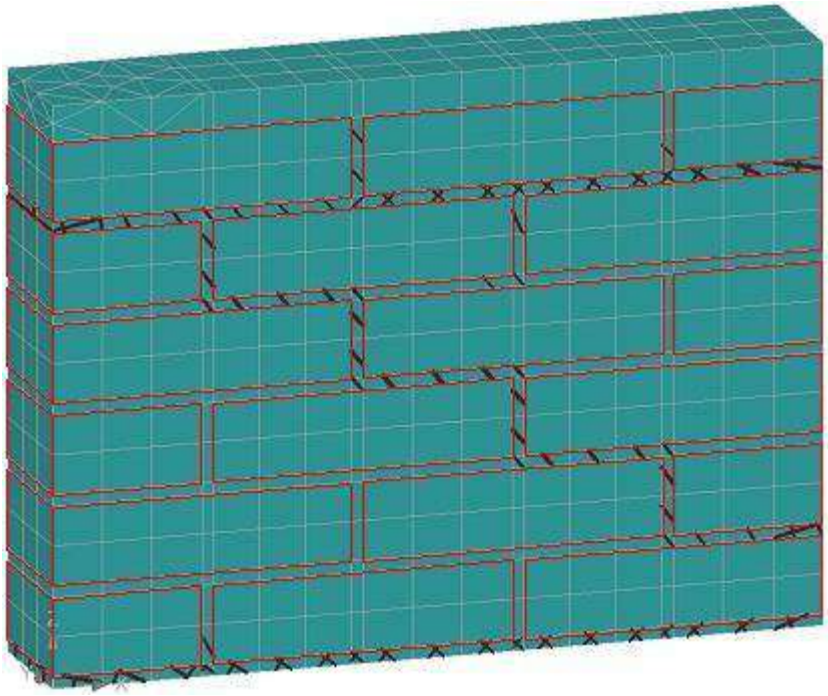
Fig. I.25. Shear walls with 10 mm thick joints and with 45 mm thick joints**[29]**

The difference in the behavior of the particular walls in the vicinity of the peak is well illustrated in Figures I.25 and I.26.

As you can see, the cracking is in the case of the wall with 10 mm thick joints very gradual. The state of the crack distribution 0,015 mm before peak is almost the same as in the peak itself and it necessary to go 0,06 mm beyond the peak to reach the cracking of a diagonal.



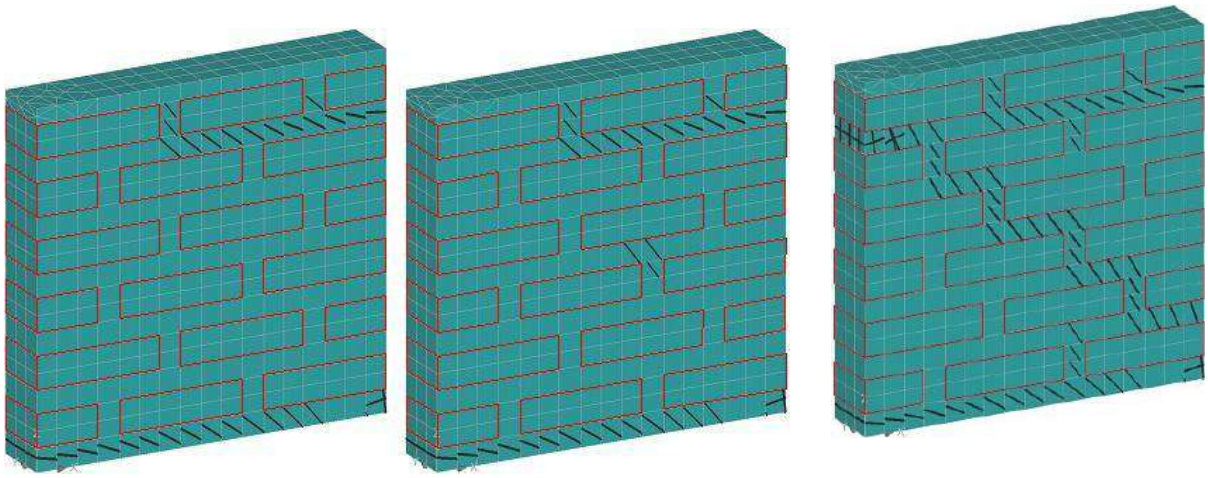
(a) 0,015 mm before peak *(b) peak*



(c) 0,06 mm beyond peak

Fig. I.26. Behavior of wall with 10 mm thick joints in vicinity of peak **[29]**

On the contrary, in the case of 45 mm joints, a small change on the diagonal is visible even between 0,015 mm before peak and peak itself, and the diagonal completely cracks 0,01 mm beyond peak only. The crack evolution is really fast beyond the peak.



(a) 0,015 mm before peak *(b) peak* *(c) 0,01 mm beyond peak*

Fig.I.27. Behavior of wall with 45 mm thick joints in vicinity of peak **[29]**

I.6.10 Head Joints

An interesting idea is to observe the influence of head joints (the vertical ones) on load-bearing capacity of the wall. This strategy was inspired by Maheri et al. (2008) **[34]**.

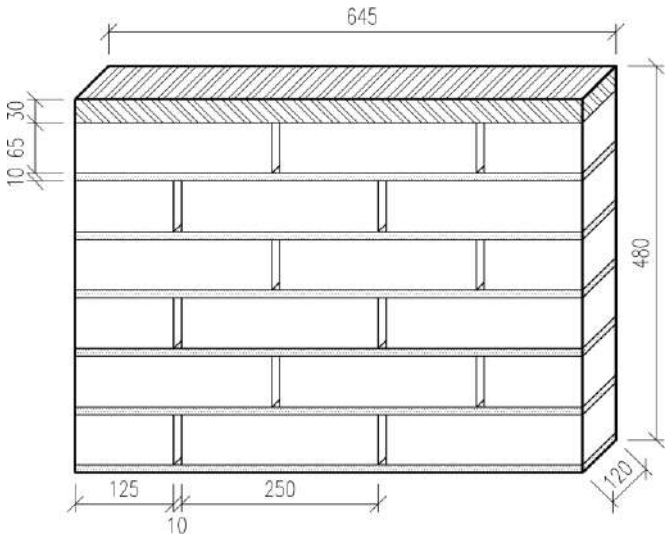
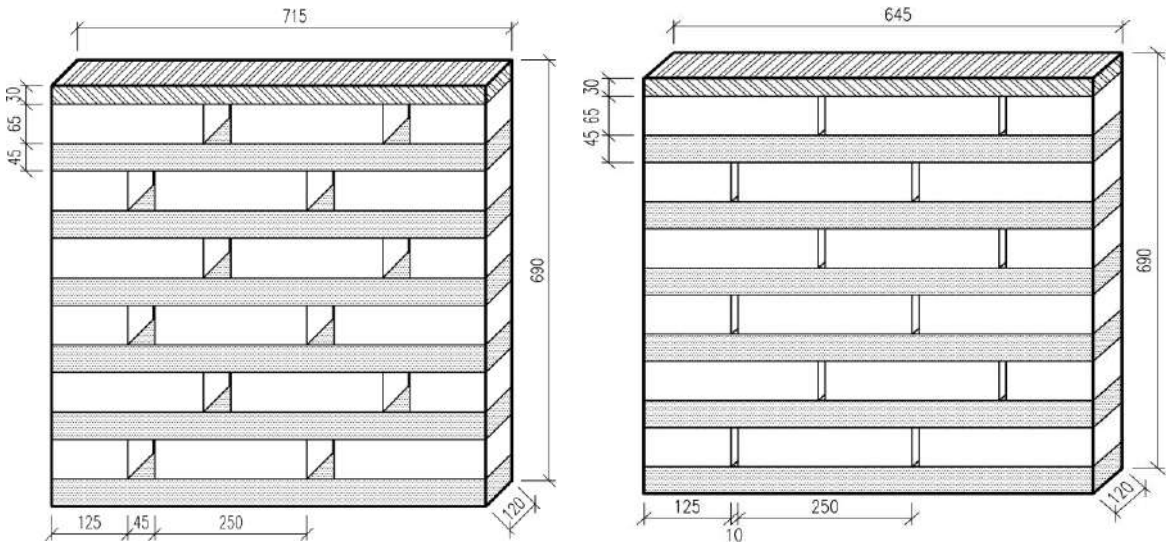


Fig. I.28. Shear wall with 10 mm thick joints without head joints**[29]**

This strategy combined with thick joints could create a very compliant structure. Therefore, the wall with 10 mm thick joints without the head joints was modeled, see Figure 1.28, to compare the

properties of joints



(a) without 45 mm thick head joints (b) without 10 mm thick

Fig. I.29. Shear walls with 45 mm thick joints without head joints **[29]**

The wall with 45 mm thick joints without head joints was created as well. However, omission of 45 mm thick head joints looks very strange, as you can see in Figure I.29 (a), and it probably would not be practical in-situ either. Therefore, a hybrid walls with 45 mm thick bed joints and only 10 mm thick head joints, which were omitted, was modeled. It is illustrated in Figure I.29 (b).

The materials, bricks and loading procedure are the same as described in section 5.3. A comparison of the walls with 10 mm thick bed joints and with/without the head joints is in the Figure 1.30. Values of the peaks are shown in Table I.6.

Table I.6. Peak values for walls with 10 mm thick bed joints and with/without head joints **[29]**

Head joints	Displacement [mm]	Load [kN]
yes	1,11	85,38
no	0,95	59,79

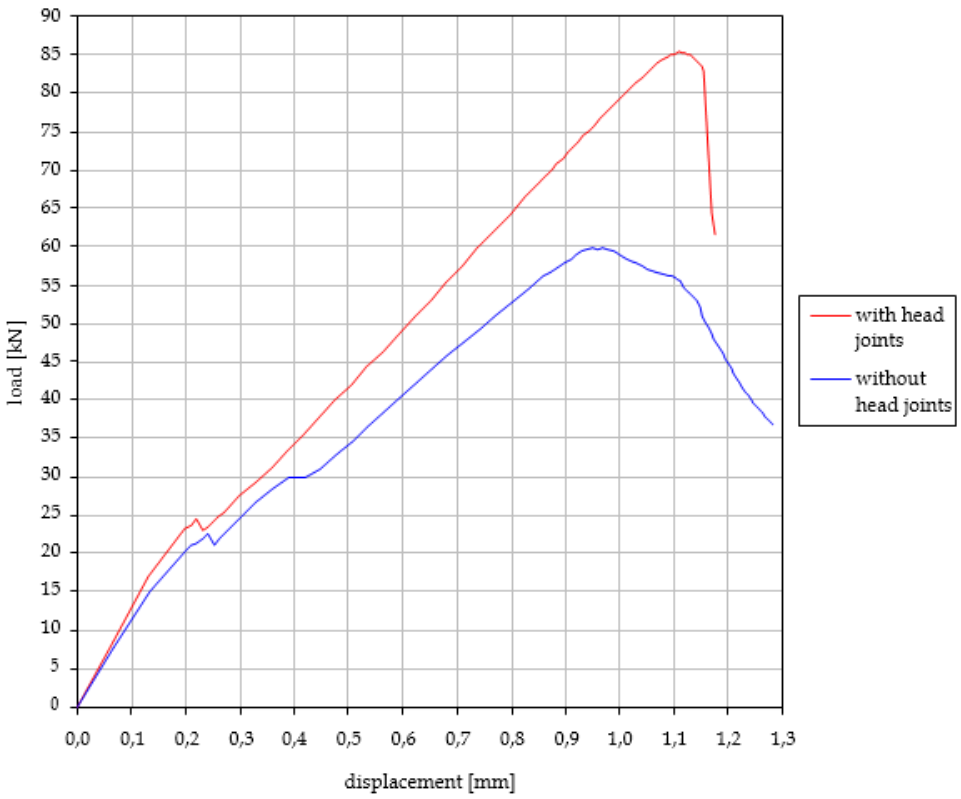


Fig. I.30. Shear walls with 10 mm thick bed joints and with/without head joints **[29]**

By mere glancing at the graph, we can say that omitting the head joints actually brought no benefits. The structure is more compliant and ductile, but the important properties, such limit deformation and load-bearing capacity, decreased significantly. The cracked wall just beyond the peak is in Figure I.31.

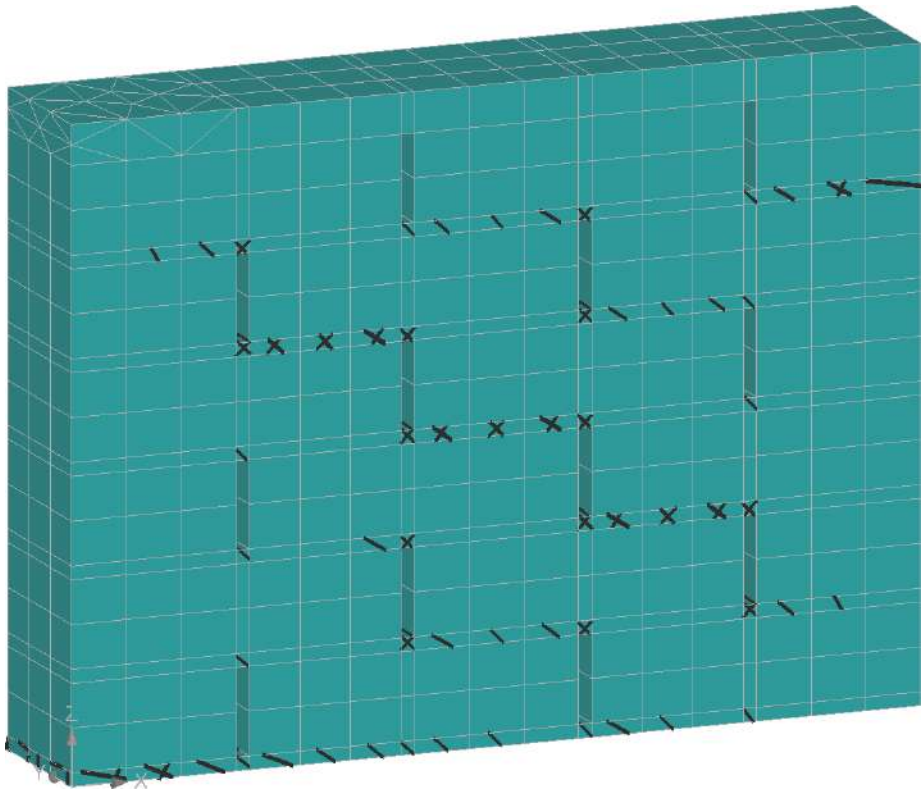


***Fig. 1.31**. Crack pattern of wall with 10 mm thick bed joints without head joints*

Results of the analyses of the walls with 45 mm thick bed joints are depicted in Figure I.32 As already mentioned, two types of the head joints (i.e. 10 mm and 45 mm) were omitted. In this case, the results of walls without the head joints are not worse so evidently. The coordinates of the peaks of the individual walls appear in Table I.7. It is obvious that if we want to omit any head joints, then definitely the thinner ones. **[29]**

Table I.7. Peak values for walls with 45 mm thick bed joints and with/without head joints **[29]**

Head joints	Displacement [mm]	Load [kN]
yes	1,74	83,85
no - 10 mm	2,40	65,17
no - 45 mm	1,98	57,45

The omission of the 45 mm thick head joints meant growth of limit displacement, but resistance of the

structure decreased considerably. The wall without 10 mm thick head joints shows similar properties, but in a way that is more favorable, because limit displacement increased even more than in the case of omitted 45 mm joints, and the wall is also able to withstand higher load, but still lower than in the case of the full joints. The crack distribution of both cases is shown in Figure I.33.

In summary, omitting the head joints in the case of the wall with thin joints has no positive effect. However, in the case of the wall with thick joints, the omission of the thin head joints can be helpful. If we need a structure that is more compliant and, at the same time, we know that load-bearing capacity of such a weakened structure is still high enough, then the wall with 45 mm thick bed joints and without 10 mm head joints is a wise choice.

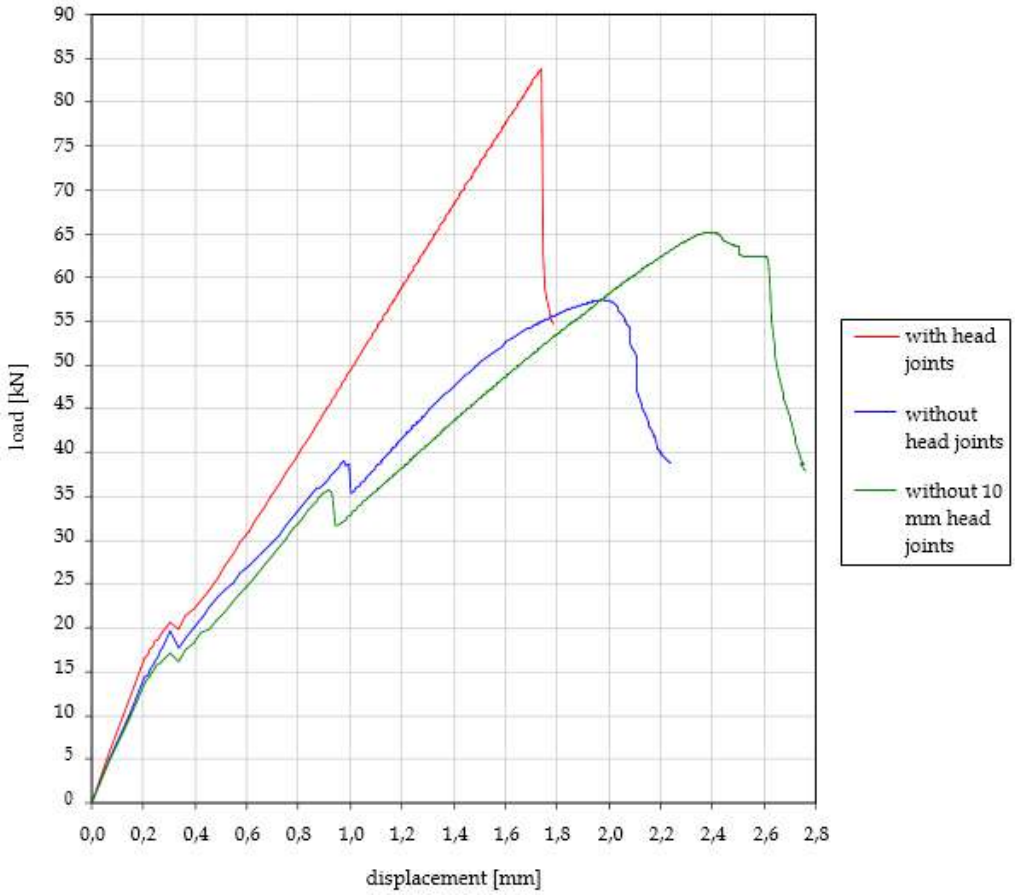
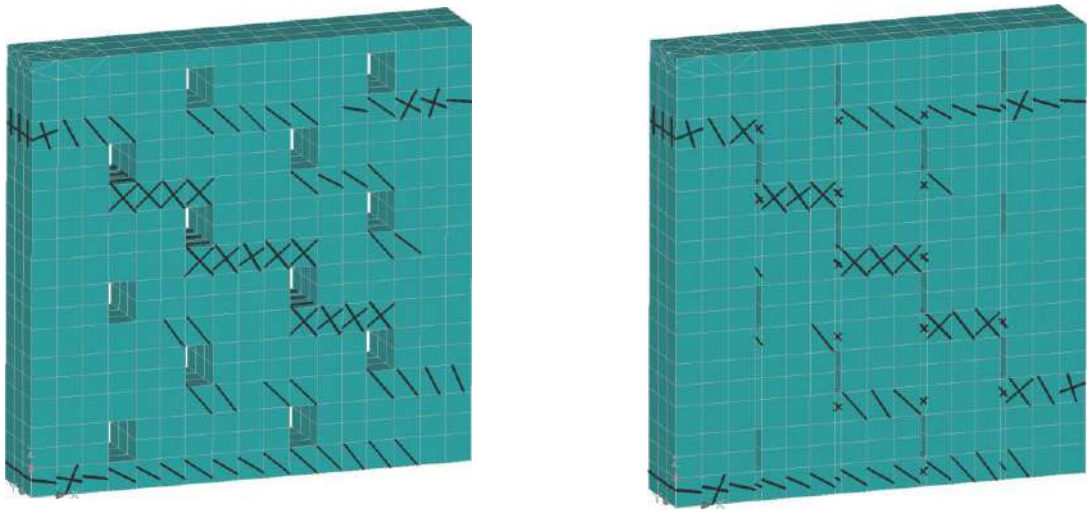


***Fig. I.32**. Shear walls with 45 mm thick bed joints and with/without head joints* **[29]**



(a) without 45 mm thick head joints *(b) without 10 mm thick head joints*

Fig. I.33. Crack pattern of wall with 45 mm thick bed joints without head joints **[29]**

I.6 Influence of Material Properties

In this section, an impact of different material properties on behavior of the walls is investigated. Now, the walls have always the same dimensions, i.e. all the walls have 45 mm thick joints and no joints are omitted, as shown in Figure I.34, and it is not changed all through the section.

The same bricks with the same properties as in previous section are used, but properties of the cocciopesto mortar are changed from case to case, as described next.

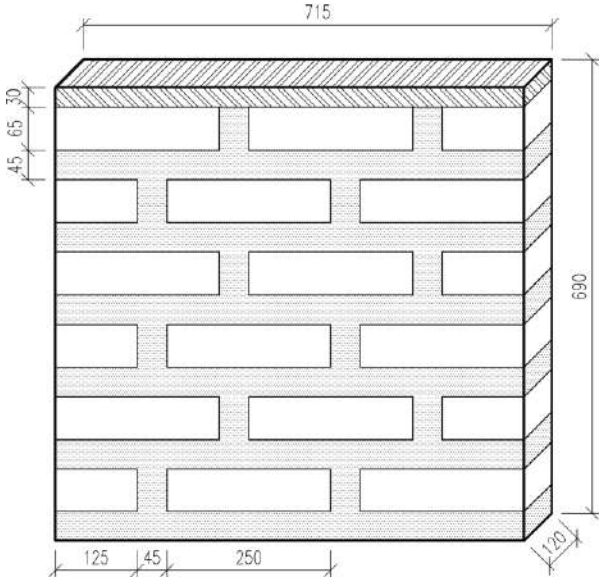


Fig. I.34. Shear wall with 45 mm thick joints **[29]**

Young's Modulus

Default value of the modulus is 2200 MPa. This value was being gradually lowered to 2000, 1800, 1600 and finally to 1400 MPa. To better see the trend of the response of the wall with different moduli, the value 3000 MPa was added.

Curves of all the analyses are plotted in Figure 1.35. Apparently, the shapes of the curves are absolutely the same. Just inclinations are different, but it is not surprising, if we take into account that the Young's modulus determines the angle between the horizontal axis and the elastic curve. However, also the peak values change. The summary of the peak coordinates, in dependence on the Young's modulus, is in the Table 1.8.

The tendency is clear. With decreasing elastic modulus, the limit displacement increases, while load-bearing capacity decreases. It can be interpreted by means of the internal strain energy again. The higher is the Young's modulus, the faster the curve reaches higher values of loading. If the product of stress and strain should be kept constant, the limit displacement must be inevitably lower.Of course, there are small deviations not matching the explanation, especially in the case of the values of moduli 2200 MPa and 2000 MPa, where the maximum loads differ, whereas the limit displacements are the same. Nevertheless, the difference of their load-displacement products is just 4%, which is not significant and can be caused by many irrelevant factors. Therefore, it is negligible. Figures of the cracked walls are very similar for all moduli, E=2200 MPa is shown.

Table I.8. Summary of peak values for different Young's modulis **[29]**

Young's modulus E [MPa]	Displacement [mm]	Load [kN]
3000	1,61	88,89
2200	1,74	83,85
2000	1,74	80,47
1800	1,75	76,86
1600	1,78	73,63
1400	1,82	70,05

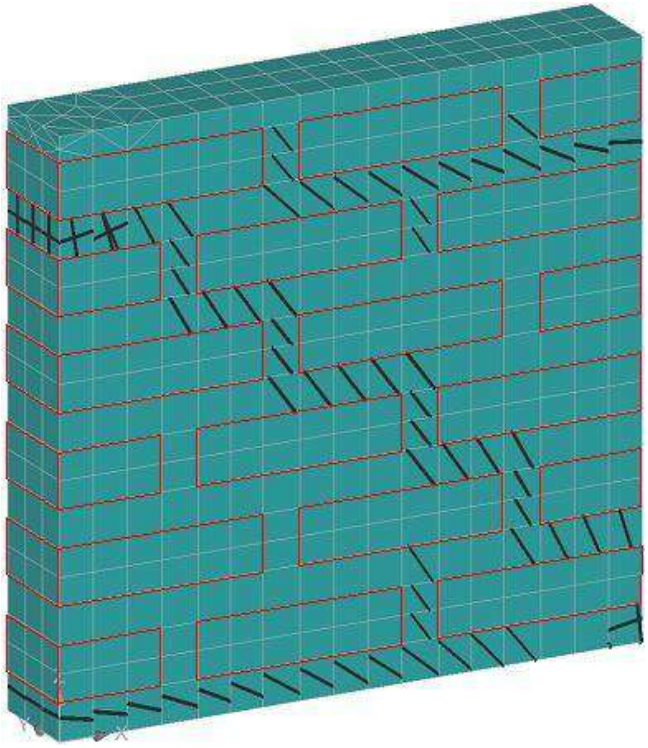


Fig. I.35. Crack pattern of wall with 45 mm thick joints and Young's modulus 2200 MPa **[29]**

Fracture Energy

It was discussed in Section 5.3.1 that the sharp peak of the wall with 45 mm thick joints is caused by reaching of the fracture energy, which did not allow the wall to exhaust its load-bearing capacity. On the contrary, peak of the wall with 10 mm thick joints was rounded, due to gradual cracking, because the strength was exceeded. This explanation can be now verified by changing values of the fracture energy.

Default value of the fracture energy is 19,55 Jm-2. It was then increased 5 times and 10 times and also decreased 5 times and 10 times.

Graphs of the analyses are plotted in Figure 1.36. As expected, the shape of the peak really changed. When the fracture energy was increased, either 5 or 10 times, it became so high that the limit of a load-bearing capacity was reached sooner than the limit of fracture energy, causing a gradual cracking of the wall. The fact that the peak stays sharp, if the fracture energy is either 5 or 10 times lowered, only confirms the idea of the different reasons of collapse. **[29]**

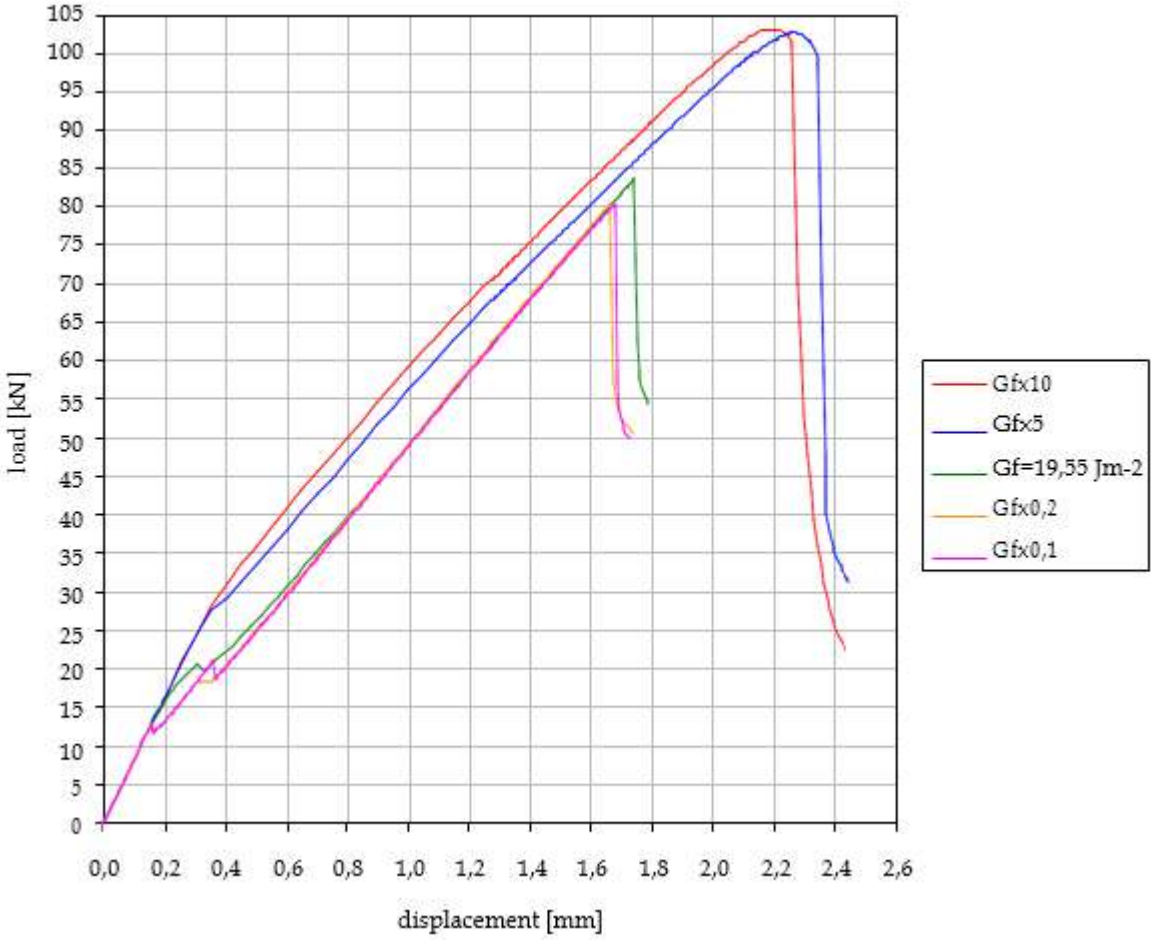


Fig. 1.36. Shear walls with different values of fracture energy **[29]**

The values of the individual peaks are gathered in Table 1.9. Both the limit displacement and limit load increased quite significantly. It actually shows where the material strength limits of the structure are, if it is not limited by the fracture energy. After first glance, it may seem strange that limit displacement of Gfx10 is lower than for Gfx5, but it can be easily explained. There is a break on the Gfx5 curve in an initial phase of loading, approximately at 28 kN. It is caused by first cracks, but the Gfx10 curve is smooth in this area. It is clear, because in the case of Gfx10, the energy necessary for first cracks was so high that it was not reached. As a result of this difference, the Gfx10 curve is, for the most of the time, higher than the Gfx5 curve. Nevertheless, if the areas below the graphs should be equal, then the value of the limit displacement of the Gfx10 curve must be lower. **[29]**

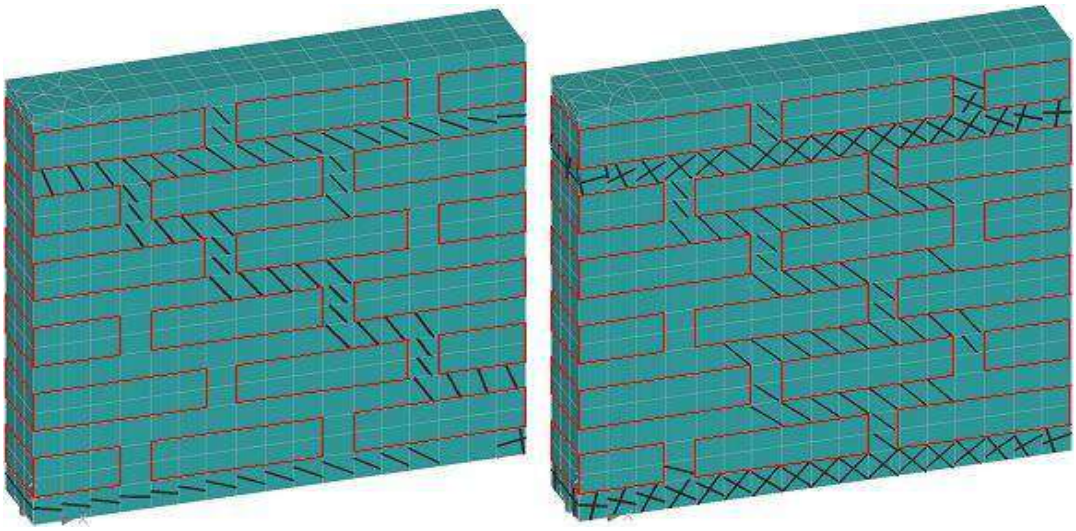
If the value of the fracture energy is lowered, the curve develops in the same manner, as in the case of the default fracture energy, also the shape of the peak is still sharp, just the collapse comes sooner. Further lowering of the fracture energy plays a negligible role, as you can see

from both graphs and table.

***Table 1.9**. Summary of peak values for different fracture energies* **[29]**

Fracture energy G_f [Jm^{-2}]	Displacement [mm]	Load [kN]
G_fx10	2,19	103,30
G_fx5	2,27	102,80
G_f=19,55	1,74	83,85
G_fx0,2	1,66	80,62
G_fx0,1	1,67	80,60

Crack patterns are relatively different for each value of the fracture energy. Therefore, there are depicted two representatives of extreme values, i.e. Gfx0,1 and Gfx10 in Figure 1.37. We can see that the cracks are really distributed differently. In the case of Gfx0,1 the diagonal is obviously decisive.



(a) fracture energy G_fx 0,1 *(b) fracture energy G_f x 10*

***Fig. 1.37**. Crack pattern of wall with 45 mm thick joints and different fracture energies* **[29]**

Tensile Strength

Since materials like concrete or mortar are known for their low tensile strengths, it is possible to expect that changes in the strength will have a certain effect on the overall structural behavior. The default value

is 0,7 MPa. It was then increased to 0,9 and 1,1 MPa and also decreased to 0,5 and 0,3 MPa.

Results of the analyses are plotted in Figure 1.38. All the curves have very similar shape with the same inclination and only the peak values differ. However, we can see that the peak values change considerably, as the tensile strength changes. By increasing the default value about 0,4 MPa only, the peak moved higher and further, in the coordinate axes, than in any other case of material property or geometry change, and this is also similarly valid vice versa. If the default value is lowered about 0,4 MPa only, the limit properties of the wall are very unfavorable.

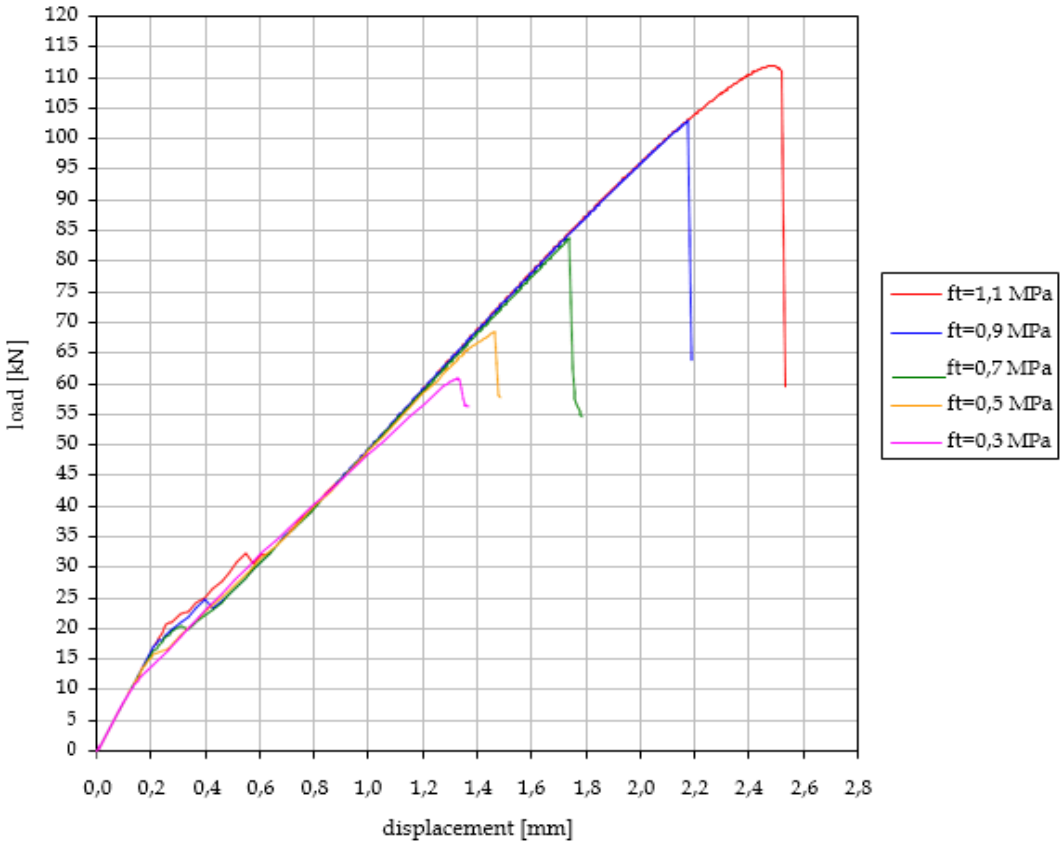


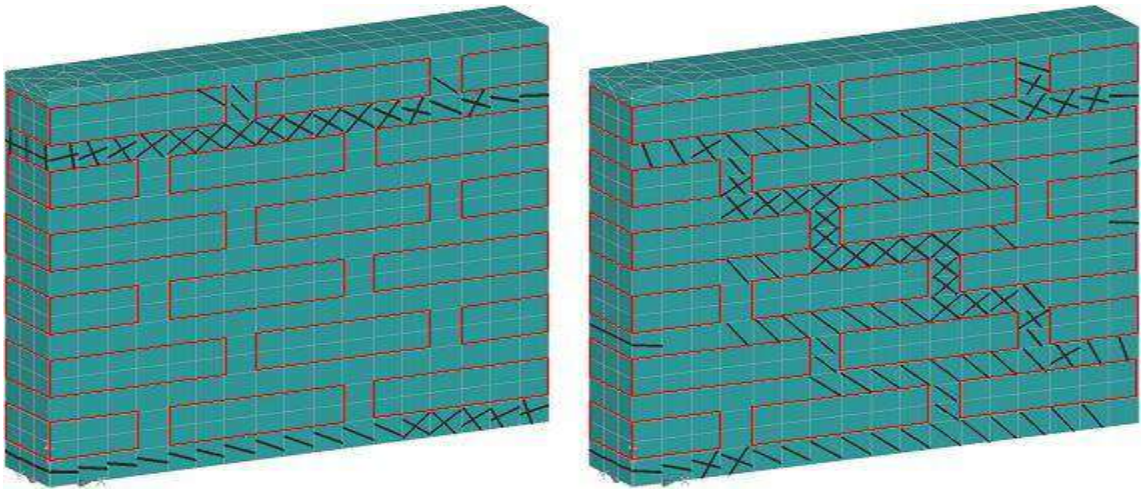
Fig. 1.38. Shear walls with different values of tensile strength **[29]**

Table I.10 illustrates the changes of the peak values by concrete numbers. From this, a conclusion can be drawn that the tensile strength influences the behavior very significantly.

Table I.10. Summary of peak values for different tensile strengths **[29]**

Tensile strength f_t [MPa]	Displacement [mm]	Load [kN]
1,1	2,49	111,90
0,9	2,17	102,90
0,7	1,74	83,85
0,5	1,46	68,48
0,3	1,32	60,90

Crack patterns also change together with the change of the tensile strength. In the case of a high tensile strength (i.e. 1,1 MPa), the collapse comes due to severe cracking of the two most exposed joints. As the tensile strength of the mortar is high, even a crack in a brick in the left top corner appears, as you can see in Figure I.39 (a). When a low value of the tensile strength (i.e. 0,3 MPa) is set, the wall shows many cracks spread through the joints, because even small tension is enough to initiate cracking. This is illustrated in Figure I.39 (b).



(a) tensile strength 1,1 MPa *(b) tensile strength 0,3 MPa*

Fig. 1.39. Crack pattern of wall with 45 mm thick joints and different tensile strengths **[29]**

Compressive Strength

It is expected that the compressive strength will not influence the response of the wall in such extent as the tensile strength. The default compressive strength is 5 MPa, which was lowered to 3 MPa and then

increased to 7, 9, and 11 MPa for next analyses.

Graphs of the analyses are depicted in Figure I.40. The effect of the changed strengths is even lower than the expectations. We can see that all the curves, excepting 3 MPa, are extremely similar, almost identical.

This fact is just confirmed by Table I.11, where the similarity of the peak values can be easily compared. **[29]**

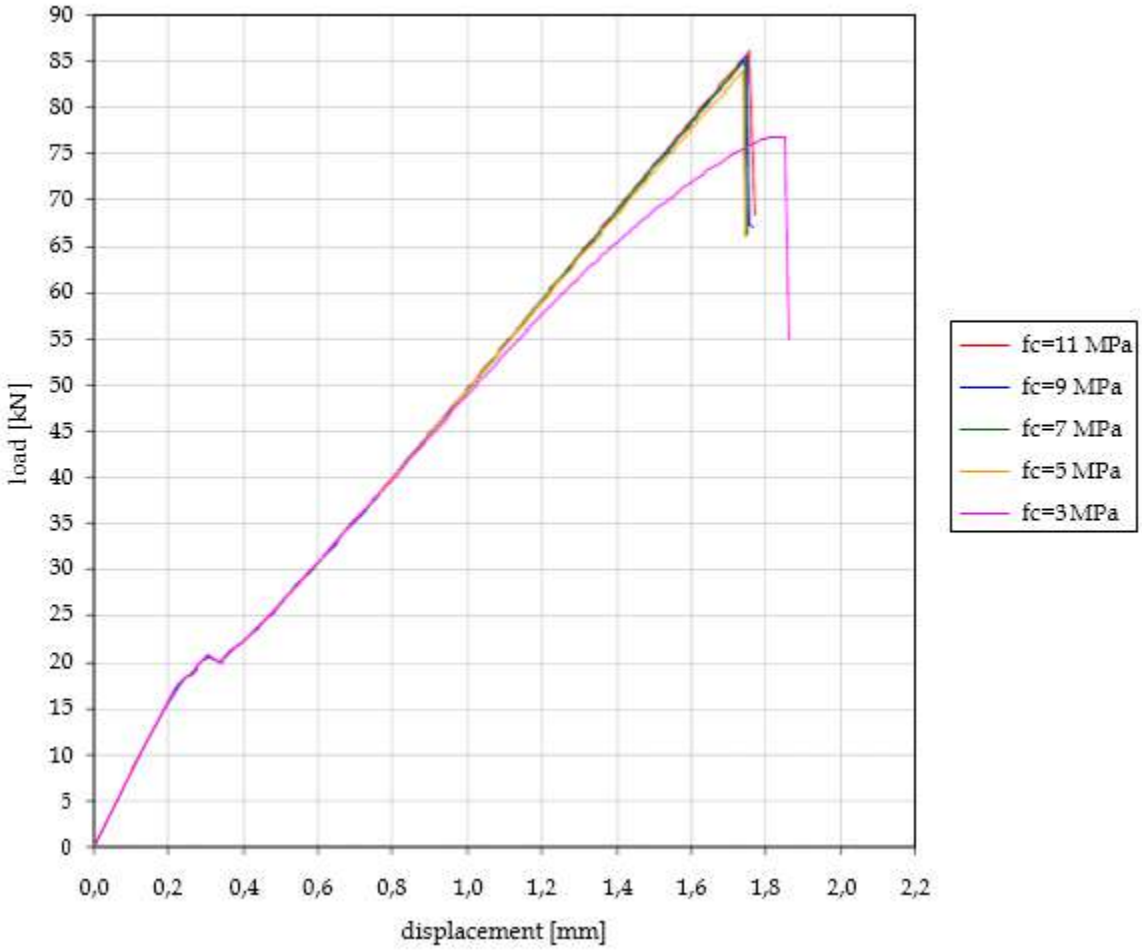


Fig. 1.40. Shear walls with different values of compressive strength **[29]**

When the compressive strength is equal to 3 MPa, the mortar is weak in compression and therefore even a relatively low compression causes a crushing of the mortar. It makes the wall more compliant, which is illustrated by a slightly different shape of the corresponding curve.

Table 1.11. Summary of peak values for different compressive strengths **[29]**

Tensile strength f_c [MPa]	Displacement [mm]	Load [kN]
11	1,76	86,10
9	1,75	85,50
7	1,74	85,02
5	1,74	83,85
3	1,70	76,85

Crack patterns are very similar for all values of the compressive strengths, therefore just one representative Figure 5.28 for fc=5 MPa is shown.

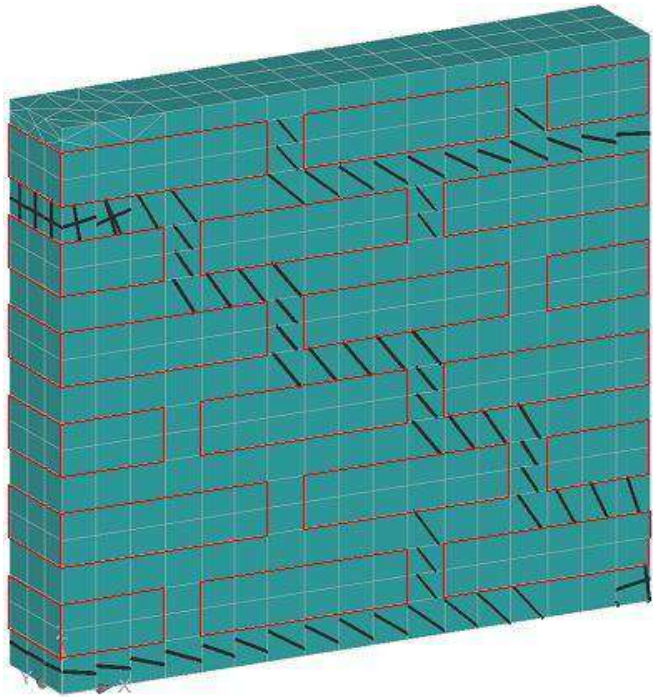


Fig. I.41. Crack pattern of wall with 45 mm thick joints and compressive strength 5 MPa **[29]**

Chapter 2 :

SIMULATION

II.1 Materials and tests

II.1.1 Introduction

This chapter is interested in the simulation so it will introduce the plan of work which will contain 8 tests using ANSYS APDL

II.1.2- Materials:

The testing process will be with two (2) different materials:

- Brick:

All the parameters of these materials are fixed in all tests.

- Mortar:

Only one mortar is used with different parameters (Uniaxial Crashing Stress) in first five (5) vertical loads tests.

After that two (2) mortars with different parameters (Uniaxial Crashing Stress) in last three (3) horizontal loads tests.

II.1.3. Loads:

All tests have (BLOCKING) in the bottom level (y=0), in the five first tests vertical loads are applied (uy) on level (y=250).

In each of these tests the goal is to know exactly the value of load which will cause the first crack.

the three (3) last tests horizontal loads are applied in this order:

- **First test :**

Horizontal load is on the left side (x = 0 mm) on all nodes

- **Second test:**

Horizontal load is on the right side (x = 410 mm) on all nodes.

- **Third test:**

It contains both loads on the left and right side (x = 0 mm) and (x = 410 mm) on all nodes

- **Fourth test :**

Horizontal load is on the left side (x = 0 mm) only on top nodes (level y = 250 mm)

- **Fifth test :**

The horizontal load is on the left side (x = 410 mm) only on top nodes (level y = 250 mm)

II.2 Modeling:

This is the main model which is created by ANSYS APDL:

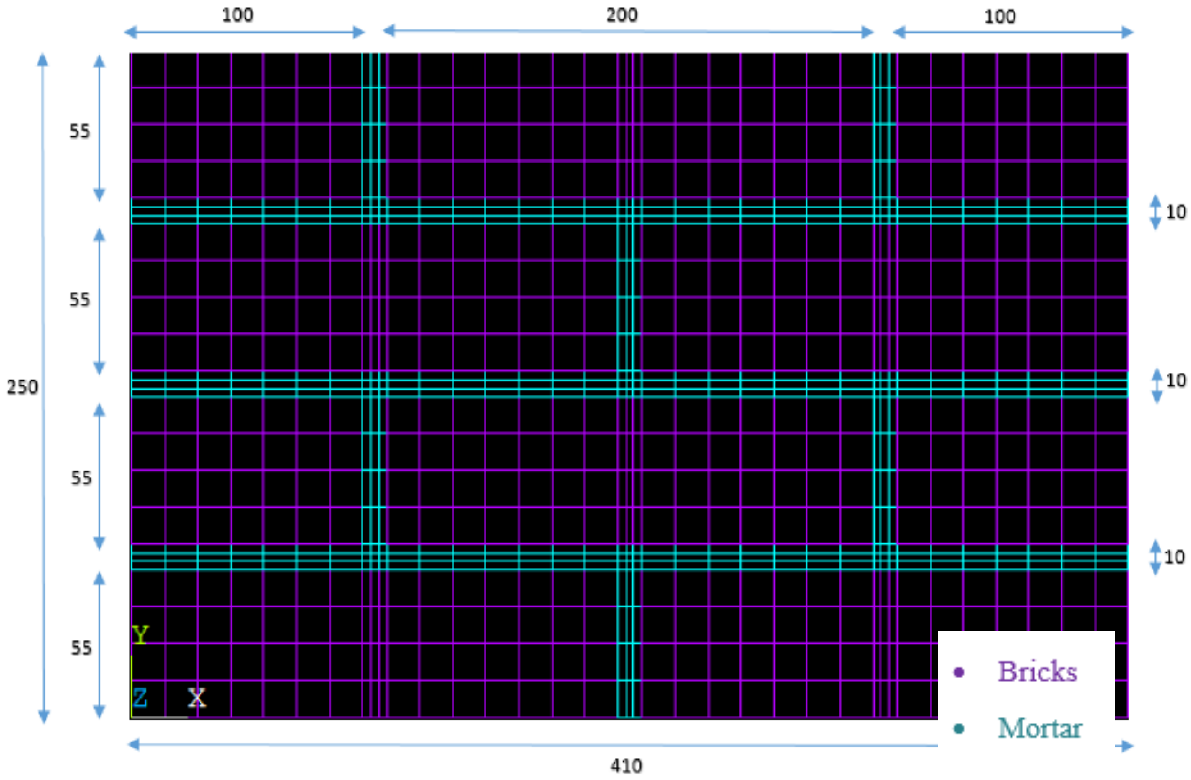


Fig II.1: main model (Ansys APDL)

II.2.1 Execution

Both vertical and horizontal loads are tested on our main model.

- **Vertical loads:**

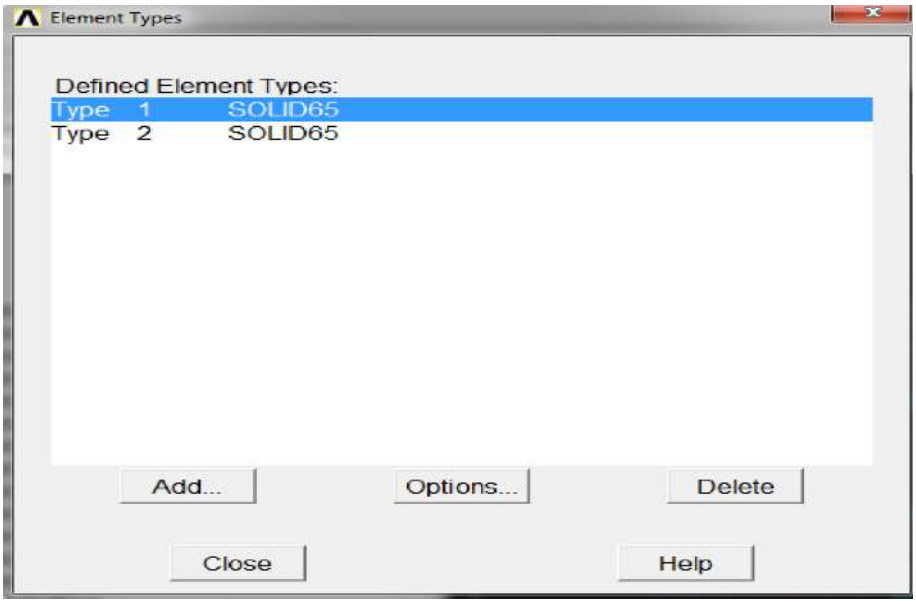
This table shows the required loads and the applied Uniaxial Crashing Stress for each crack with its own mortar:

TableII.1: parameters of each test

Test	Load (MPa)	Uniaxial Crashing Stress (MPa)
1	-0.09	15
2	-0.095	20
3	-0.1	25
4	-0.11	30
5	-0.111	35

➢ **First test:**

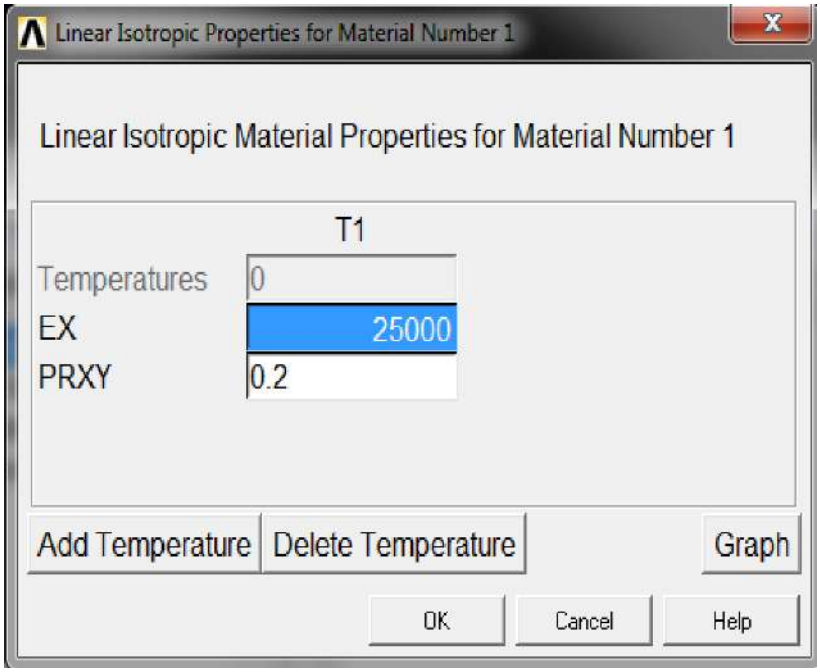
Two (2) element types (materials) Solid 65 are used



FigII.2: element types

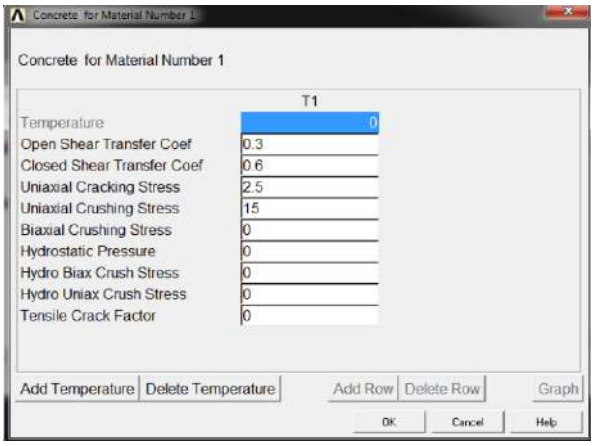
- SOLID 65 type 1: mortar
- SOLID 65 type 2: bricks

In the first test the bricks parameters are fixed and other parameters are shown on tables above:

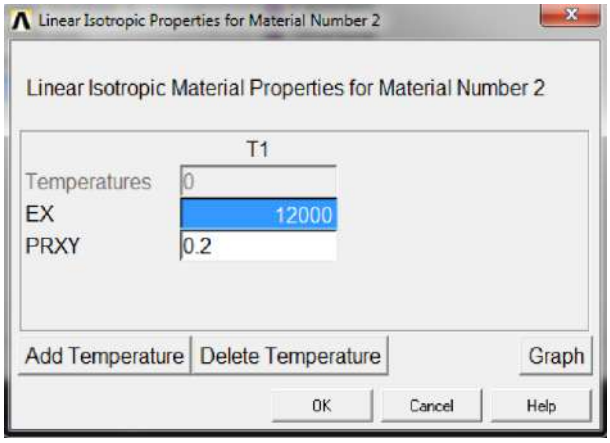


FigII.3: linear isotropic properties for material (1)

- EX (young modulus): 25000 MPa
- PRXY (Major Poisson's ratio, x-y plane): 0,2

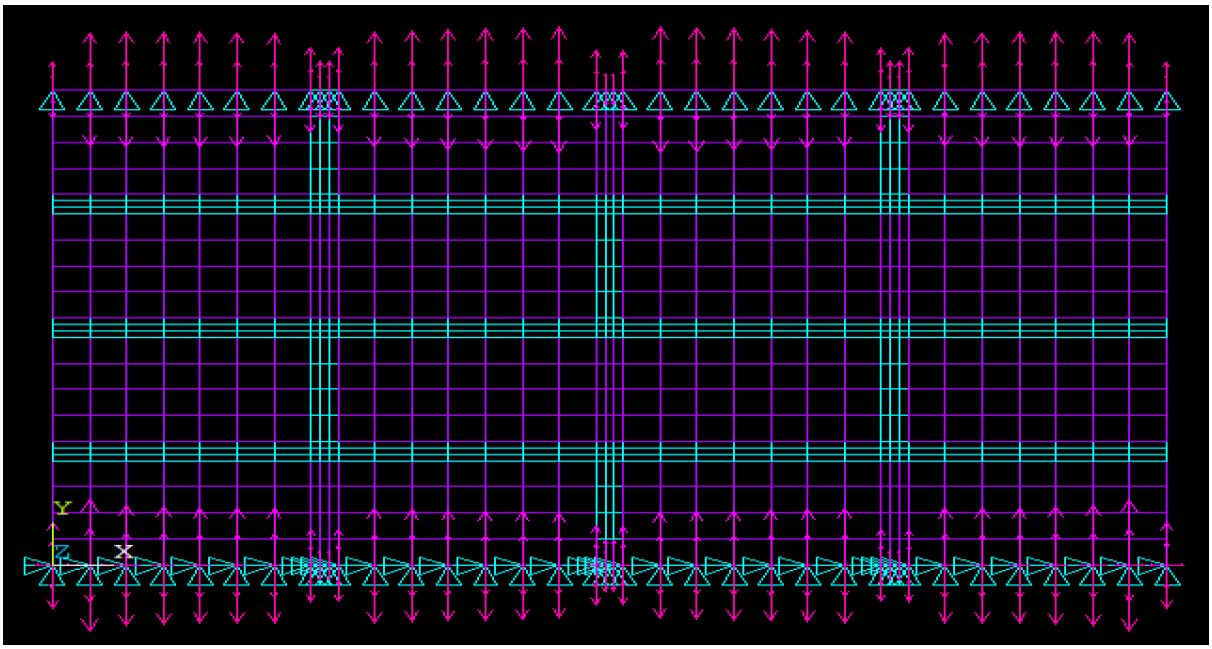


FigII.4: parameters for material (1)



FigII.5: linear isotropic properties material (2)

- EX (young module): 12000 MPa
- PRXY (Major Poisson's ratio, x-y plane): 0.2

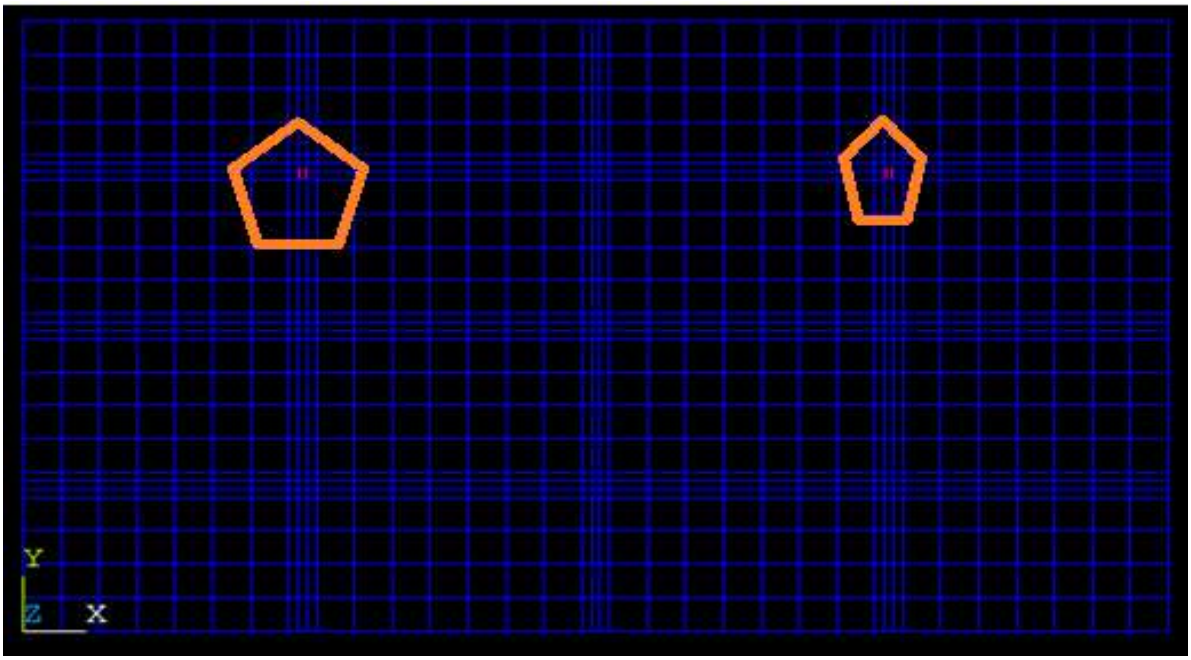


FigII.6: loads distribution

 : Blocking (3D) on level (y = 0 mm)

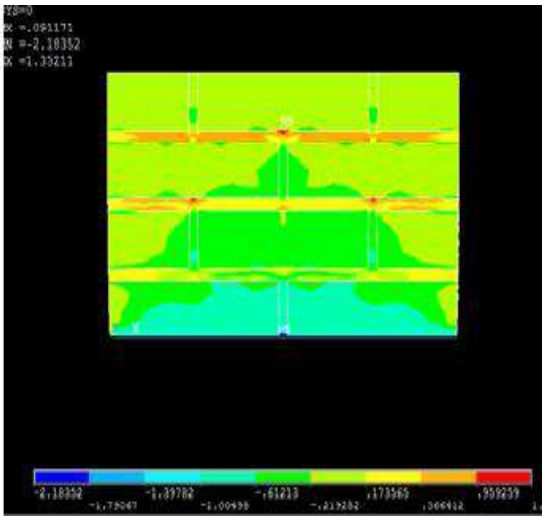
 : load (-0.09 MPa) on level (y = 250 mm) obtained from the first crack

First crack appears on the nearest points of applied loads and specifically on the intersection of horizontal and vertical mortar

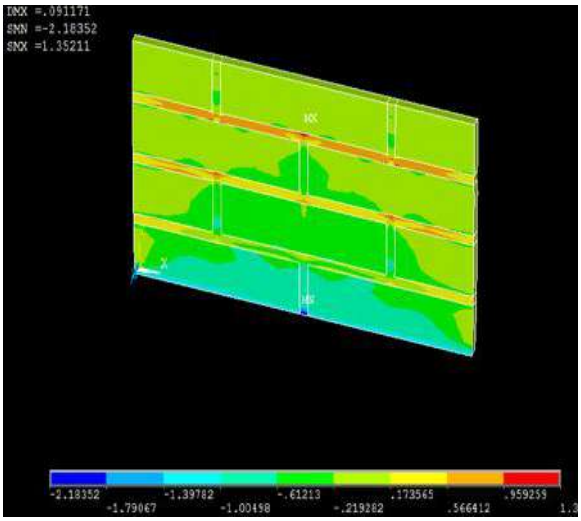


FigII.7: first cracks

When load is applied on the whole superior level we can see that there is a repartition of stress in a symmetrical way concerning the vertical axe of the wall, also we observe a stress concentration (traction) on the intersection of horizontal and vertical mortar



FigII.8: stress 2D



FigII.9: stress 3D

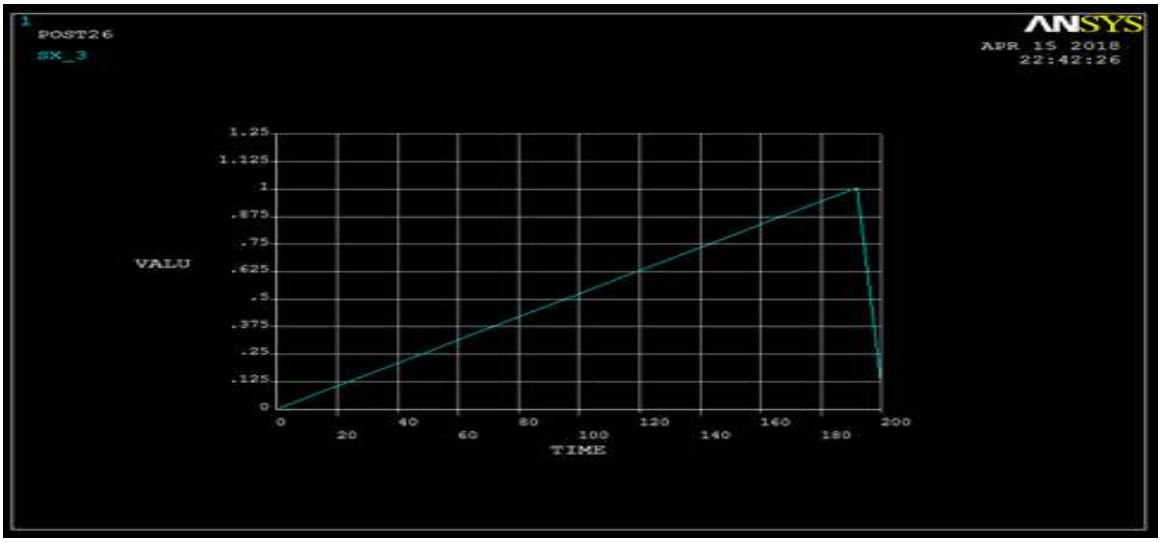
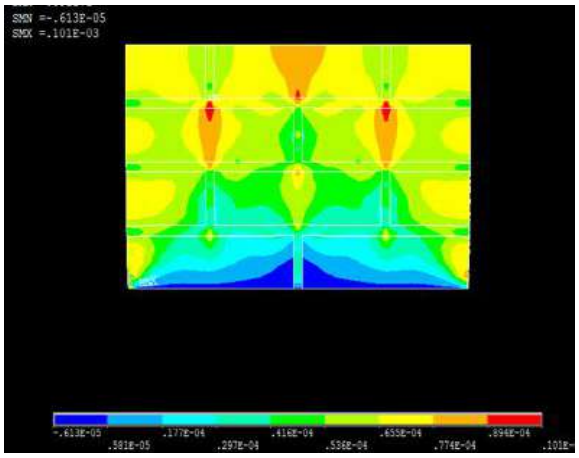
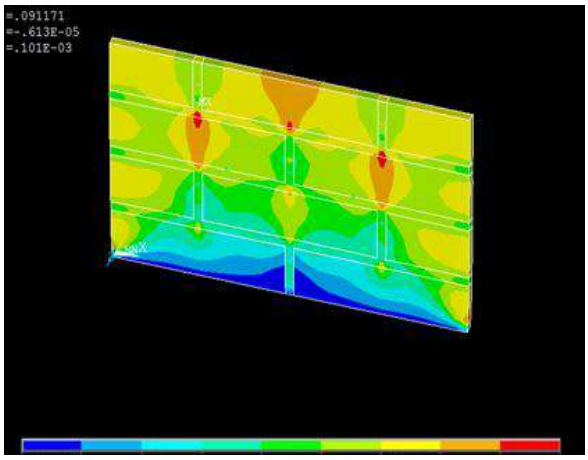


Fig2.10: stress in function of time

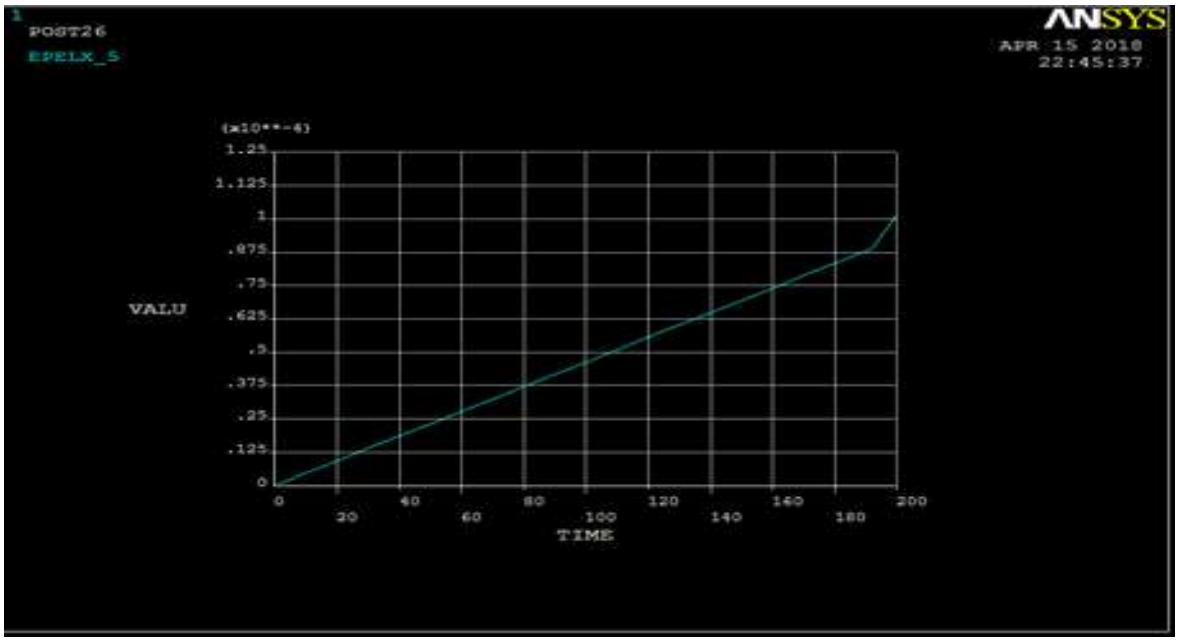
When load is applied on the whole superior level we can see that there is a repartition of elastic strain in a symmetrical way concerning the vertical axe of the wall, also we observe an elastic strain concentration (deformation) on the intersection of horizontal and vertical mortar



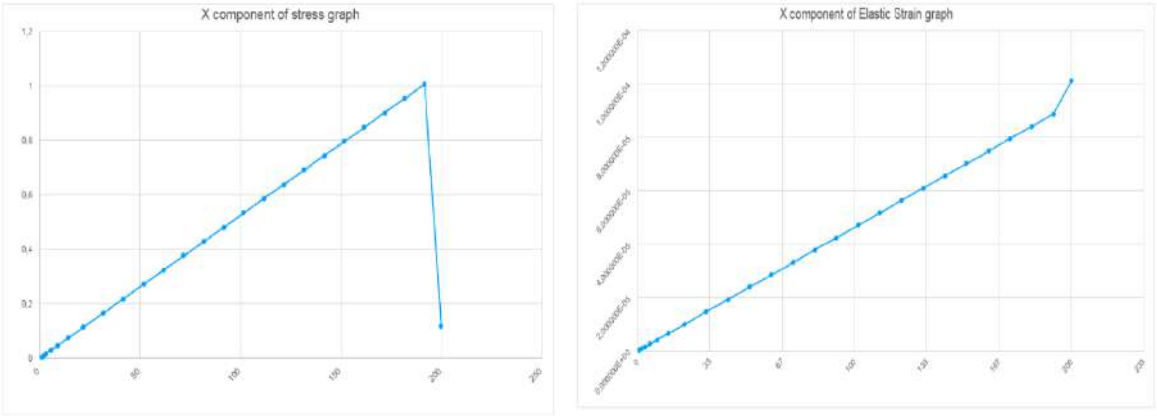
FigII.11: elastic strain 2D



FigII.12: elastic strain 3D



FigII.13: elastic strain in function of time

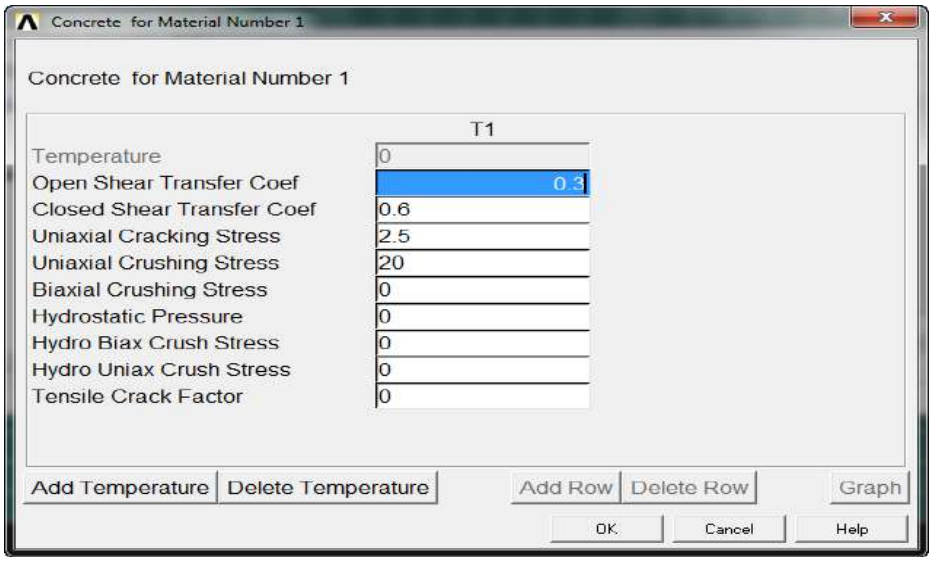


(a) (b)

FigII.14: stress (a) and elastic strain (b) in function of time

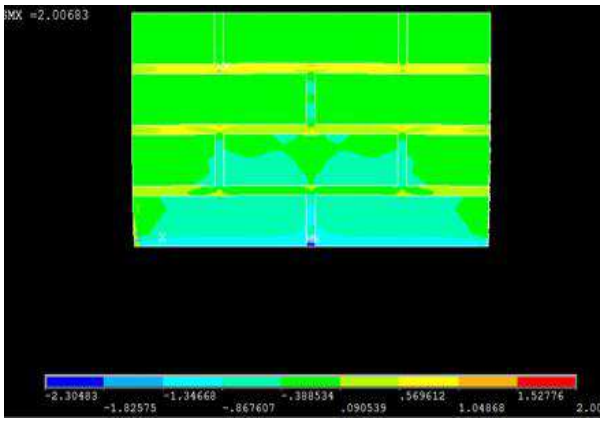
- **Second test :**

It's same as the first test, only with different parameters (Uniaxial Crashing Stress)

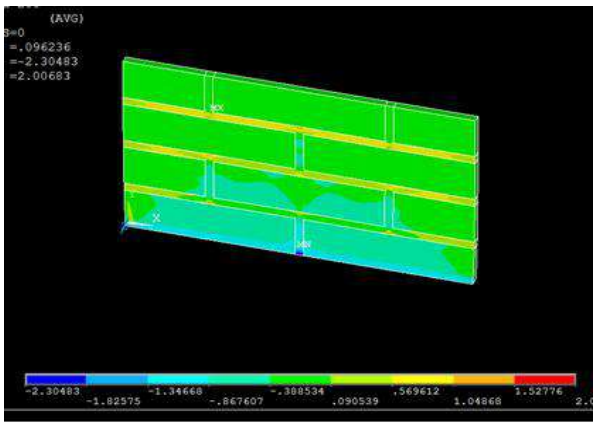


FigII.15: parameters for material (1)

When load is applied on the whole superior level we can see that there is a repartition of stress in a symmetrical way concerning the vertical axe of the wall, also we observe a stress concentration (traction) on the intersection of horizontal and vertical mortar



FigII.16: stress 2D



FigII.17: stress 3D

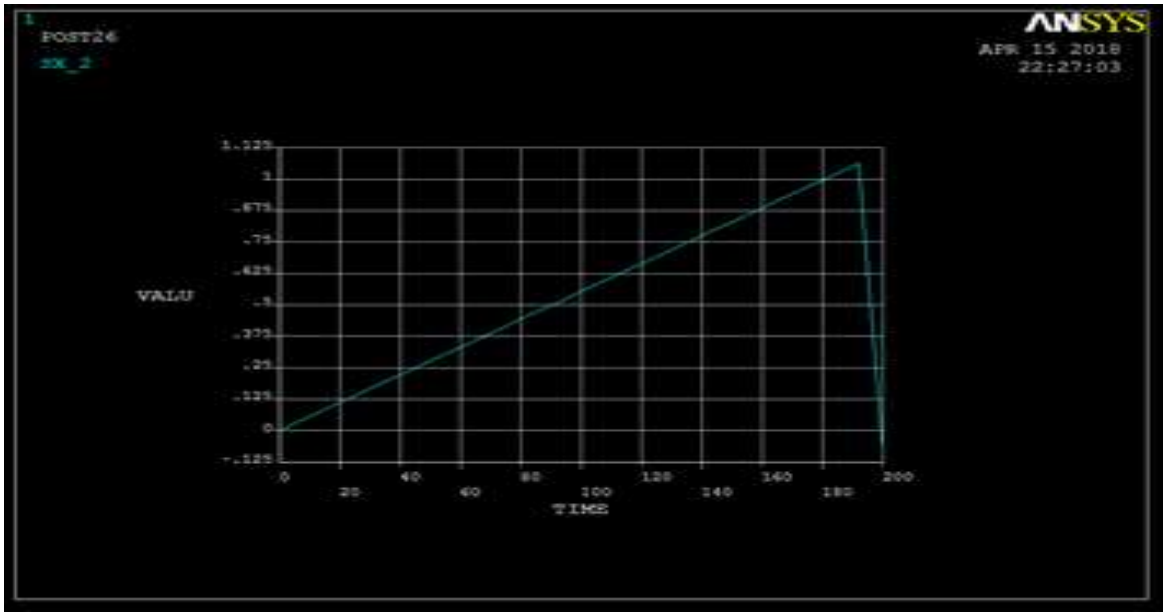
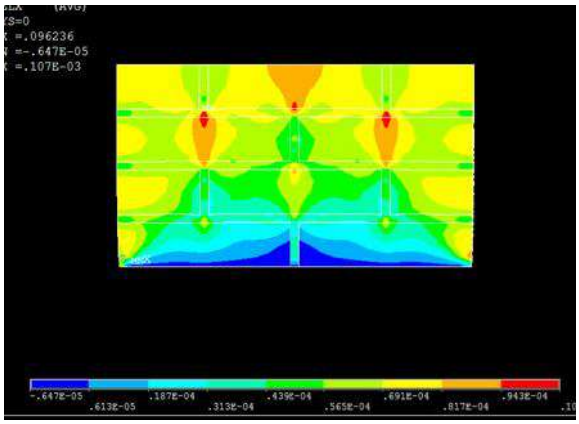
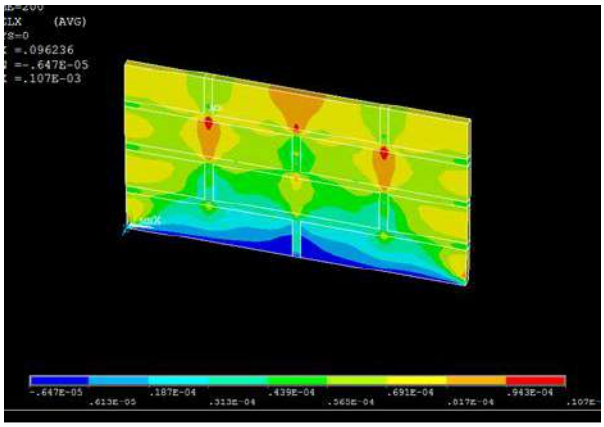


Fig2.18: stress in function of time

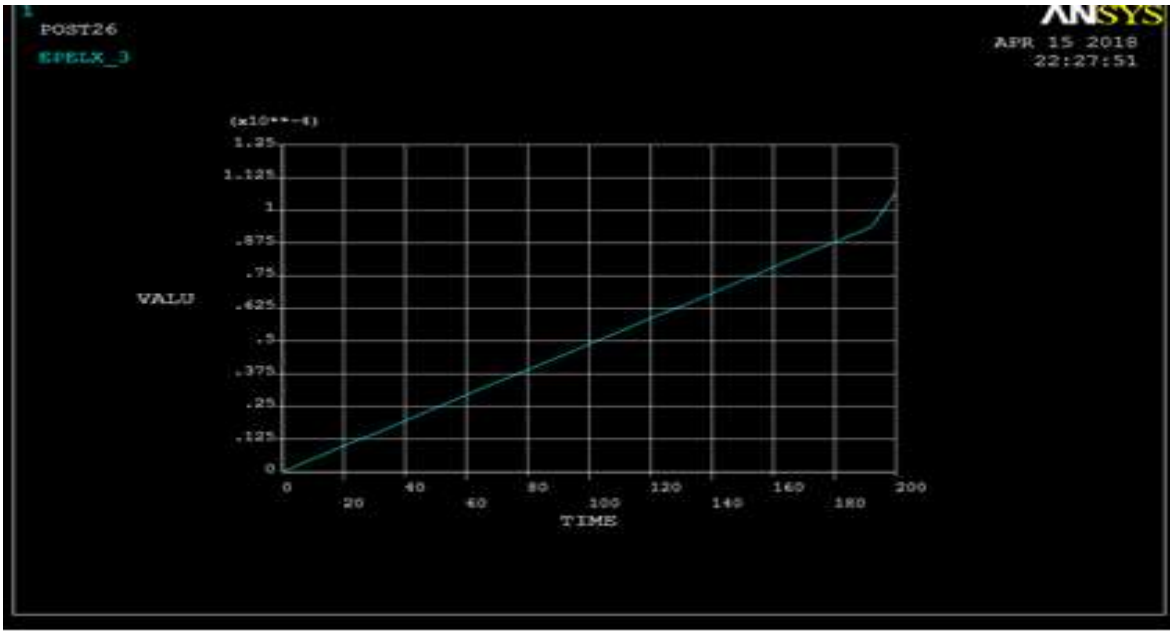
When load is applied on the whole superior level we can see that there is a repartition of elastic strain in a symmetrical way concerning the vertical axe of the wall, also we observe an elastic strain concentration (deformation) on the intersection of horizontal and vertical mortar



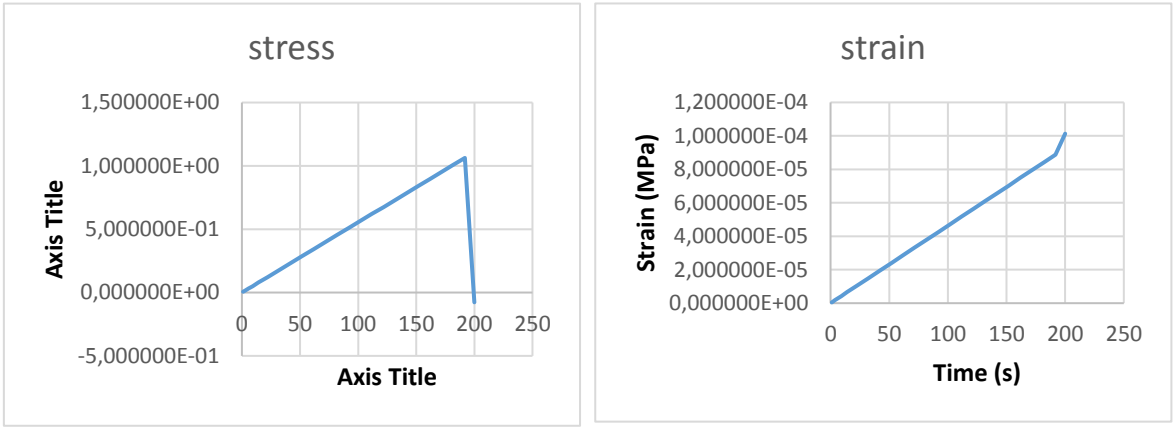
FigII.19: elastic strain 2D



FigII.20: elastic strain 3D



FigII.21: elastic strain in function of time

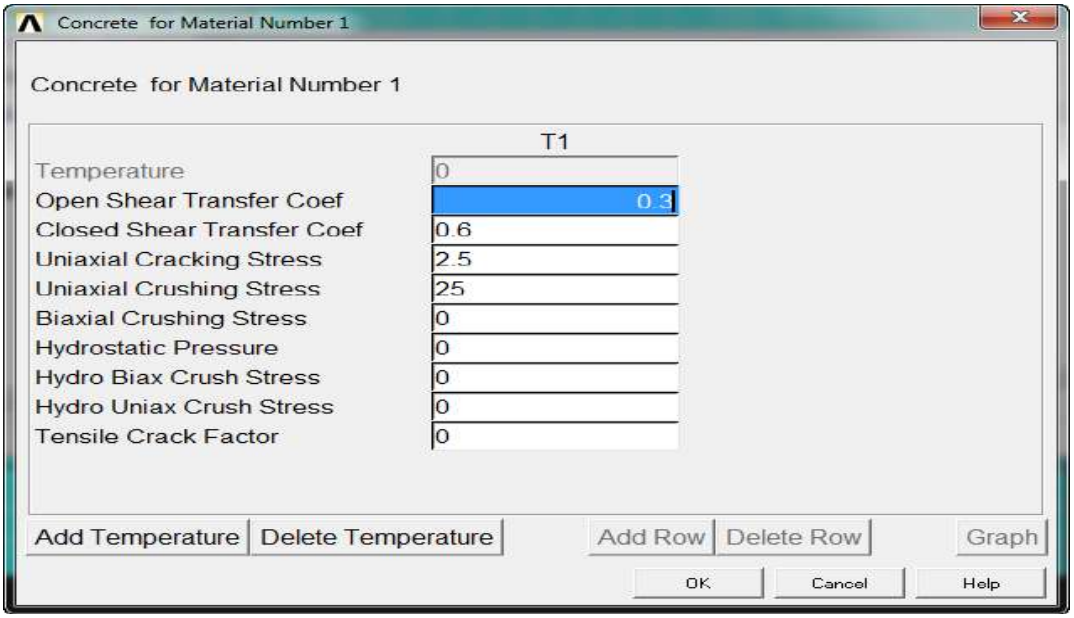


(a) **(b)**

FigII.22: stress (a) and elastic strain (b) in function of time

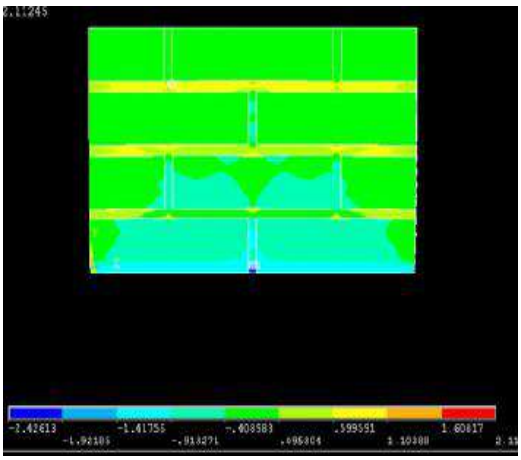
- **Third Test :**

It's same as the first test, only with different Uniaxial Crashing Stress

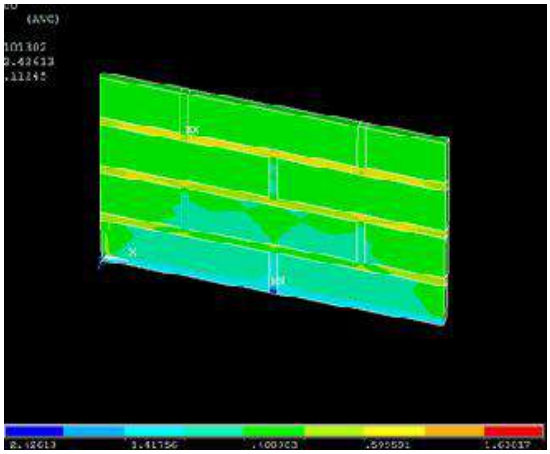


FigII.23: parameters for material (1)

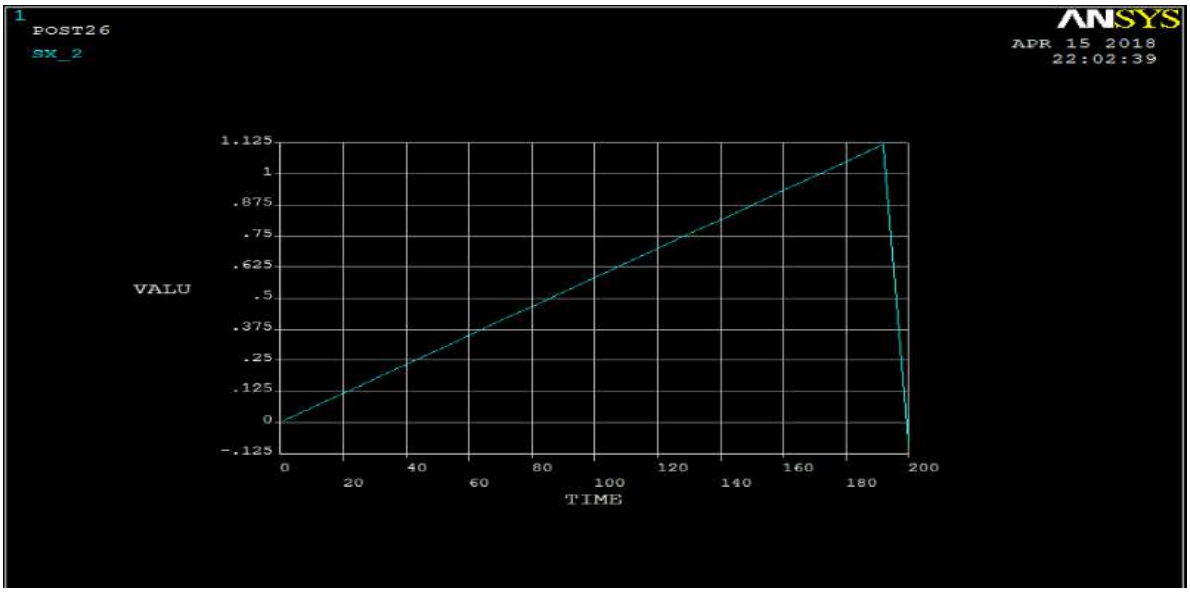
When load is applied on the whole superior level we can see that there is a repartition of stress in a symmetrical way concerning the vertical axe of the wall, also we observe a stress concentration (traction) on the intersection of horizontal and vertical mortar



FigII.24: stress 2D

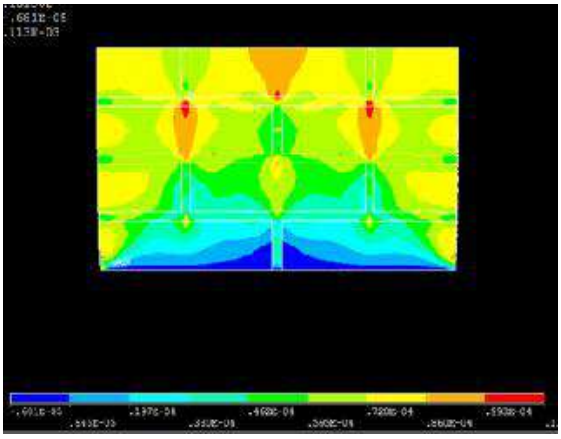


FigII.25: stress 3D

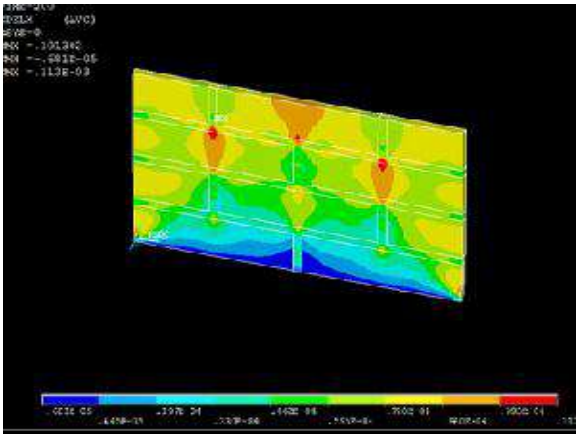


FigII.26: stress in function of time

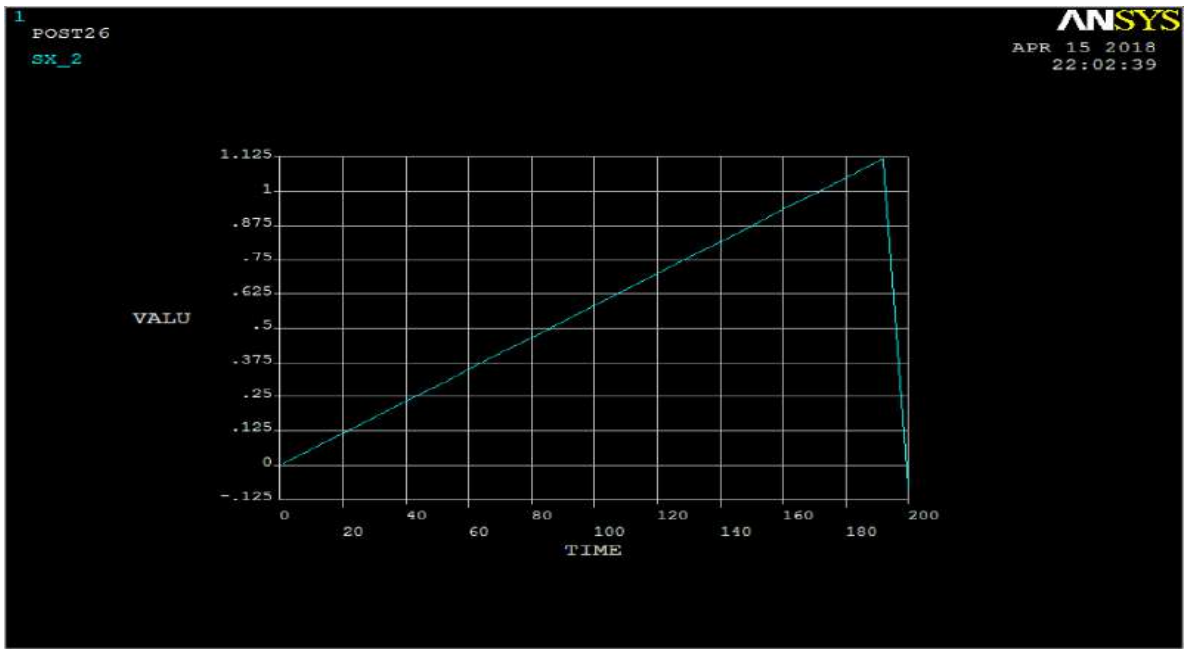
When load is applied on the whole superior level we can see that there is a repartition of elastic strain in a symmetrical way concerning the vertical axe of the wall, also we observe an elastic strain concentration (deformation) on the intersection of horizontal and vertical mortar



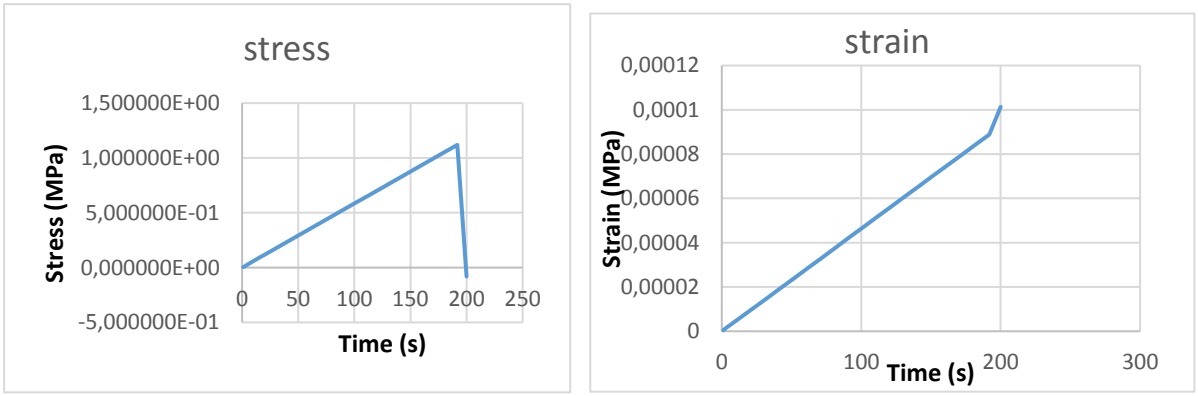
FigII.28: elastic strain 2D



FigII.27: elastic strain 3D



FigII.29: elastic strain in function of time

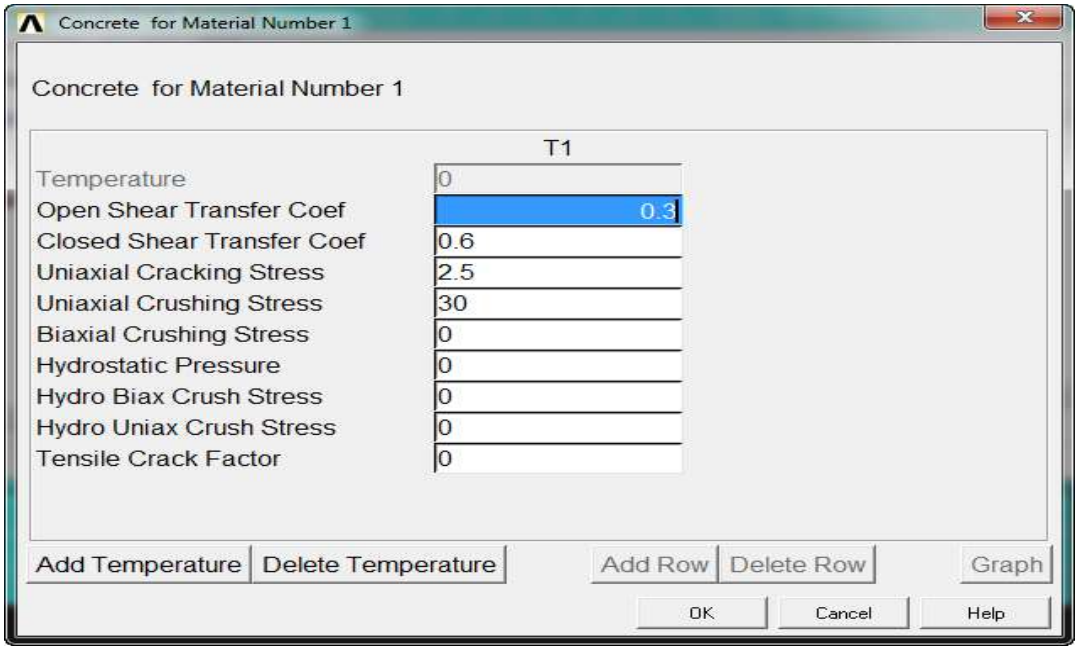


(a) (b)

FigII.30: stress (a) and elastic strain (b) in function of time

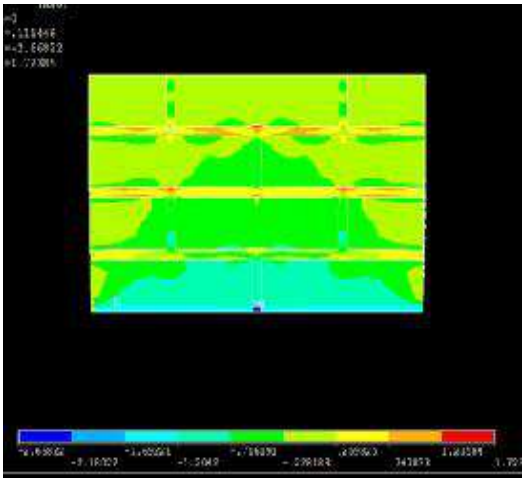
- **Fourth test :**

  It's same as the first test, only with different Uniaxial Crashing Stress

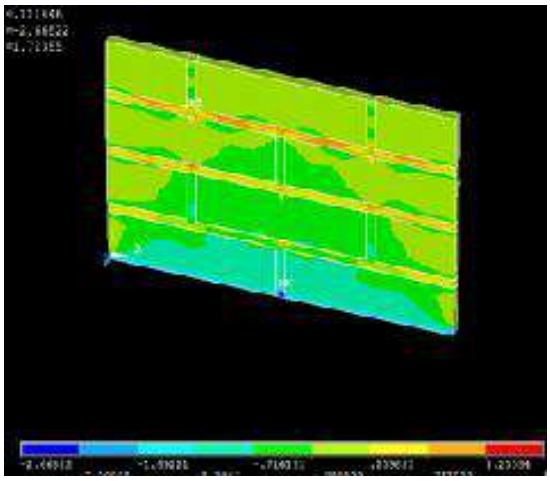


FigII.31: parameters for material (1)

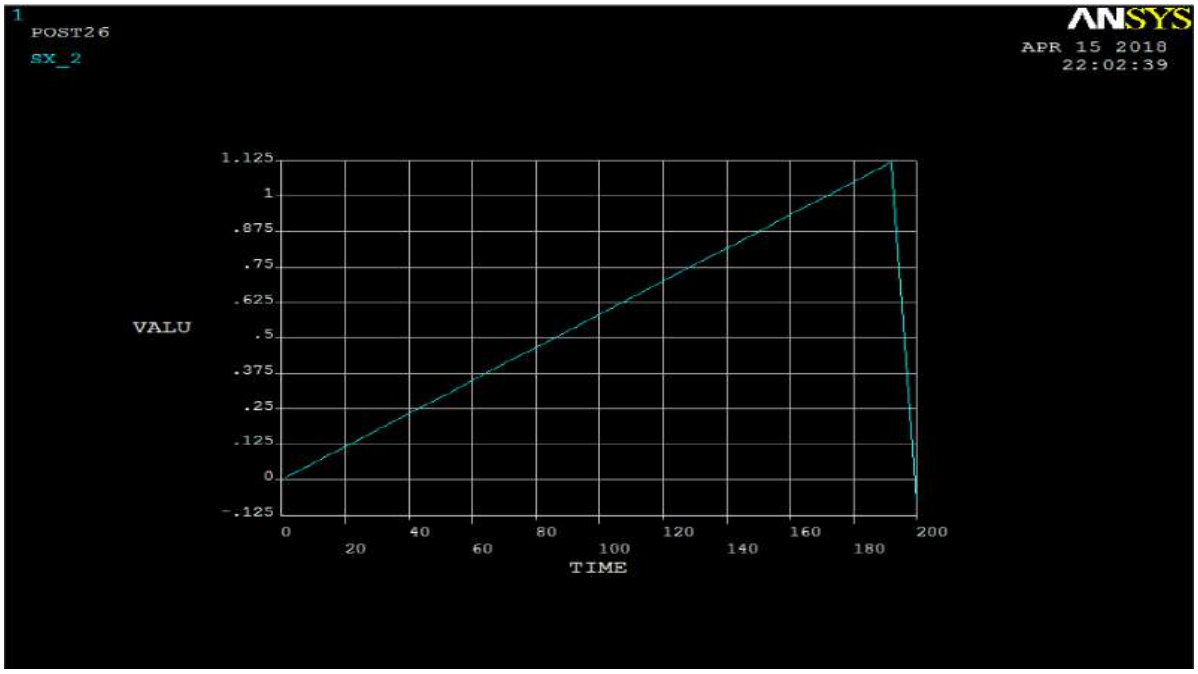
When load is applied on the whole superior level we can see that there is a repartition of stress in a symmetrical way concerning the vertical axe of the wall, also we observe a stress concentration (traction) on the intersection of horizontal and vertical mortar



FigII.32: stress 2D

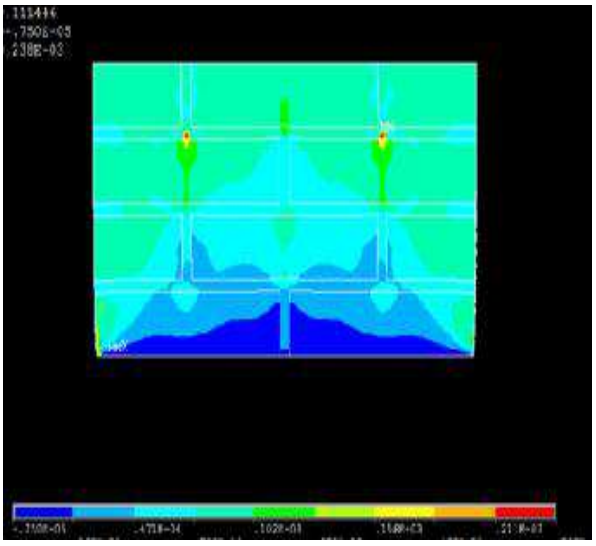


FigII.33: stress 3D

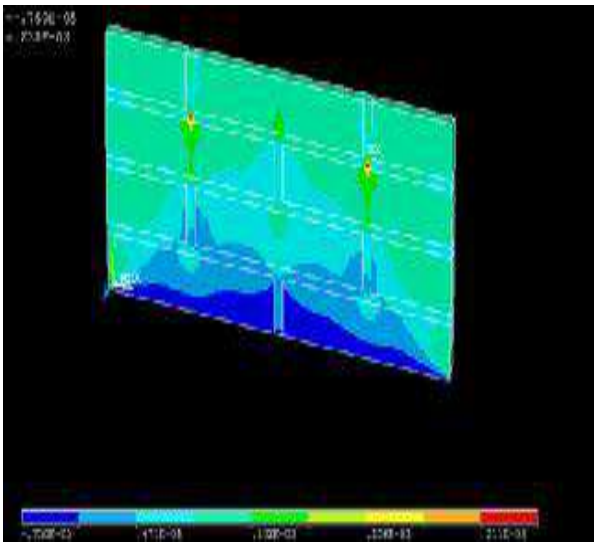


FigII.34: stress in function of time

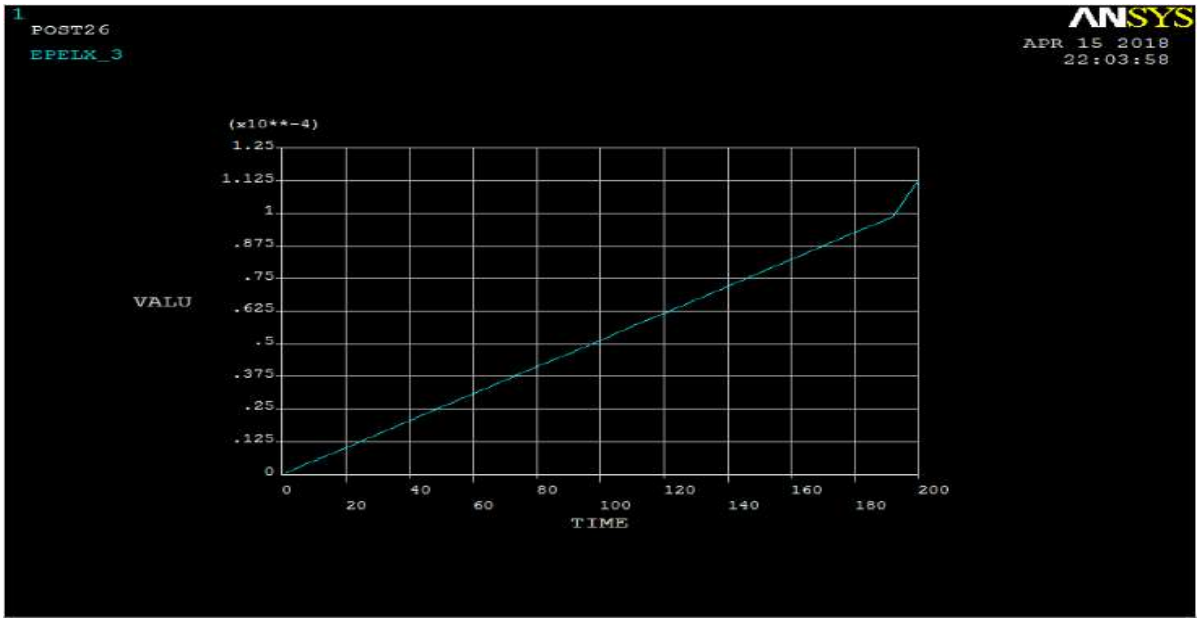
When load is applied on the whole superior level we can see that there is a repartition of elastic strain in a symmetrical way concerning the vertical axe of the wall, also we observe an elastic strain concentration (deformation) on the intersection of horizontal and vertical mortar



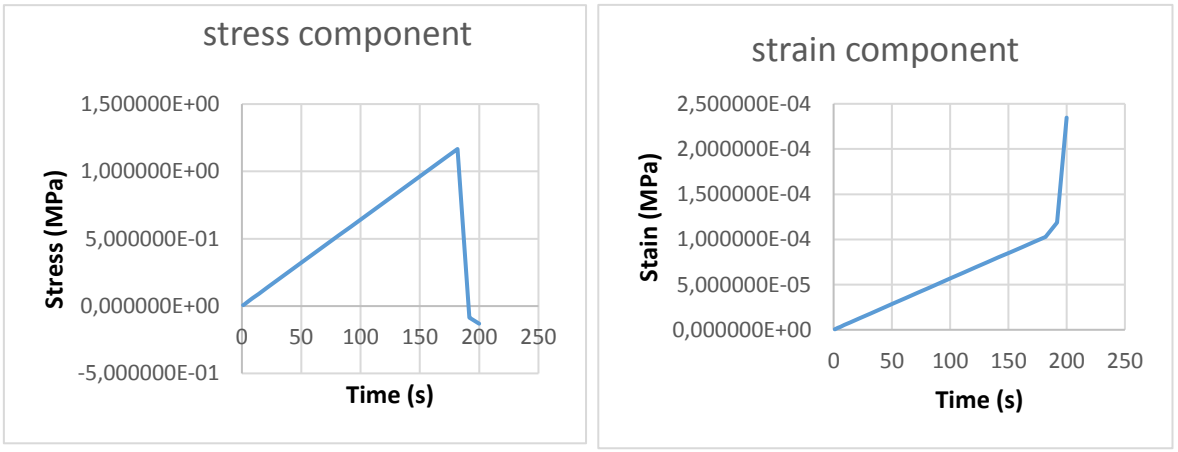
FigII.35: elastic strain 2D



FigII.36: elastic strain 3D



FigII.37: elastic strain in function of time



(a) **(b)**

FigII.38: stress (a) and elastic strain (b) in function of time

- **Fifth test :**

  It's same as first test, only with different Uniaxial Crashing Stress

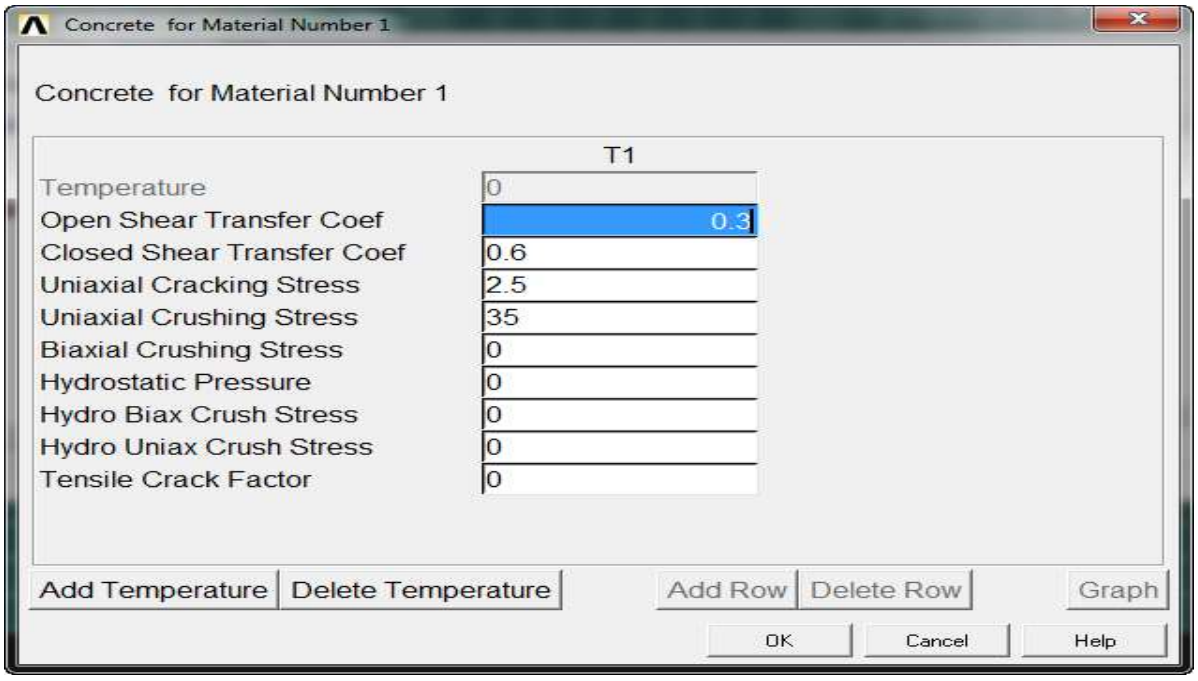
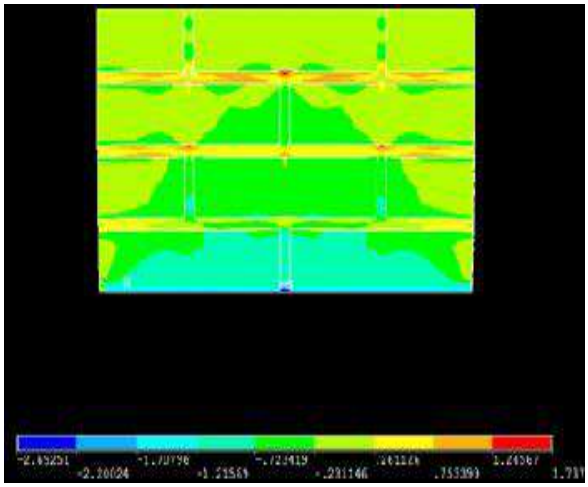
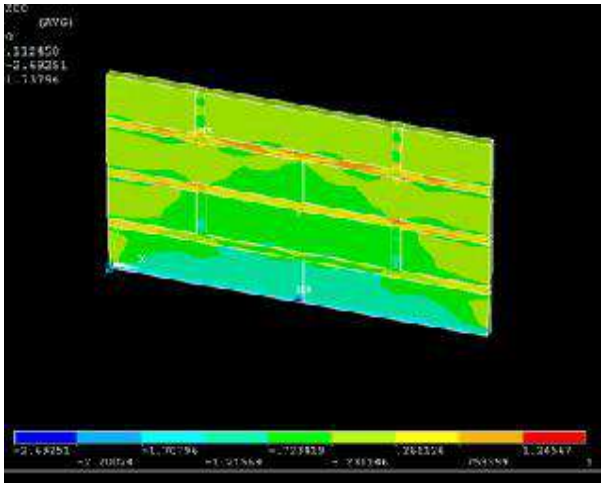


Fig II.39: parameters for material (1)

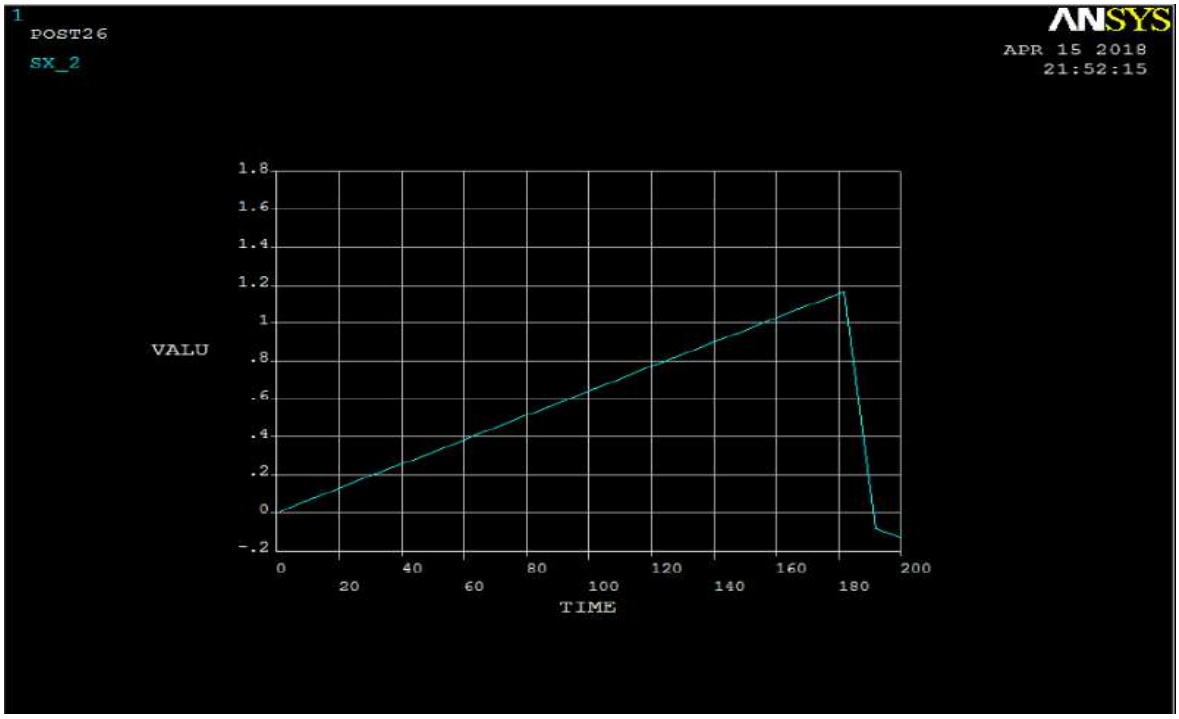
When load is applied on the whole superior level we can see that there is a repartition of stress in a symmetrical way concerning the vertical axe of the wall, also we observe a stress concentration (traction) on the intersection of horizontal and vertical mortar



FigII.40: stress 2D

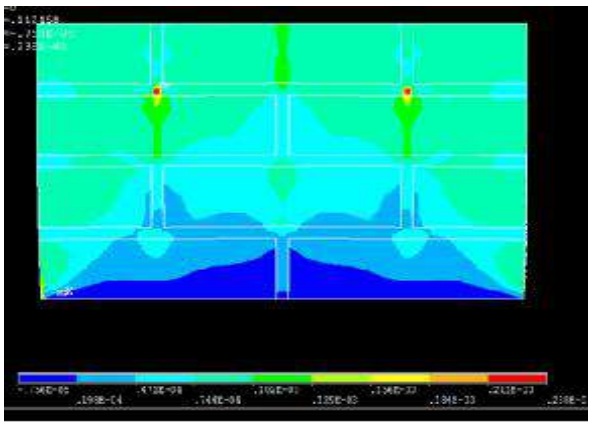


FigII.41: stress 3D

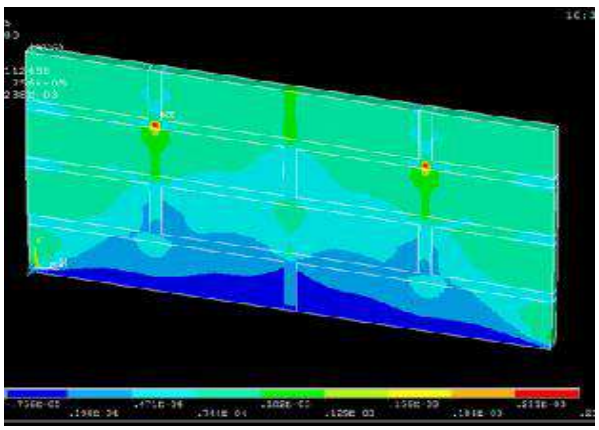


FigII.42: stress in function of time

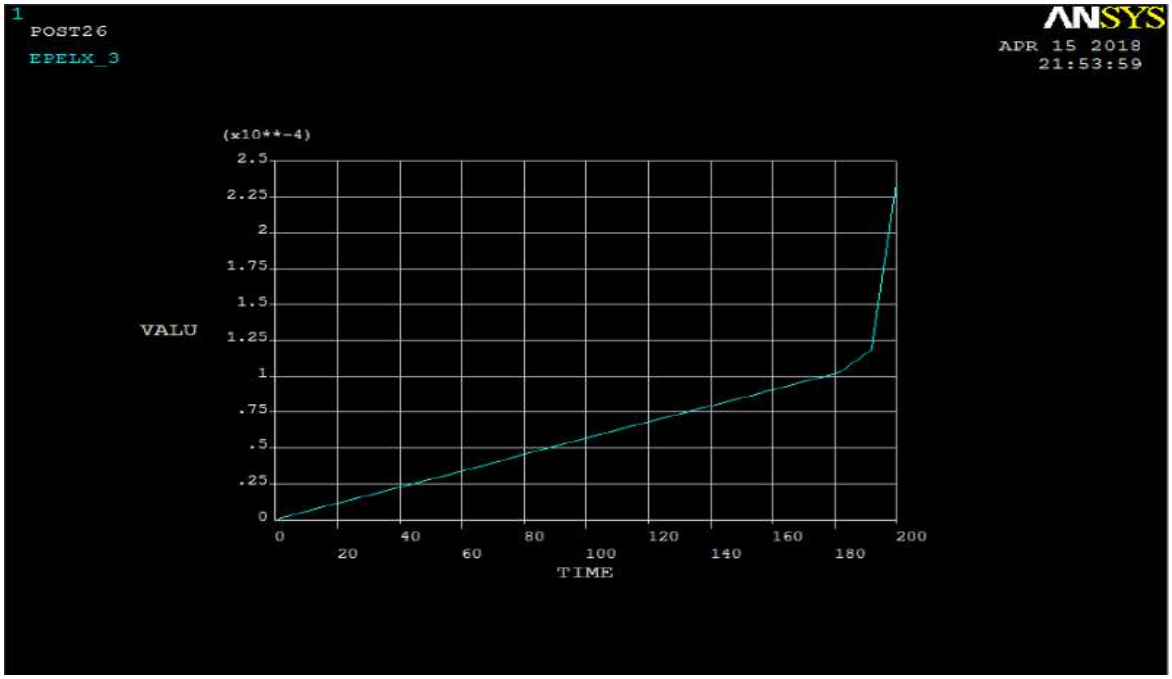
When load is applied on the whole superior level we can see that there is a repartition of elastic strain in a symmetrical way concerning the vertical axe of the wall, also we observe an elastic strain concentration (deformation) on the intersection of horizontal and vertical mortar



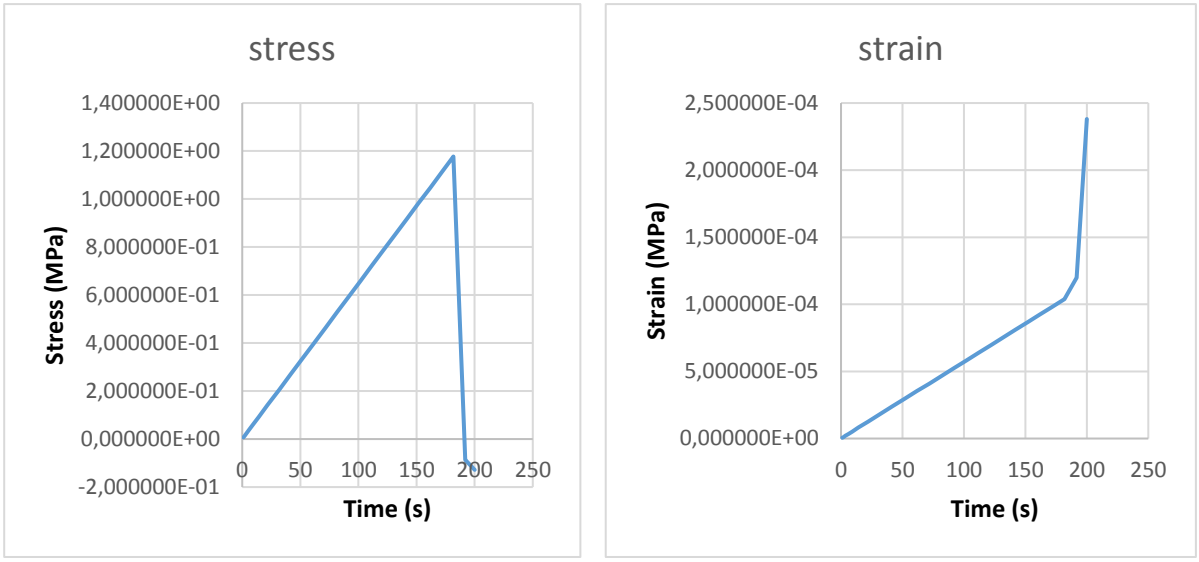
FigII.43: elastic strain 2D



FigII.44: elastic strain 3D



FigII.45: elastic strain in function of time



FigII.46: stress and elastic strain in function of time

- **Horizontal loads:**

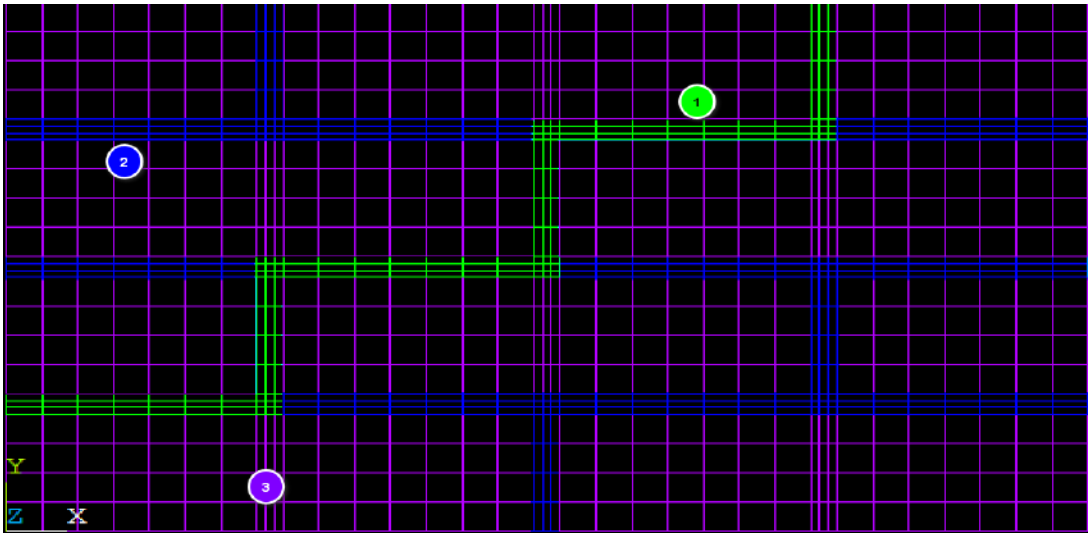
These are the required loads for each crack with its own mortar

TableII.2: Parameters of each test

Test	LOAD (MPA)
1	-0.22
2	-0.22
3	0.096 / -0.096

- **First Test** : (right side)

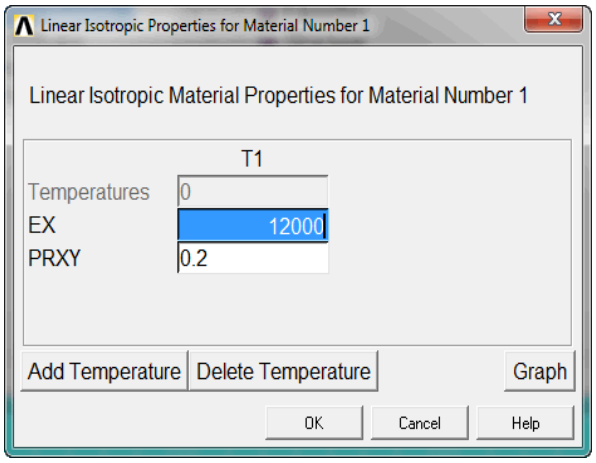
Three (3) element types (materials) Solid 65 are used to get this schema



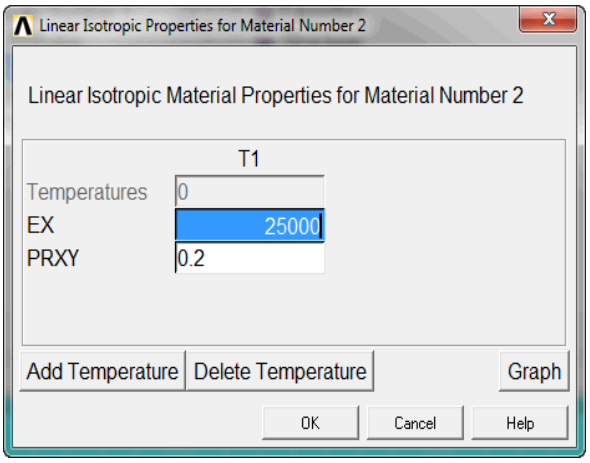
FigII.47: distribution of material

TableII.3: type of materials

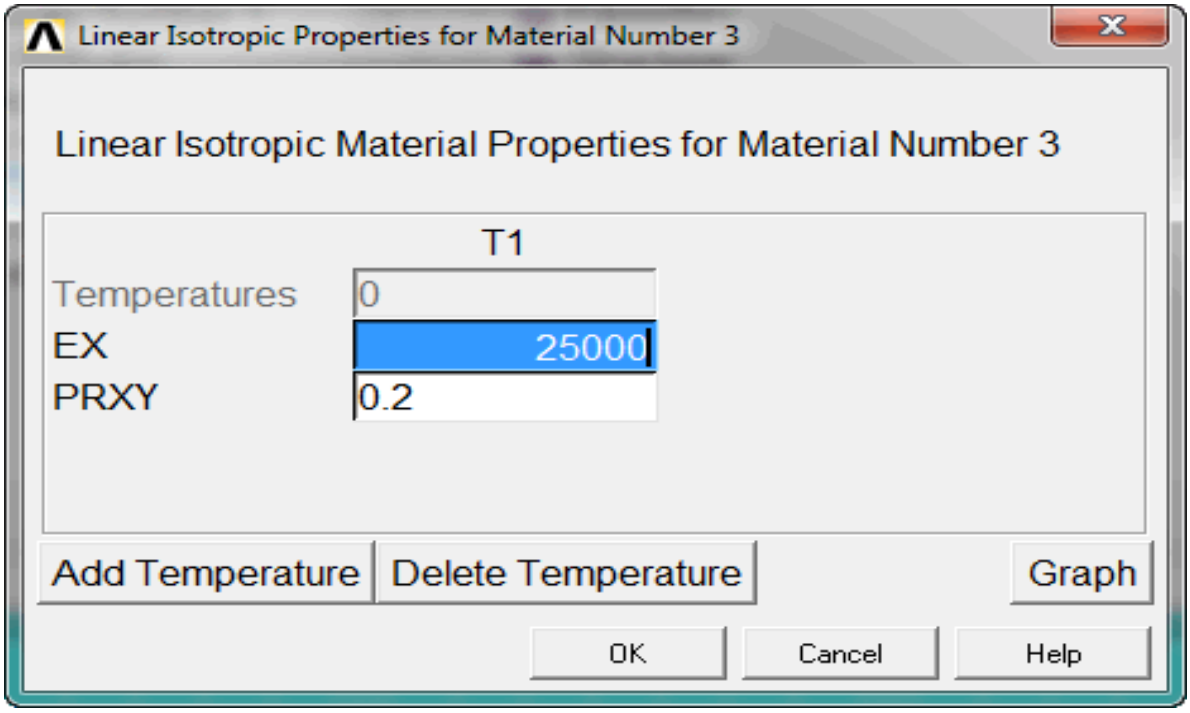
Material
1 (mortar1) low resistance
2 (morter2) good resistance
3 (bricks) standard resistance



FigII.48: properties of material (1)

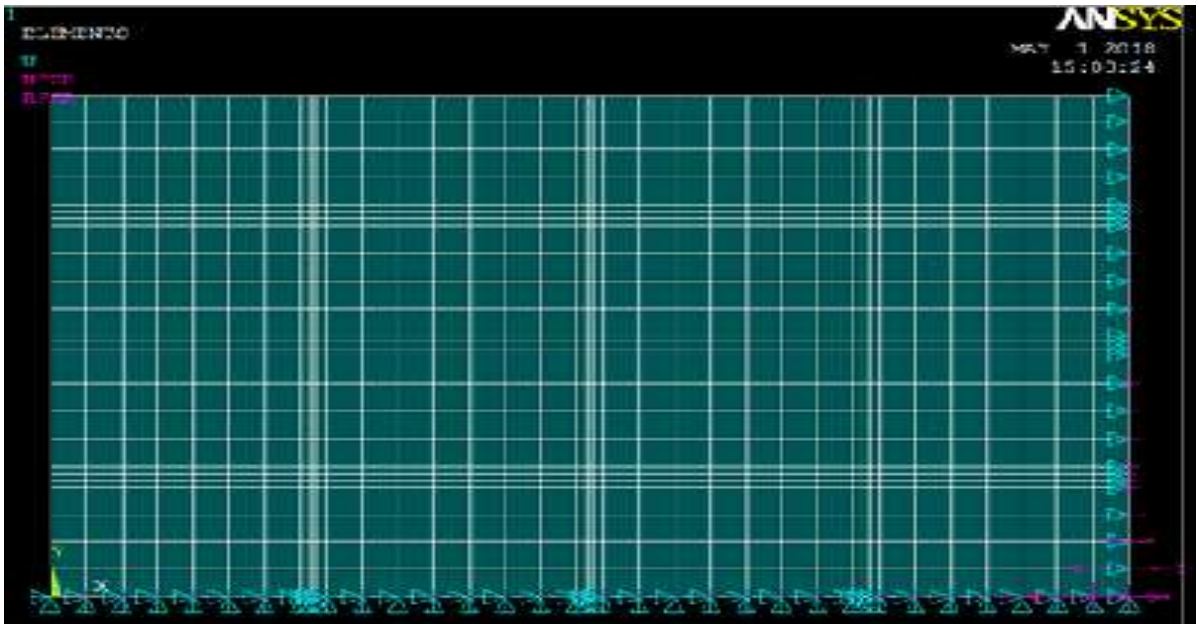


FigII.49: properties of material (2)



FigII.50: properties for material (3)

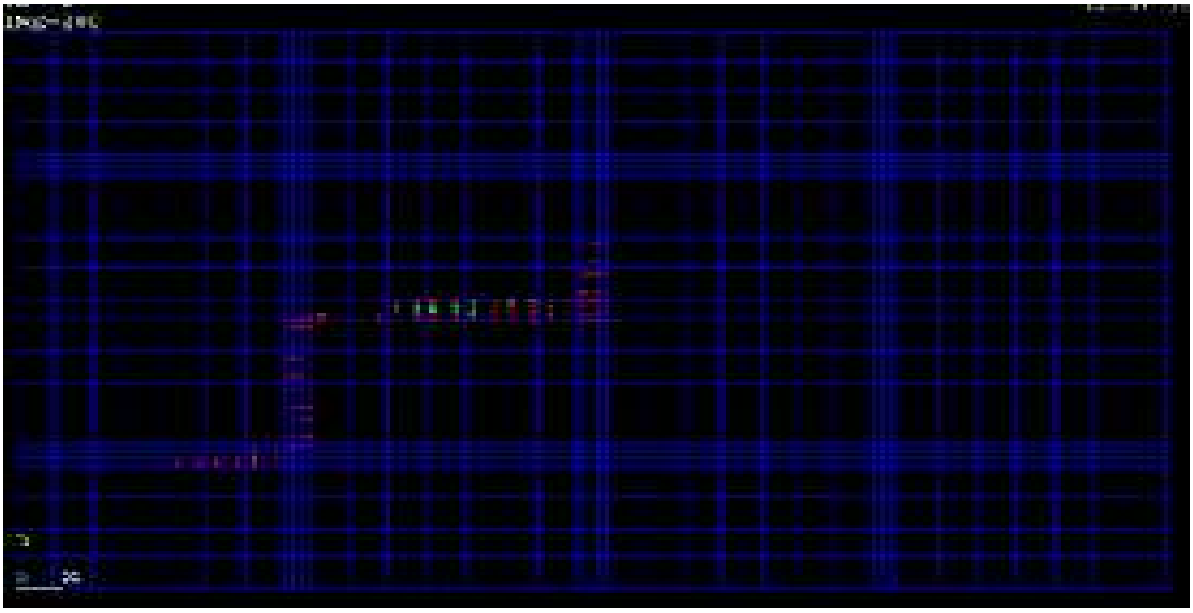
After applying loads, the distribution is like above:



FigII.51: distribution of loads

Cracks are shown above (fig2.52):

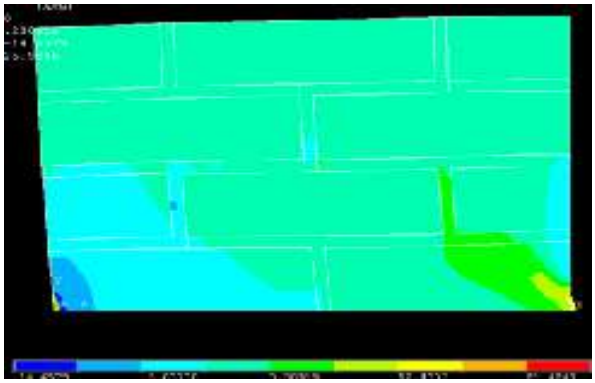
We can see that first crack appears on the same path of the weak mortar and also on the bottom



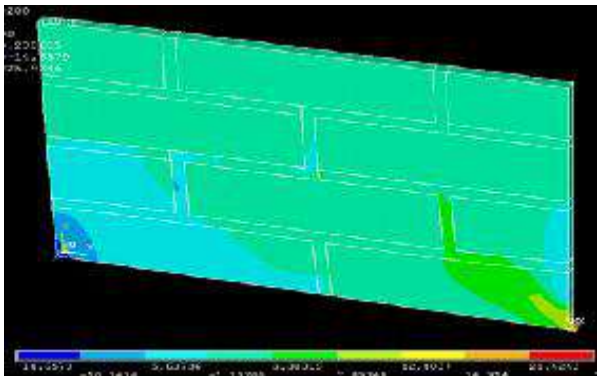
FigII.52: the first crack path

When load is applied on the right side (all nodes) we can see a compression stress on the opposite side specifically on the bottom, there is also a traction stress on the same right side.

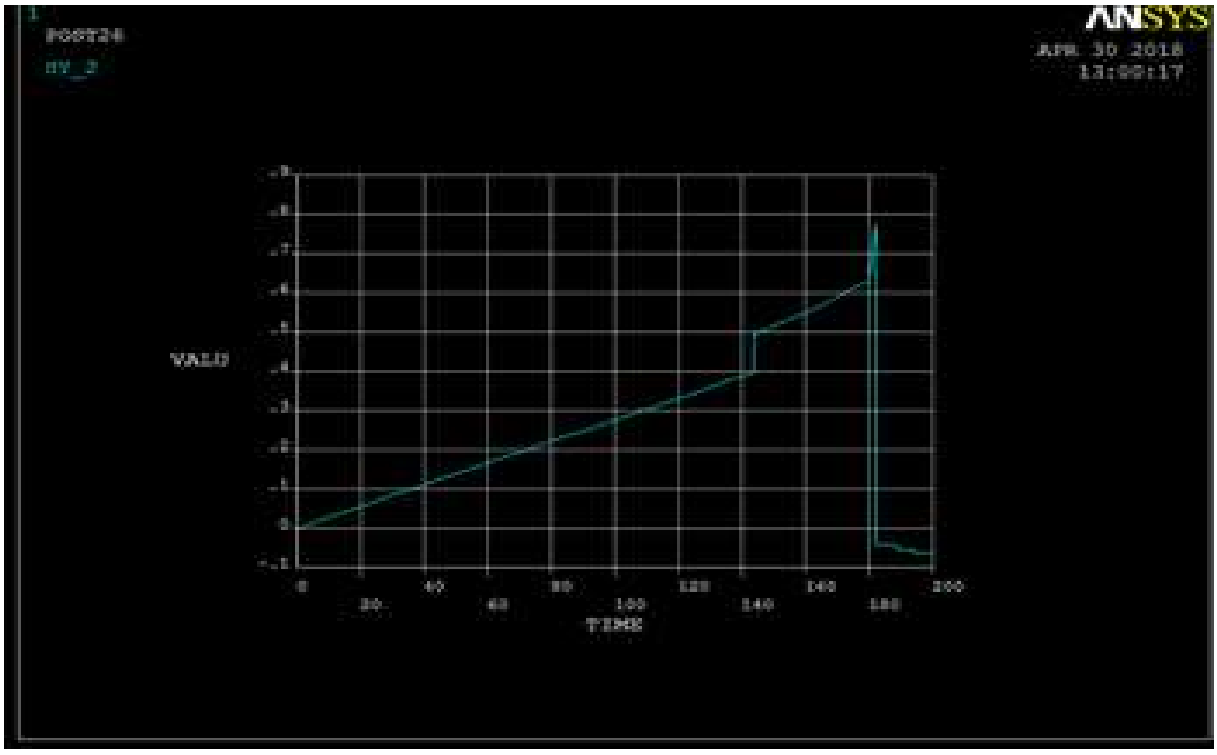
2D and 3D:



FigII.53: stress 2D



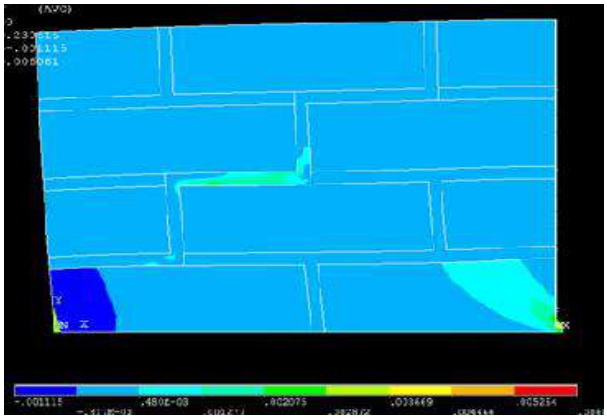
FigII.54: stress 3D



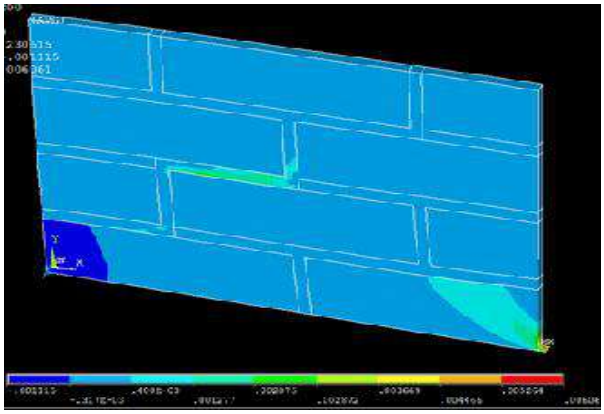
FigII.55: stress in function of time

When we apply a load on the right side (all nodes) we can see there is a repartition of elastic strain on the opposite bottom side. We observe also an elastic strain concentration on the path of weak mortar.

2D and 3D:

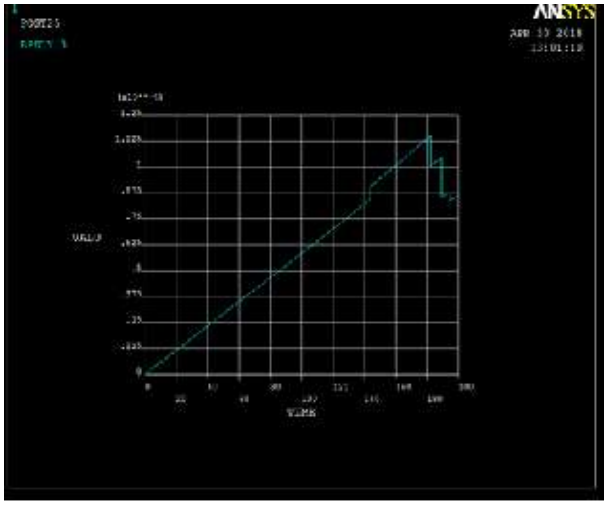


FigII.56: elastic strain 2D

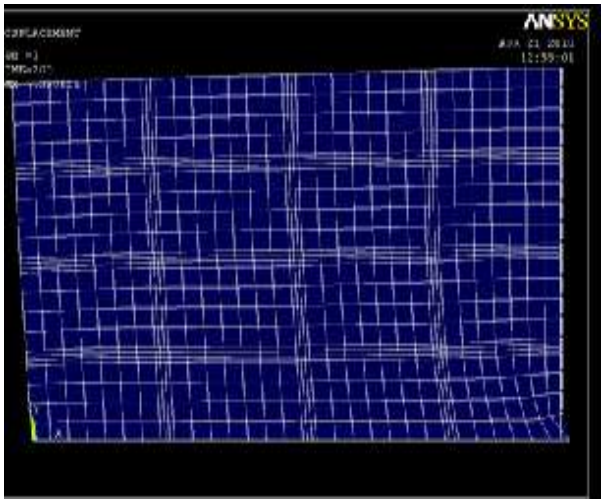


FigII.57: elastic strain 3D

Elastic strain and displacement are shown above (fig2.58 , fig2.59):



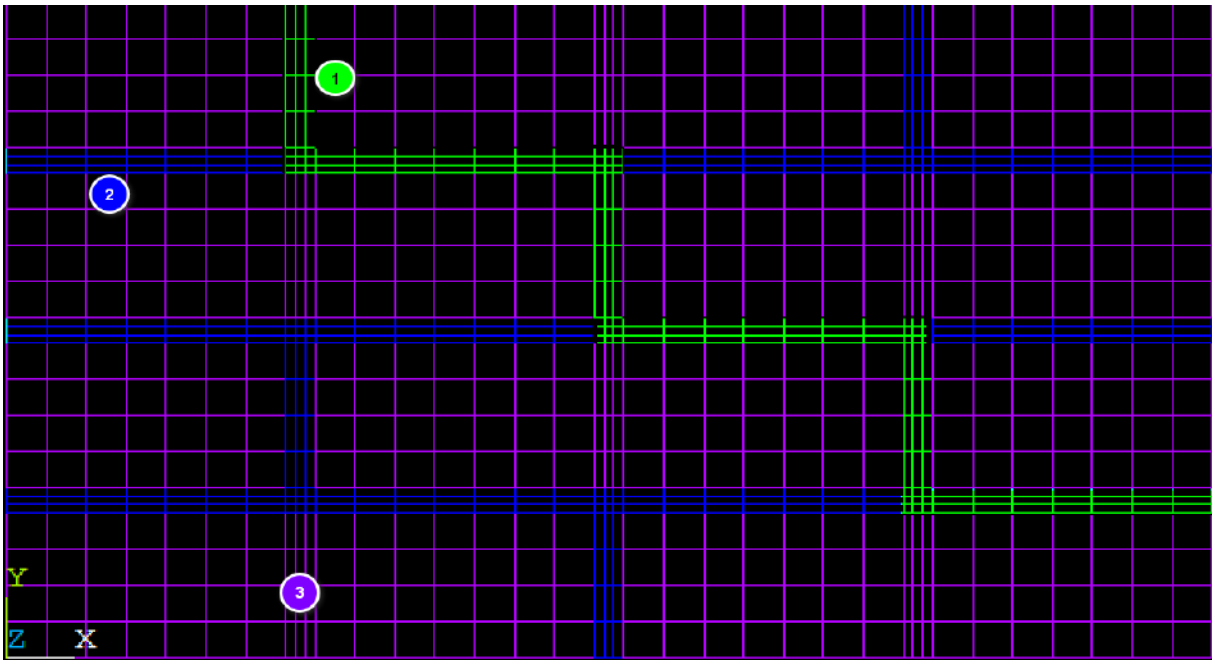
FigII.58: elastic strain in function of time



FigII.59: displacement of wall

- **Second Test** : (left side)

Three (3) element types (materials) Solid 65 are used to get this schema

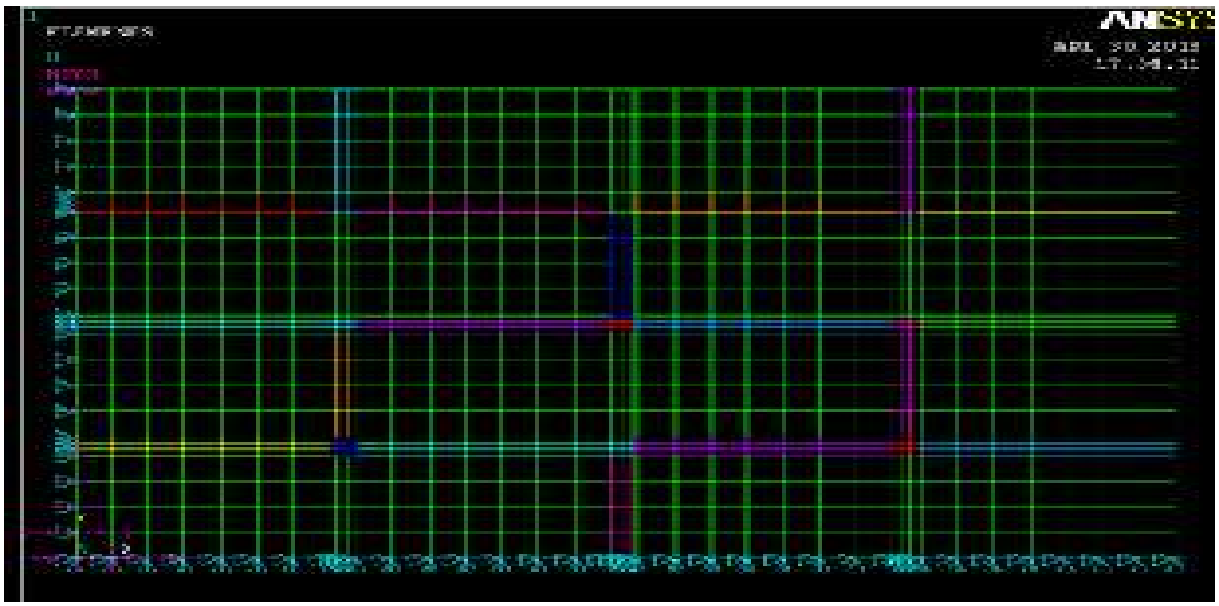


FigII.60: distribution of materials

TableII.4: type of materials

Material
1 (mortar1) low resistance
2 (morter2) good resistance
3 (bricks) standard resistance

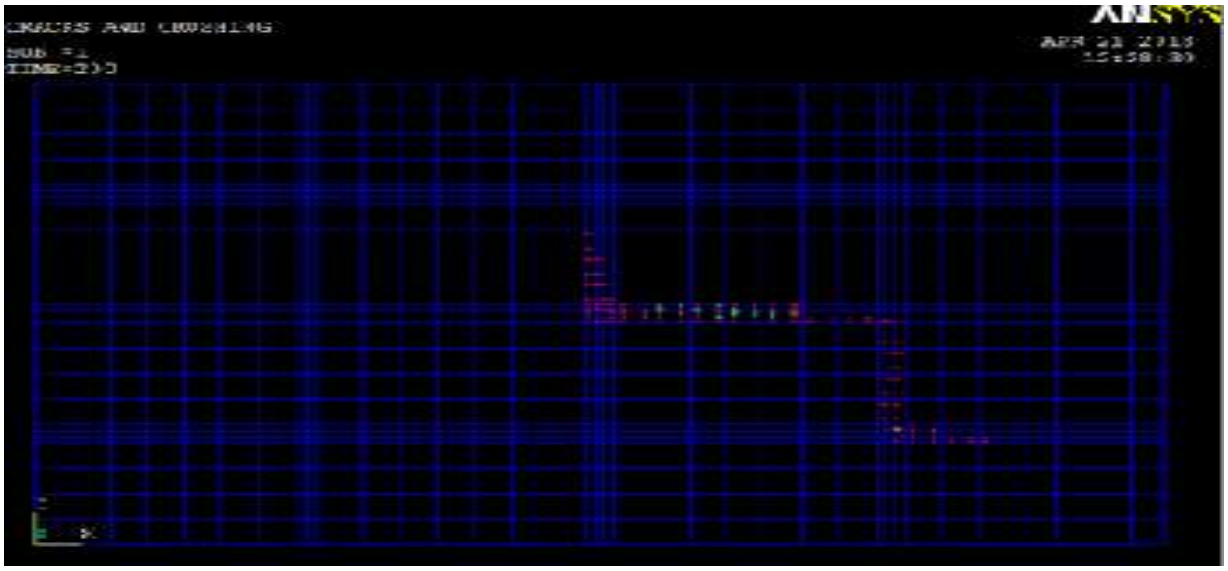
After loads are applied this is the result schema:



FigII.61: distribution of loads

Cracks are shown above (fig2.62):

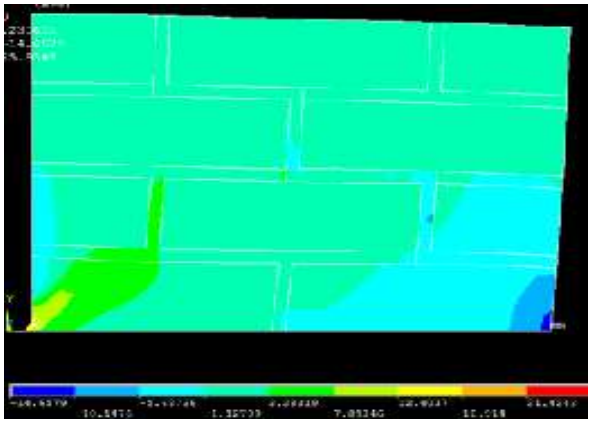
We can see that first crack appears on the same path of the weak mortar and also on the bottom



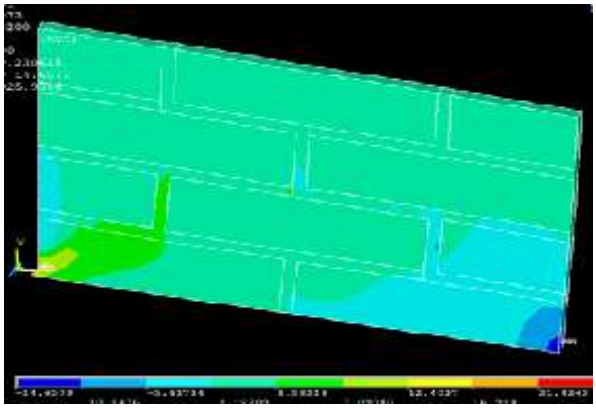
FigII.62: the first Crack path

When load is applied on the left side (all nodes) we can see a compression stress on the opposite side specifically on the bottom, there is also a traction stress on the same left side.

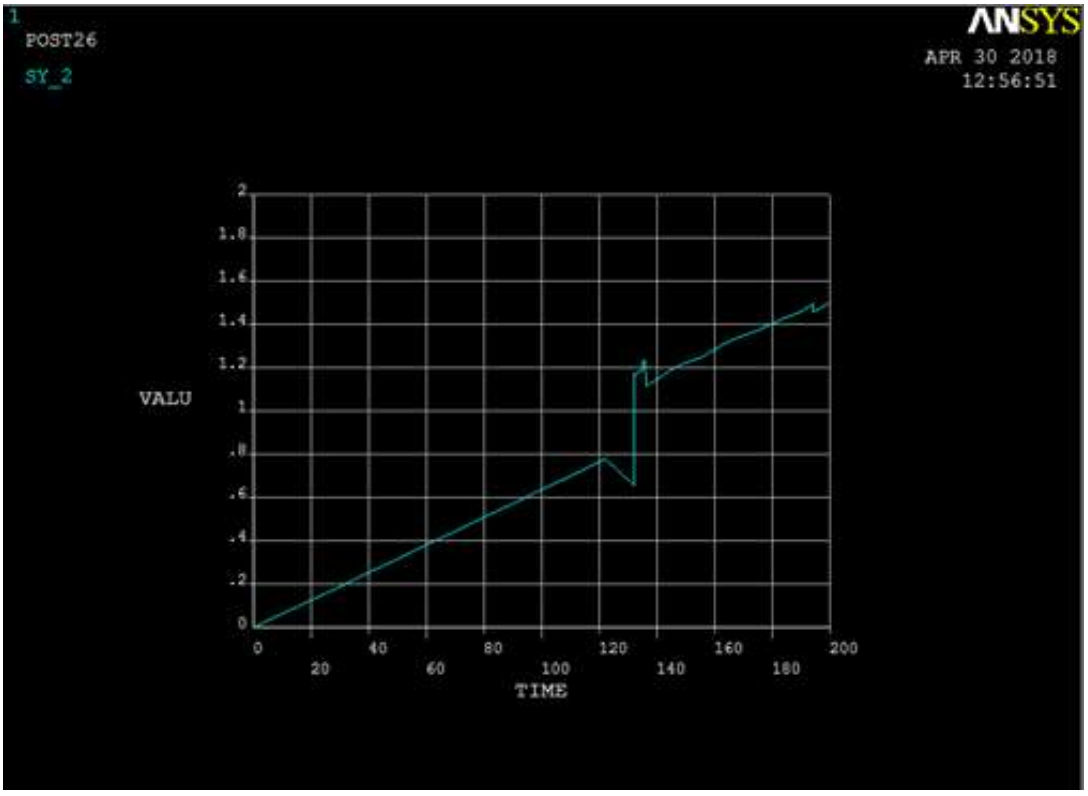
2D and 3D:



FigII.63: stress 2D



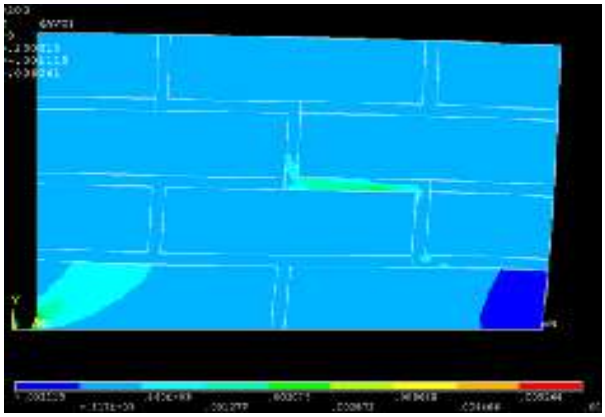
FigII.63: stress 3D



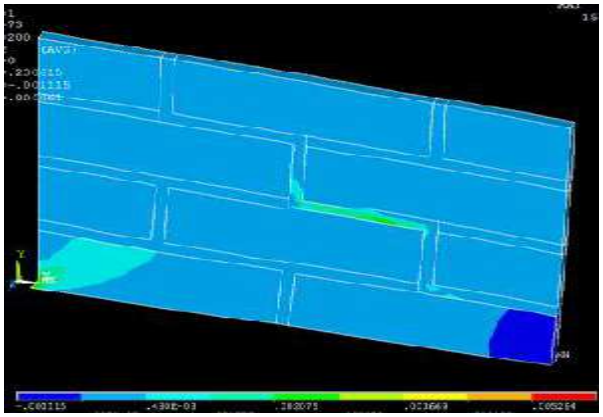
FigII.64: stress in function of time

When we apply a load on the left side (all nodes) we can see there is a repartition of elastic strain on the opposite bottom side, we observe also an elastic strain concentration on the path of weak mortar.

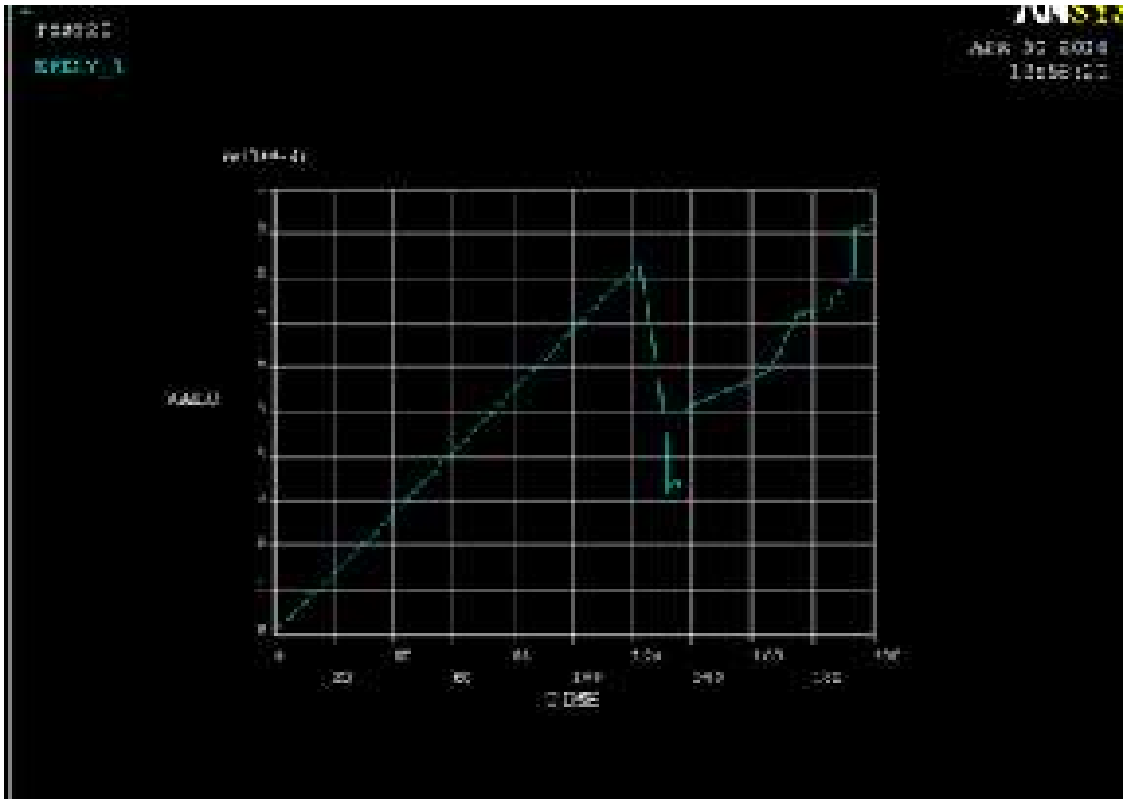
2D and 3D:



FigII.65: elastic strain 2D

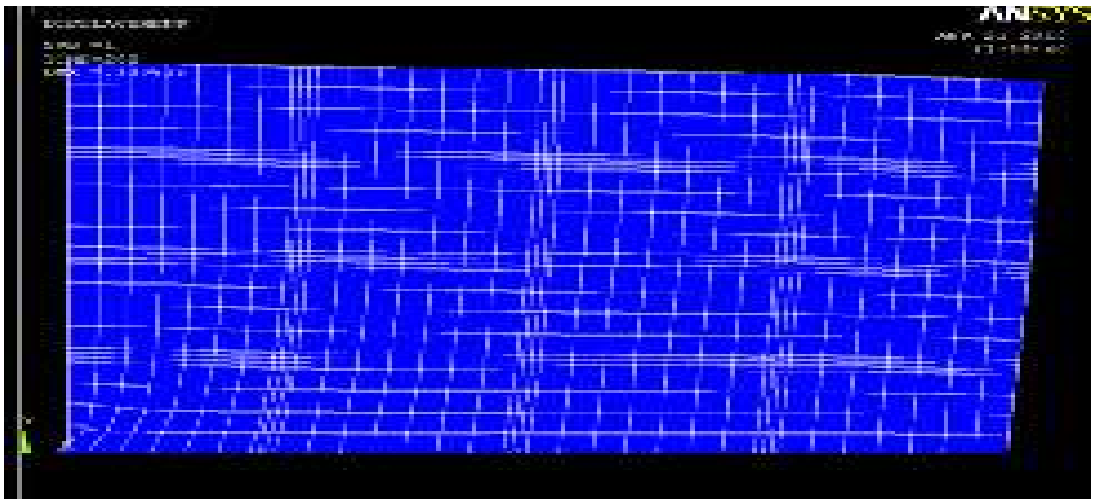


FigII.66: elastic strain 3D



FigII.67: elastic strain in function of time

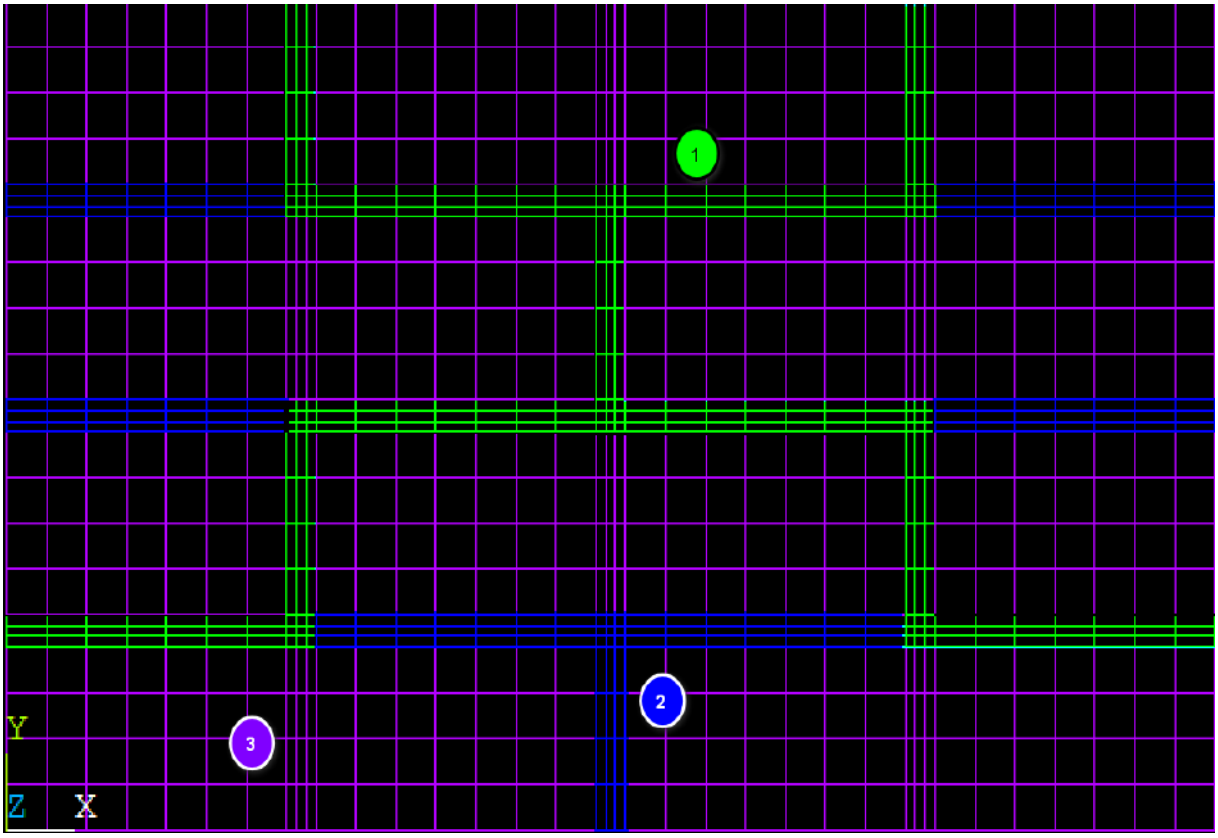
Displacement is shown above (figII.68):



FigII.68: displacement

- Third test: (both sides)

Three (3) element types (materials) Solid 65 are used to get this schema

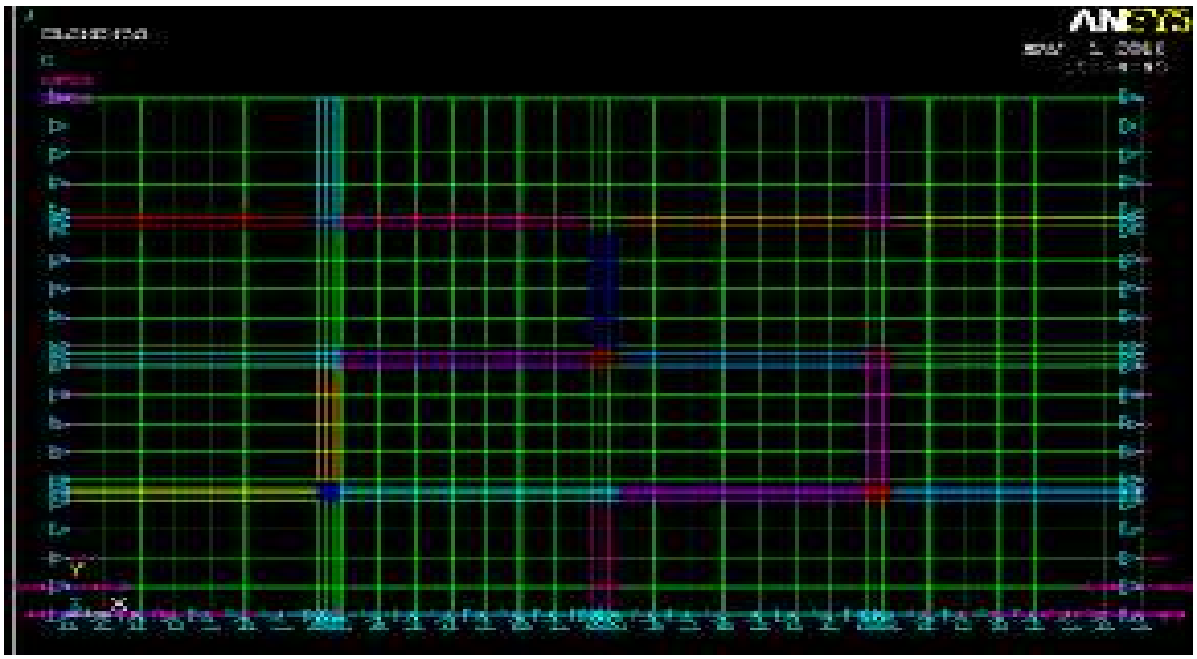


FigII.69: distribution of materials

TableII.5: type of materials

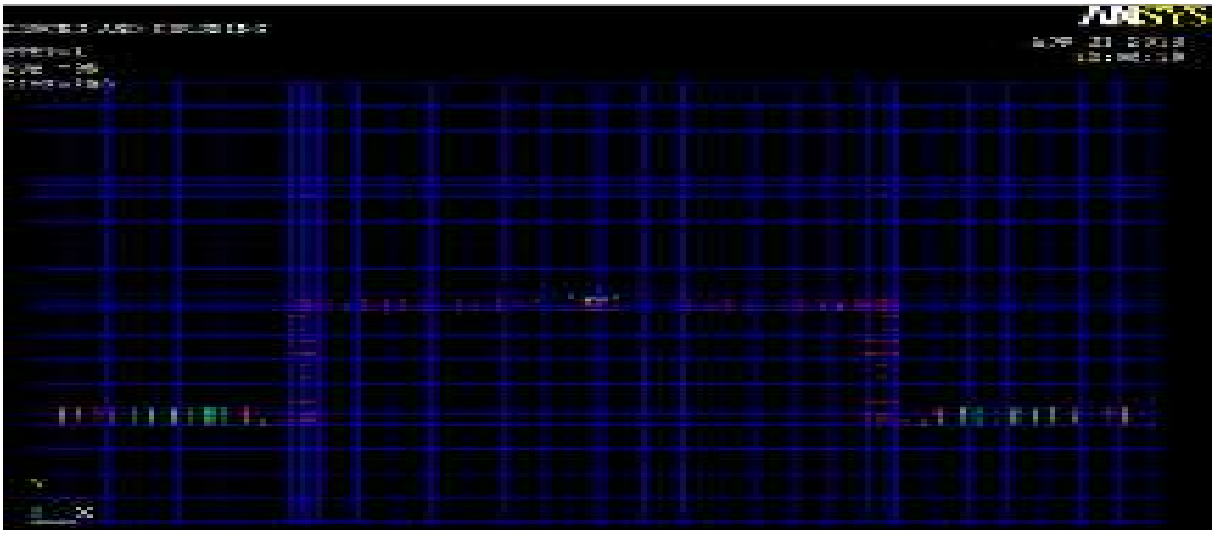
Material
1 (mortar1) low resistance
2 (morter2) good resistance
3 (bricks) standard resistance

After loads are applied this is the result schema:



FigII.70: distribution of loads

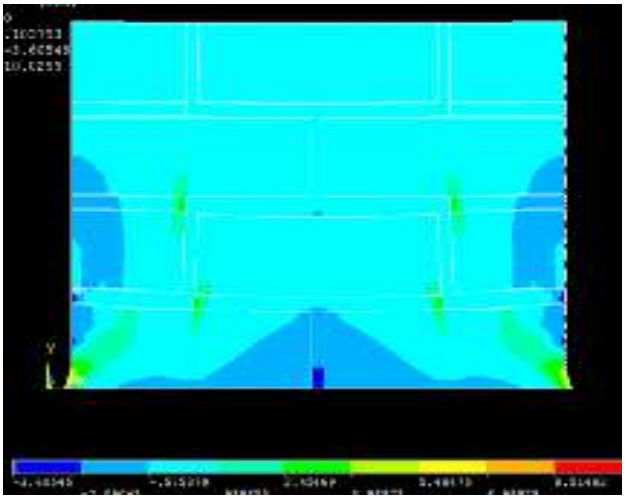
First crack appears on the same path of the weak mortar and also on the bottom in both sides



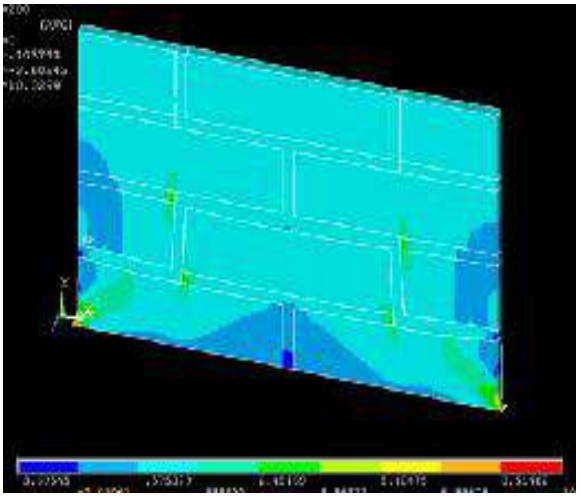
FigII.71: the first crack

When loads are applied on both sides (all nodes) we can see there is a repartition of a compression stress in a symmetrical way concerning the vertical axe of the wall, also we can see a traction stress on the both extreme bottom sides.

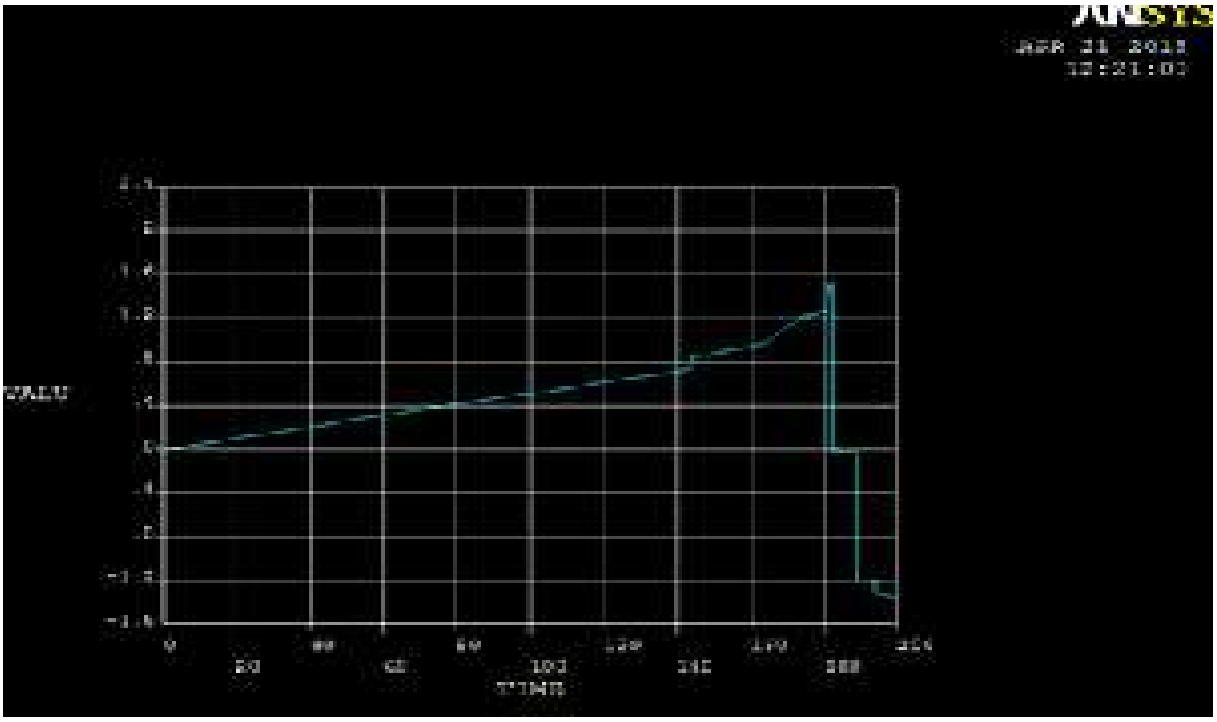
2D and 3D



FigII.72: stress 2D

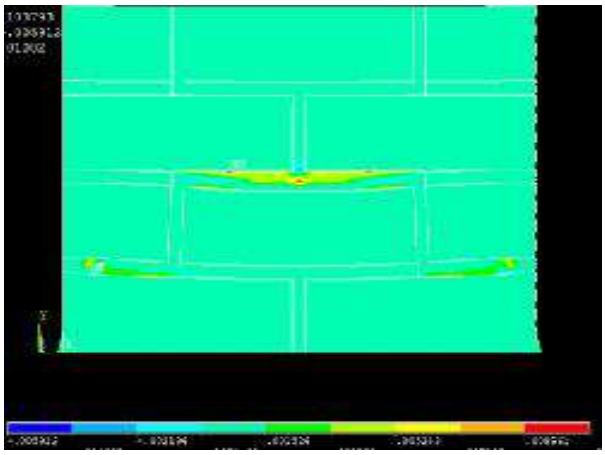


FigII.73: stress 3D

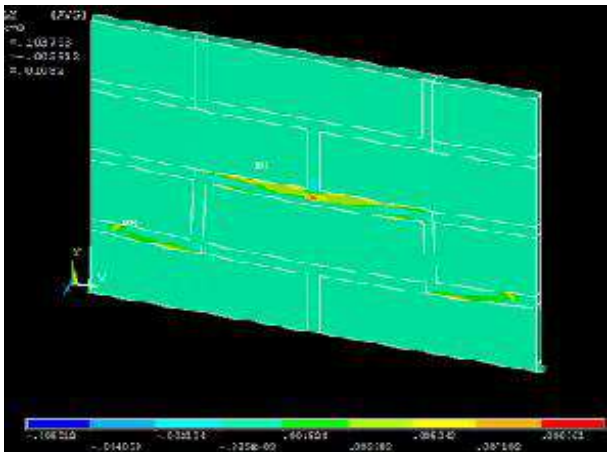


FigII.74: stress in function of time

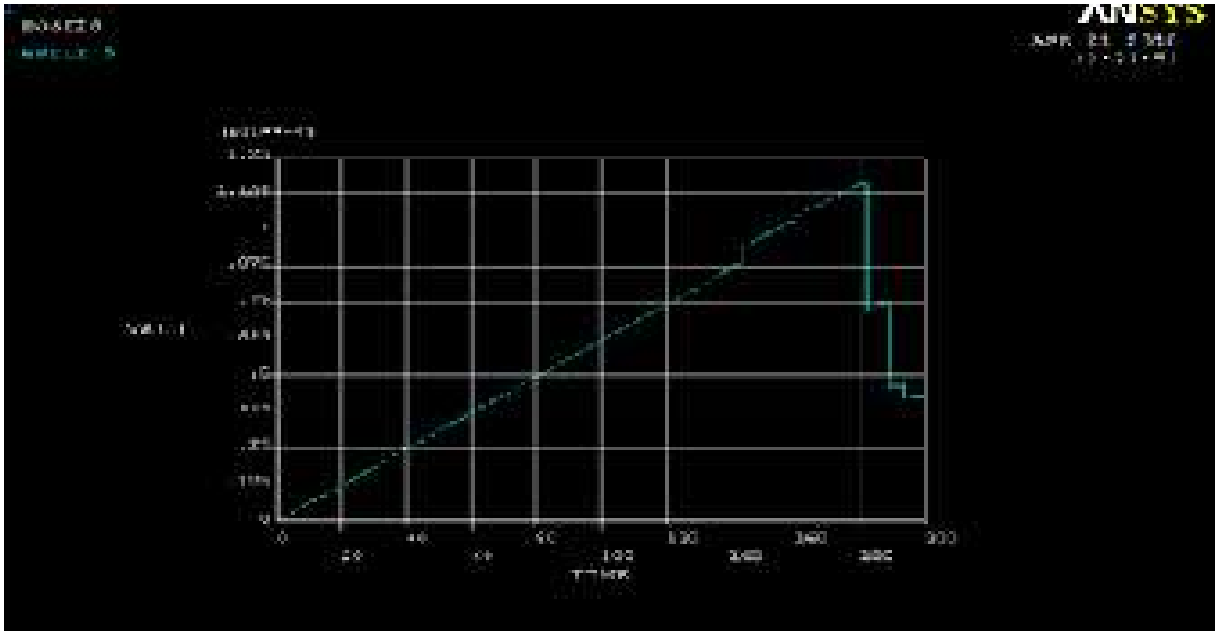
When we apply loads on both sides (all nodes) we can see there is a repartition of elastic strain in symmetrical way concerning the vertical axe of the wall.
Also we observe an elastic strain concentration (deformation) in the middle area (intersection of both horizontal mortar).



FigII.75: elastic strain 2D

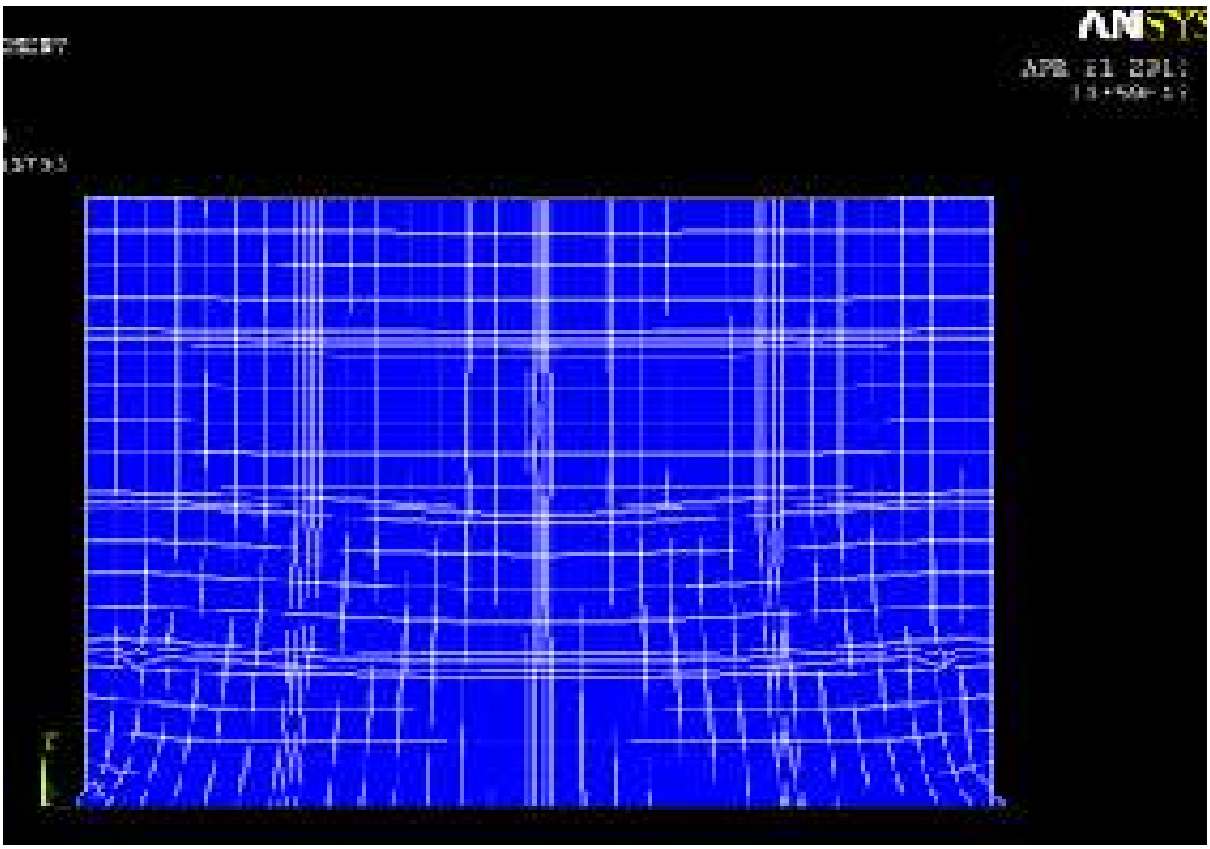


FigII.76: elastic strain 3D



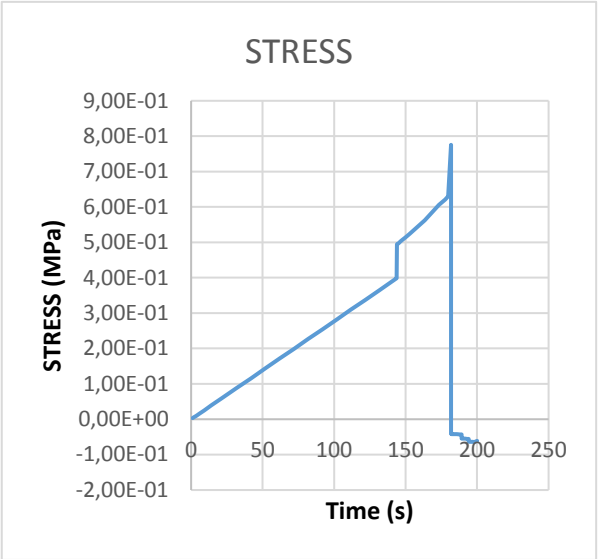
FigII.77: elastic strain in function of time

Displacement is shown above (fig2.78):

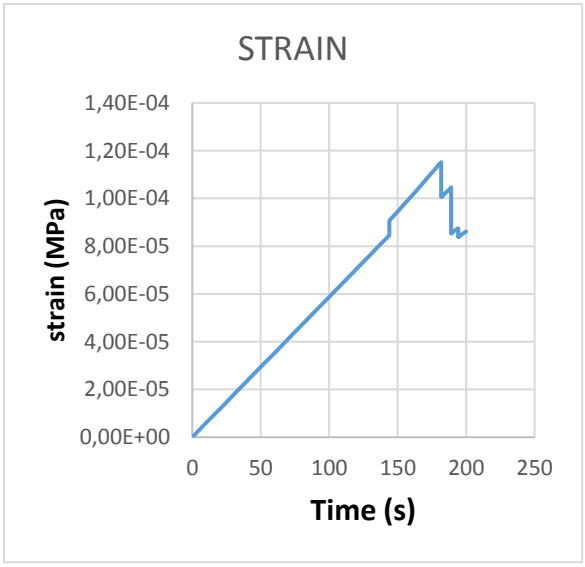


FigII.78: displacement

1. First test

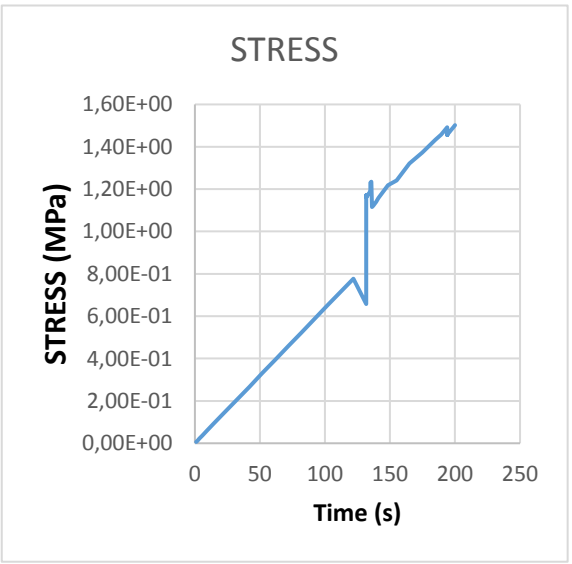


FigII.79 – stress in function of time

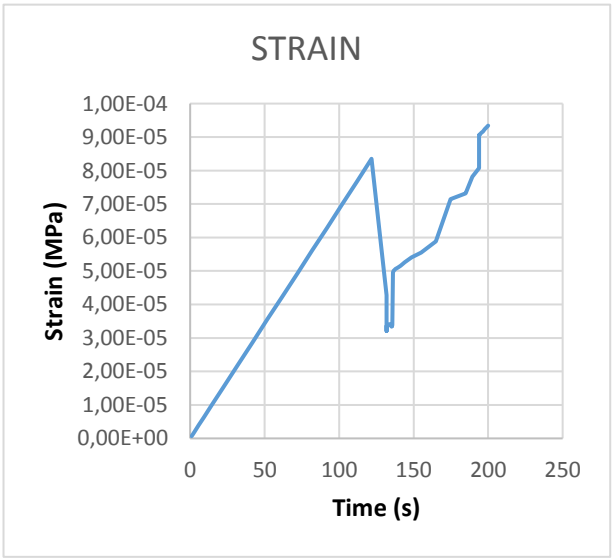


FigII.80 – strain in function of time

2. Second test :

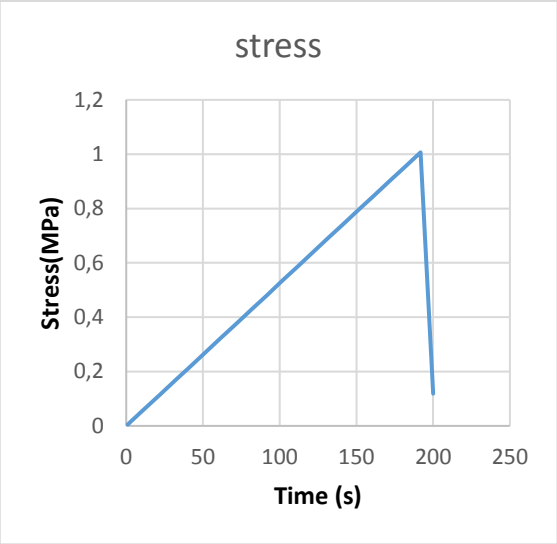


FigII.81 – stress in function of time

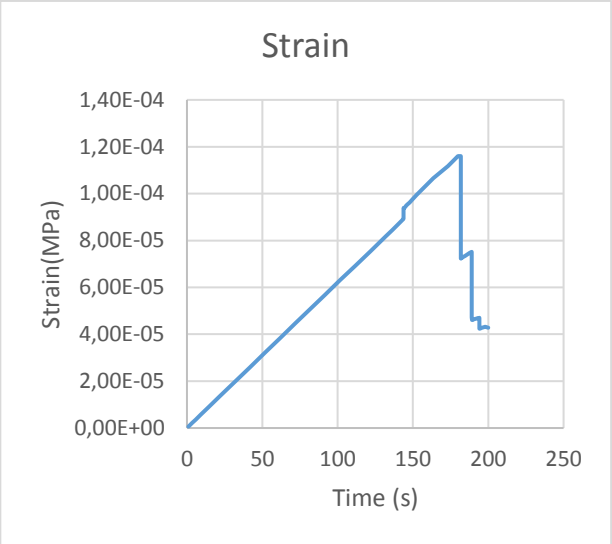


FigII.82 – strain in function of time

3. Third test:



FigII.83 – stress in function of time



FigII.84 – strain in function of time

Chapter 3 :

Results and interpretations

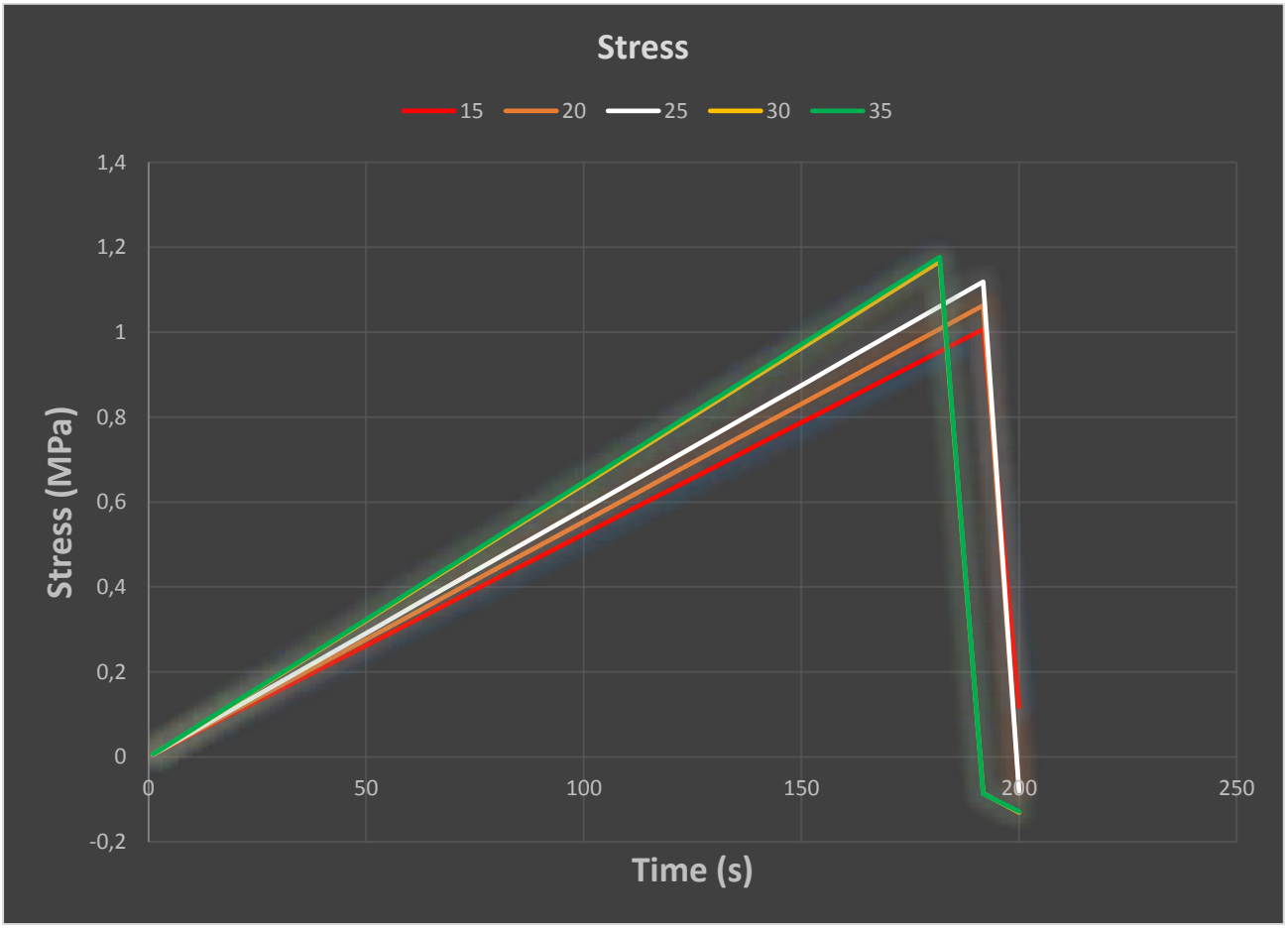
III.1 Influence of mortar parameters on wall resistance

III.1.1 Stress

This graph shows first five (5) tests combined with different applied parameters

There is a small difference between the first three parameters Uniaxial Crushing Stress [15 MPa, 20 MPa, 25MPa].

After this parameter go above 25 MPa [30MPa and 35MPa], in these two tests the difference becomes negligible.



FigIII.1. Stress in function of time (first 5 tests)

III.1.2 Strain

This graph shows first five (5) tests combined with different applied parameters

There is no difference between the first three parameters (Uniaxial Crushing Stress) [15MPa,20MPa,25MPa].

After this parameter go above 25 MPa [30MPa and 35MPa], the difference in strain becomes negligible.

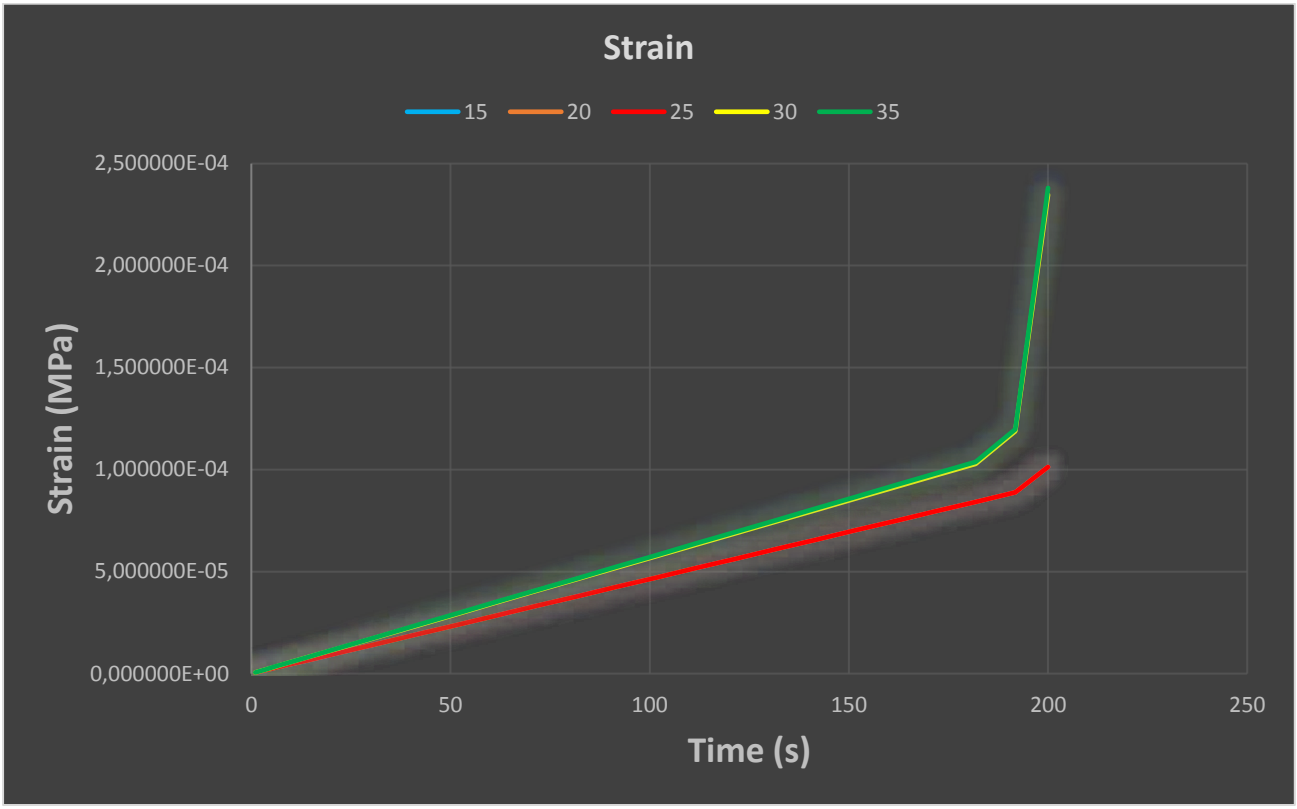


Fig III.2 Strain in function of time (first 5 tests)

III.2 Influence of applied loads sense on wall deformation

III.2.1 Vertical loads

When vertical loads are applied on the superior level (first five tests) we can see that there is a repartition of elastic strain in a symmetrical way concerning the vertical axe of the wall, also we notice an elastic strain concentration (deformation) on the intersection of horizontal and vertical mortar

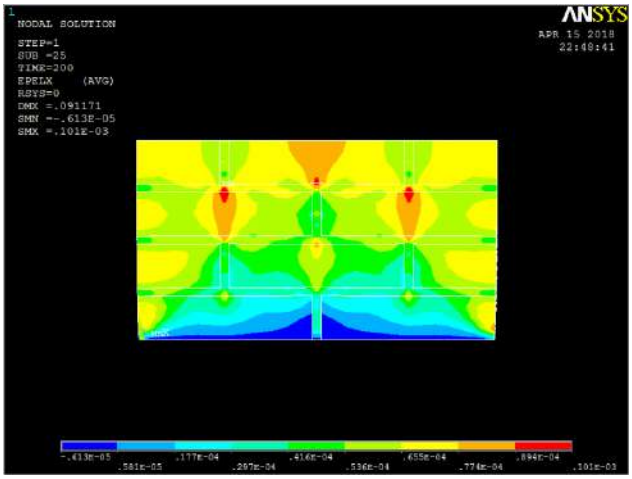


Fig III.3. Elastic Strain (Test 1)

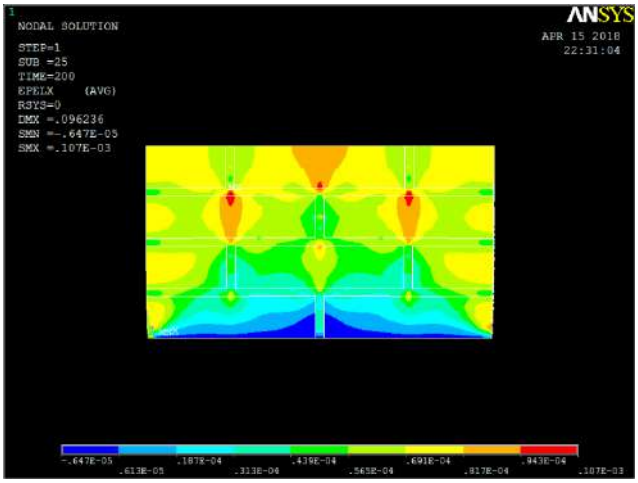


Fig III.4. Elastic Strain (Test 2)

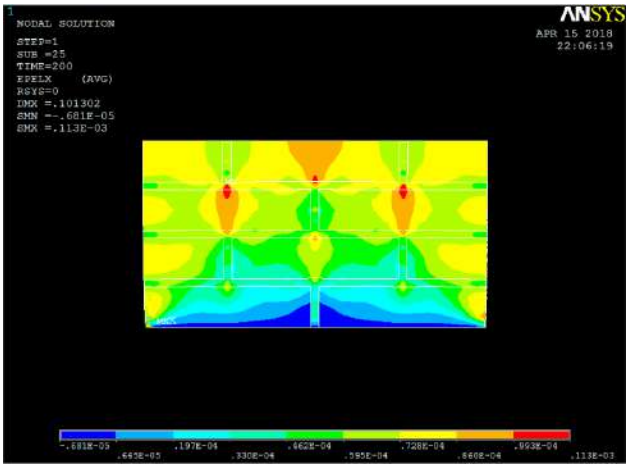


Fig III.5. Elastic Strain (Test 3)

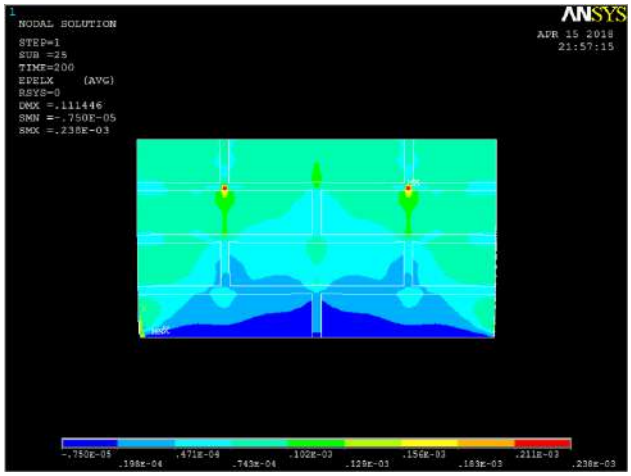


Fig **III.6.** Elastic Strain (Test 4)

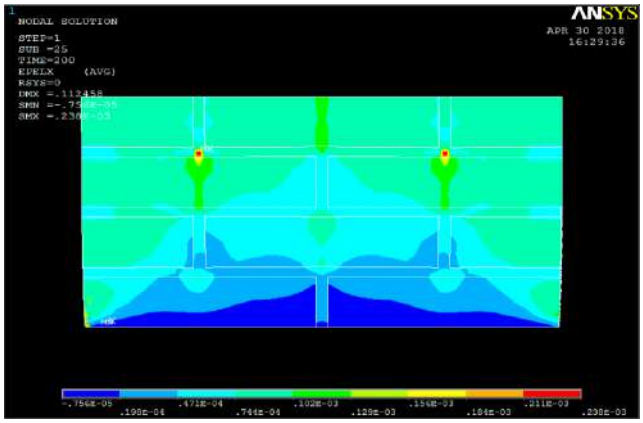


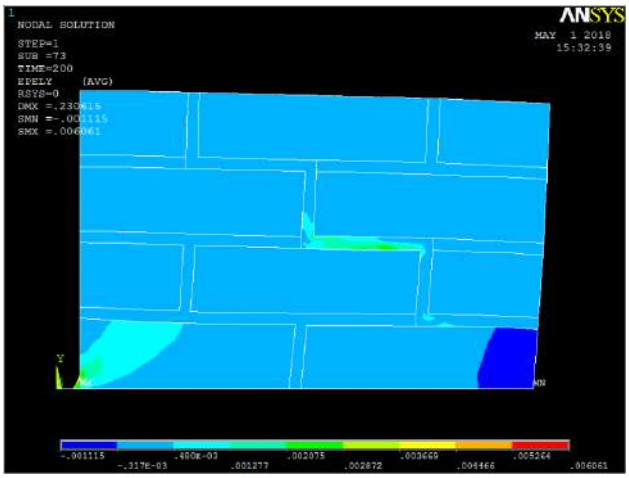
Fig III.7. Elastic Strain (Test 5)

III.2.2- Horizontal loads

When horizontal loads are applied on the (right; left or both) sides we notice that there is a repartition of elastic strain in symmetrical way concerning the vertical axe of the wall (both sides test).

Also an elastic strain concentration in the middle area (concerning LEFT and RIGHT

tests) is observed.



FigIII.8. Elastic Strain (LEFT Side)

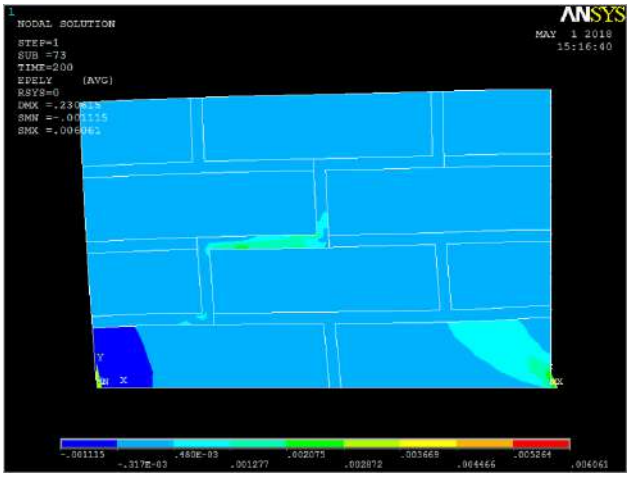
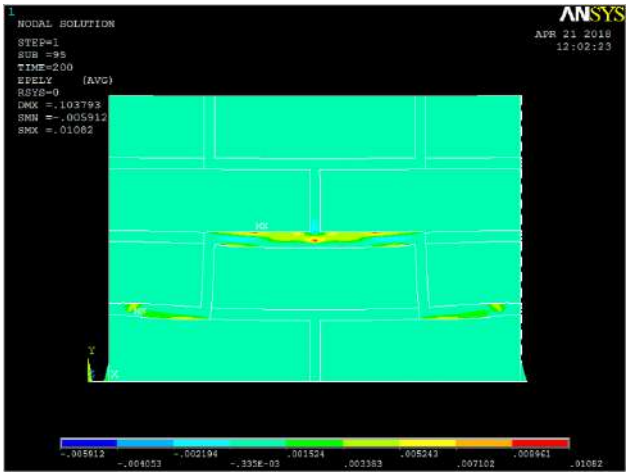


Fig III.9. Elastic Strain (RIGHT Side)



FigIII.10. Elastic Strain (Both Sides)

III.3 - Influence of mortar parameters on the crack path

When mortar parameters are changed we can see that first cracks appear on the same path of the

weak mortar (in all tests) and also on the bottom (in both sides test).

The first cracks also happen in the intersection of horizontal and vertical mortar area.



Fig III.11. Crack path (Left side)

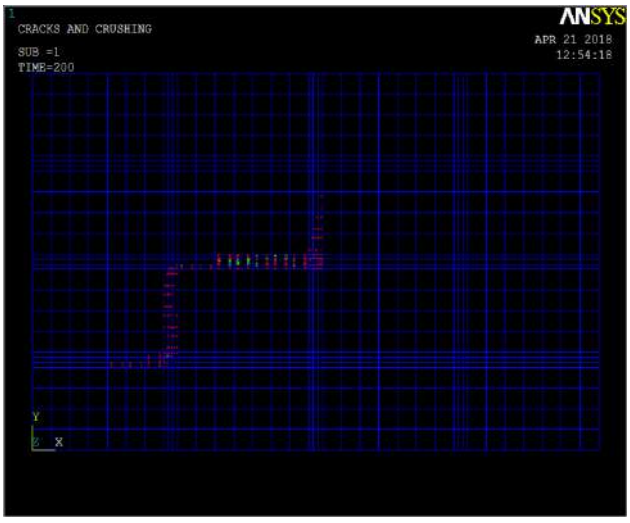


Fig III.12. Crack path (Right Sides)



Fig III.13. Crack path (Both sides)

III.4 Conclusion and perspective

The analysis of the simulation results of the influence of loads directions and mortar parameters on the behavior of wall can lead to the following conclusions:

The mortar doesn't have an essential role of supporting the masonry wall comparing to bricks element also first cracks happen always in mortar.

The mortar resistance can be increased to a certain value (OPTIMUM) to be at its best so we don't need to increase it more and that will give us the possibility to avoid wasting materials which are expensive.

Horizontal loads (like earthquake) can be more dangerous than the vertical ones because cracks and deformation will be higher on the first one.

The stress and strain will be always symmetrical to the vertical axe when applying vertical loads. Using contact elements and interface elements will allow better result and much more details on the combination of our materials.

Bibliographical references

Bibliographical references

[1]https://fr.wikipedia.org/wiki/S%C3%A9isme_du_1er_novembre_1755_%C3%A0_Lisbonne

[2] https://en.wikipedia.org/wiki/St_Mark%27s_Campanile

[3] https://en.wikipedia.org/wiki/Civic_Tower_(Pavia)

[4] https://fr.wikipedia.org/wiki/Cath%C3%A9drale_de_Noto

[5] MACCHI, G., 1992. Structural diagnosis and rehabilitation of historical buildings. Cuadernos INTEMAC, nº7.

[6] LANGENBACH, R., 1994. Architectural issues in the seismic rehabilitation of masonry buildings. D. Abrams and G. Calvi : US-Italy workshop on guidelines for seismic evaluation and rehabilitation of unreinforced masonry buildings. Technical report NCEER-94-0021.

[7] DRYSDALE, R.G.; HAMID, A.A.; BAKER, L.R., 1999. Masonry structures. Behaviour and design. The Masonry Society, Boulder, Colorado, USA.

[8] CROCI, G., 1998. The conservation and structural restoration of the architectural heritage. Computational Mechanics Publications, Shouthampton, UK.

[9] https://www.theonion.com/new-evidence-suggests-ancient-egyptians-only-ever-visit-1821874775

[10] https://en.wikipedia.org/wiki/Lion_Gate

[11] http://ancient-greece.org/archaeology/mycenae.html

[12] https://www.athensguide.com/acropolis.html

[13] DRYSDALE, R.G.; HAMID, A.A.; BAKER, L.R., 1999. Masonry structures. Behaviour and design. The Masonry Society, Boulder, Colorado, USA.

[14] http://storiesmysuitcasecouldtell.com/2016/12/12/the-colosseum/

[15] https://alternativetravelers.com/day-trip-to-segovia-from-madrid/

[16] LOURENÇO, P.B., 1998. Experimental and numerical issues in the modelling of the mechanical behavior of masonry. P. Roca et al. (eds): Structural Analysis of Historical Constructions II. CIMNE, Barcelona, pp. 57-91.

[17] LOURENÇO, P.B., 1996. Computational strategies for masonry structures. Ph.D. Dissertation, Delft University of Technology, Delft, The Netherlands.

[18] DHANASEKAR, M. PAGE, A.W. KLEEMAN, P.W., 1985. The failure of brick masonry under biaxial stresses. Proc. Instn. Civ. Engrs., Part 2, 79, pp. 295-313.

[19] HEYMAN, J., 1995. The stone skeleton. Cambridge University Press, Cambridge, UK.

[20] LOURENÇO, P.B., 2002. Computations on historic masonry structures. Prog. Struct. Engng. Mater., 4, pp. 301-319.

[21]http://faculty.uml.edu/Nelson_Eby/89.520/Instructor%20pdfs/Chapter%206.%2 0Behavior%20of%20Materials.pdf

[22] MACCHI, G., 1997. General methodology. The combined use of experimental and numerical techniques inside a single study. P. Roca et al. (eds): Structural Analysis of Historical Constructions. CIMNE, Barcelona, pp. 10-23.

[23] CROCI, G., 1998. The conservation and structural restoration of the architectural heritage. Computational Mechanics Publications, Shouthampton, UK.

[24] https://www.researchgate.net/figure/There-are-three-distinct-regions-of-the-stress-strain-curve-1-the-toe-region-2-the_fig5_241623404

[25] https://figshare.com/articles/Nonlinear_concrete_behaviour/3483020 page 59,60

[26] https://rdconcrete.com/tensile-behaviour-uhpc-digging-into-plain-concrete-tensile-response/

[27] LOURENÇO, P.B., 1996. Computational strategies for masonry structures. Ph.D. Dissertation, Delft University of Technology, Delft, The Netherlands.

[28] SUPRENANT, B.A.; SHULLER, M.P., 1994. Nondestructive evaluation & testing of masonry structures. Aberdeen Group.

[29] Michael Somr , 2011 , Numerical Simulation of Cocciopesto-based Masonry Structures

[30] BARONIO G., BINDA L., LOMBARDINI N.: The role of brick pebbles and dust in conglomerates based on hydrated lime and crushed bricks, Construction and Building Materials, Vol. 11, No. 1, 1997, pp. 33-40

[31] Michael Somr , 2011 , Numerical Simulation of Cocciopesto-based Masonry Structures, pp. 43

[32] NEŽERKA V.: Report 1 (micromechanics), internal research report, Faculty of Civil Engineering, CTU in Prague, 2011

[33] BRENCICH A., CORRADI C., GAMBAROTTA L., MANTEGAZZA G., STERPI E.: Compressive Strength of Solid Clay Brick Masonry under Eccentric Loading, Department of Structural and Geotechnical Engineering, University of Genoa, Italy

[34] MAHERI M. R., NAJAFGHOLIPOUR M. A., RAJABI A. R.: The influence of mortar head joints on the in-plane and out-of-plane seismic strength of brick masonry walls, The 14th World Conference on Earthquake Engineering, Beijing, China, 2008